Studies on Speed and Separation of High Performance Liquid Chromatography

Masahito ITO

February 2018

Studies on Speed and Separation of High Performance Liquid Chromatography

Masahito ITO
Doctoral Program in Chemistry

Submitted to the Graduate School of
Pure and Applied Sciences
in Partial Fulfillment of the Requirements
for the Degree of Doctor of Philosophy in
Science

at the
University of Tsukuba

Contents

Chapter 1. General Introduction

1-1 Theory on separation of pressure-driven chromatography 1

1-2 Technique speeding-up or enhancing separation 1

1-3 Graphical method to analyze separation conditions 5

1-3 Purpose and content of this thesis 7

1-4 References 8

Chapter 2. Three-Dimensional Representation Method Using Pressure, Time, and Column Efficiency to Analyze Separation Conditions

2-1 Introduction 10

2-2 Theoretical 10

2-3 Experimental 13

2-4 Results and discussion 13

2-5 Summary 24

2-6 References 24

Chapter 3. Mathematical Study on Three-Dimensional Graph, and New Coefficients on Two-Dimensional Curved Surface

3-1 Introduction 25

3-2 Theoretical

3-2-1 Logarithmically rotational transformation 25

3-2-2 Pressure-application coefficients 28

3-3 Results and discussion 33

3-4 Summary 43

3-5 References 43

Chapter 4. Applicational Experiments Using Velocity near Optimal Velocity

4-1 Introduction

4-1-1 Optimal velocity 44

4-1-2 Ginsenosides 44

4-1-3 Vitamins A and E 45

4-1-4 β-Carotene 46

4-2 Experimental

4-2-1 Ginsenosides 47

4-2-2 Vitamins A and E 50

4-2-3 β-Carotene 52

4-3 Results and discussion

4-3-1 Ginsenosides 53

4-3-2 Vitamins A and E 61

4-3-3 β-Carotene 67

4-4 Summary 71

4-5 References 72

Chapter 5. Applicational Experiments Using Larger Velocity than Optimal Velocity

5-1 Introduction

5-1-1 Capsaicinoids 75

5-1-2 Capsaicin in gochujang 76

5-2 Experimental

5-2-1 Capsaicinoids 77

5-2-2 Capsaicin in gochujang 78

5-3 Results and discussion

5-3-1 Capsaicinoids 79

5-3-2 Capsaicin in gochujang 84

5-4 Summary 93

5-5 References 93

Chapter 6. Conclusions 95

Acknowledgements 96

List of Publications 97

Chapter 1. General Introduction

1-1 Theory on separation of pressure-driven chromatography

Various types of packing support, such as particle and monolithic columns, are widely used especially for reversed-phase chromatography in HPLC, to obtain high resolution or rapid analytical time.[1-11] However, it is difficult to select the optimal packing support, and to find suitable separation conditions, given a specific pressure in an HPLC system; and peripheral studies on the theory have thus far been limited.[12-27] In 2005, Desmet *et al.* invented kinetic performance methods[28] by expanding both Bristow and Knox's,[29] and Poppe's[30] methods. At that time, van Deemter plots of height equivalent to a theoretical plate (H) and linear velocity (u_0) were used to analyze the minimal height (H_{min}) and optimal velocity ($u_{0,opt}$).[28,31] From the viewpoint of pressure-driven chromatography, the kinetic plot methods use column permeability (K_V) to find the minimal hold-up time (t_0) and maximal number of theoretical plates (N), given a specified pressure drop (ΔP). K_V is a physical constant that depends on the diameter of the packing particles and the specific surface area, and is inversely proportional to the flow resistance against ΔP. The methods give us a kinetic performance limit (KPL)[32] of t_0 and N, incorporating the length of the column (L), uniquely calculated with u_0 as an operating parameter. L is the other operating parameter, and the largest limit to be automatically obtained at u_0 with the specified ΔP.

1-2 Technique speeding-up or enhancing separation

UHPLC (Ultra HPLC) has led 2-micrometer packings of ODS (octadecylsilyl) silica or less. Two-micrometer packings have a feature to almost keep H_{min} at higher u_0 than $u_{0,opt}$, compared with 3- or 5-micrometer. Therefore, in case of 2-micrometer, it is comparatively easy to speed up analytical methods by increasing u_0 while almost keeping N.

On the other hand, according to the traditional methodology[12-15], when speeding up analytical method, $u_{0,opt}$ should be used as the most efficient velocity with H_{min}. Therefore, when requiring a certain N, L is determined uniquely at $u_{0,opt}$. Then both ΔP and t_0 are also determined necessarily. For example, an analytical method for glycated hemoglobin Hb A1c[33] takes a velocity near $u_{0,opt}$ (Fig. 1-1a). And there is another method with lager N. In that case, although L should be made larger, ΔP becomes too high, because the HPLC system or the column has realistically a limitation of pressure. Figure 1-2 shows a relationship between N and the retention time (t_R) of Hb A1c with limitation of ΔP. As the result, a chromatogram with larger N was obtained without use of $u_{0,opt}$ (Fig. 1-1b).

The apparatus was Hitachi Model L-9100 glycated hemoglobin analyzer. It had two analytical

methods: high-speed mode (Fig. 1-1a) and high-resolution mode (Fig. 1-1b). The two modes used the same mobile phase A = 64 mM potassium phosphate buffer (pH 6.2); mobile phase B = 75 mM potassium phosphate buffer (pH 6.2); and mobile phase C = 207 mM sodium phosphate buffer (pH 6.1). In the high-speed modes, a 35 mm x 4.6 mm I. D. column packed with weak cation-exchange polymethacrylate resin was used. The particle diameter of resin was 3.5 μm. The flow rate was 1.4 ml/min. samples were injected at 3.3-min intervals.

In the high-resolution mode, an 80 mm x 4.6 mm I. D. column with the same resin in the high-speed mode was used. The flow rate was 1.0 ml/min. samples were injected at 7.0-min intervals. Other conditions for two modes were identical. The column temperature was 40˚C. The absorbance at 415 nm, using the absorbance at 530 nm as a reference. Samples were whole blood diluted 160-fold with water. The injection volume was 10 μl.

The high-resolution mode was developed by using the schematic graph of Fig. 1-2. Firstly, the blue line means the result of $u_{0,\mathrm{opt}}$ derived from 1.4 ml/min. N is proportional to L, then t_R of Hb A1c is also proportional to L with the constant flow rate. The high-speed mode adopted L of 35 mm and resulted in t_R of approximate 2 min. The dashed curve shows the result obtained under a restricted condition of the pressure limit, that is 8 MPa. The curve is a function on square root of t_R, because the flow rate should be decreased to increase L under the pressure limit. That is a kind of KPL. The high-resolution mode adopted L of 80 mm, then the flow rate should become about 1.0 ml/min under the pressure limit of 8 MPa. The mode resulted in t_R of approximate 5 min. The high-speed mode utilized the optimized method of $u_{0,\mathrm{opt}}$ until reaching a pressure limit. And the high-resolution mode was based on KPL with the maximum pressure.

As a summary, in case of speeding-up, it is possible to increase u_0 up to the maximum of ΔP ($\Delta P_{\max}$) with an adequate column of L to obtain required N. When using 2-micrometer packings, almost the same N can be expected. In case of enhancing separation, first of all, L should be chosen to obtain required N at $u_{0,\mathrm{opt}}$. If ΔP is $\Delta P_{\max}$ or less, the analysis time can be taken without change. If ΔP is larger than $\Delta P_{\max}$, u_0 should be decreased down to $\Delta P_{\max}$ to gain sufficient L. As a result, the analysis time becomes one after decreasing u_0.

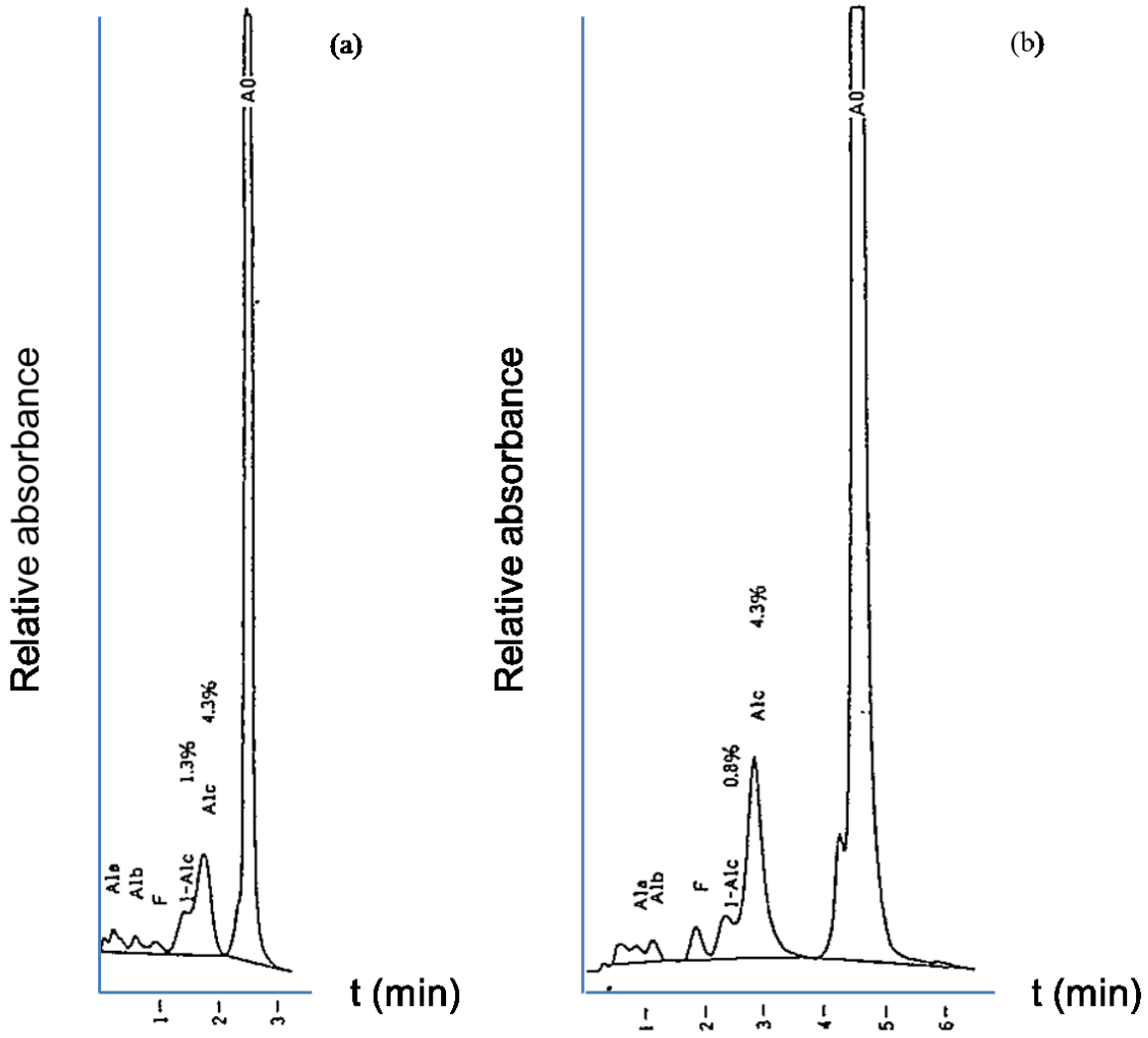

Fig. 1-1 Representative chromatograms of glycated hemoglobin Hb A1c. (a) High-speed mode with 35 mm x 4.6 mm I. D. by flow rate of 1.4 mL/min; (b) High-resolution mode with 80 mm x 4.6 mm I. D. by flow rate of 1.0 mL/min.

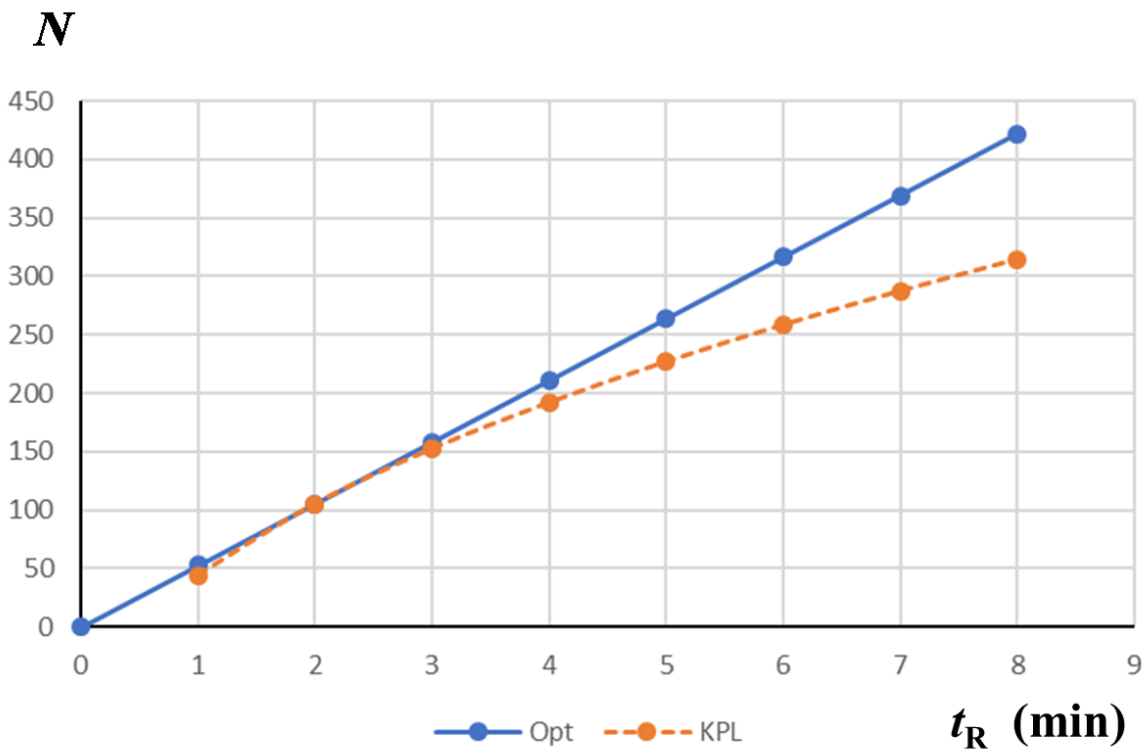

Fig. 1-2 Schematic graph of *N* and retention time of Hb A1c

The pressure limit is ignored in Opt. method. The pressure limit of 8 MPa is considered in KPL method. Therefore, a kind of saturation makes the curved line of KPL. The straight line of Opt. almost exceeds the limit of 8 MPa.

1-3 Graphical method to analyze separation conditions

Desmet et al. has introduced kinetic plot method to show graphs of t_0-N. The method is based on an idea that ΔP_{max} can give the best combination of speed and separation, that is KPL. [32]

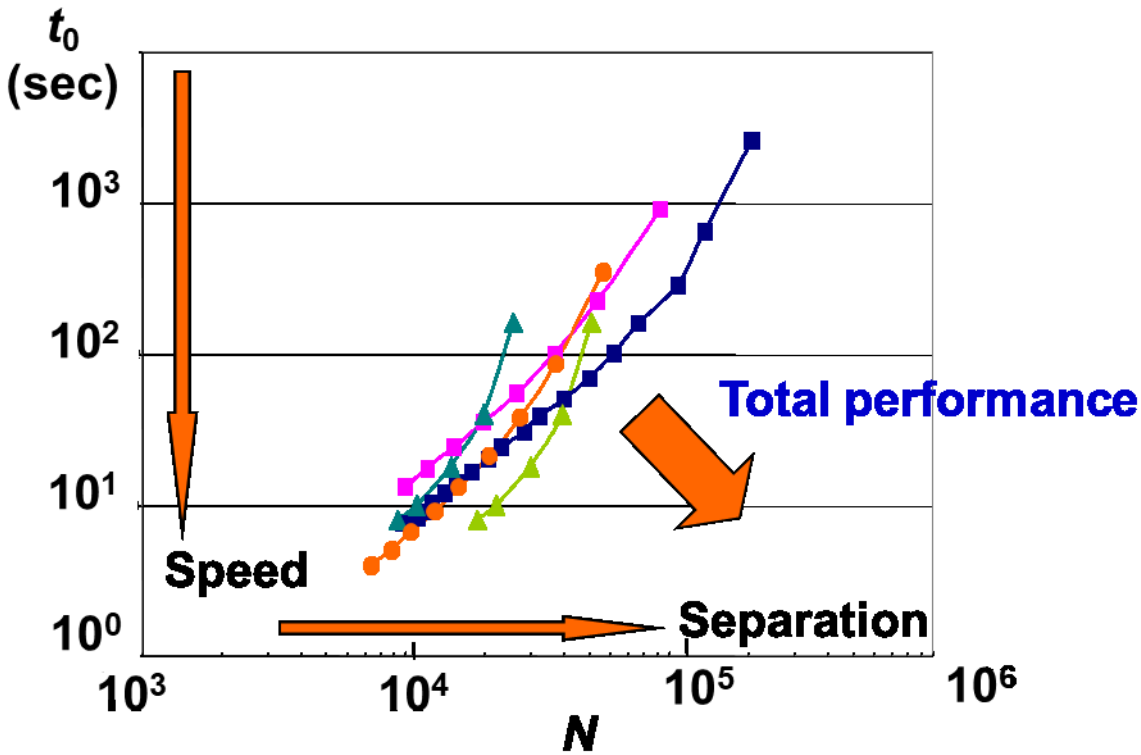

Fig. 1-3 t_0-N plot of KPL

The plots of t_0 and N are calculated by using each H (u_0) and L permitted at the pressure limit of 50 MPa

On the other hand, Weber et al. show a contour map[20] of u_0, L, and N, that is a kind of three-dimensional graph of N (u_0, L). The graph means that N coming from separation conditions of u_0 and L. It is important that Weber's graph can widely treat u_0 without limiting $u_{0,opt}$. The graph can show separation condition comprehensively with various possibilities of L.

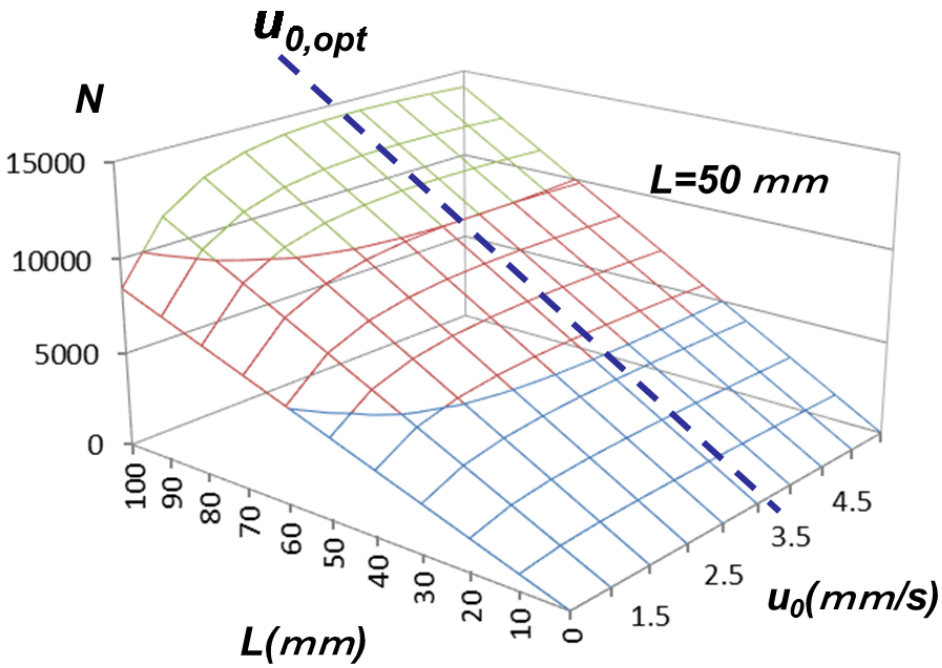

Fig. 1-4 Three-dimensional representation based on Weber's contour map

1-4 Purpose and content of this thesis

The purpose of this thesis is understanding the relationship between speed and separation of HPLC. There should be a logic to explain the strong correlation between the two performances. The logic is studied theoretically with basic experimental data, then practical methods based on the theory are proposed to represent the relationship and to evaluate the separation condition. And some applicational experiments are shown with the practical methods.

The thesis consists of six chapters.

In chapter 1, some representative theories of separation are shown in HPLC. Example methods are shown to speed up in UHPLC, or to enhance the separation in HPLC analysis of glycated hemoglobin. Then two graphical methods are outlined. One is the graph of KPL to show the two performances of speed and separation by Desmet et al. The other is a contour map of N (u_0, L) based on separation condition by Weber et al.

In chapter 2, u_0, L, Π, t_0, and N are taken as five objective variables based on a separation model to clarify the issues. Velocity length product of Π is introduced as a new essential variable instead of pressure drop of columns. And a new three-dimensional graph of N (Π, t_0) is invented to show the correlation between speed and separation. The experimental data of ODS silica were measured by using three types of packing particle and monolithic silica column.

In chapter 3, LRT (Logarithmically Rotational Transformation) correspondence is found out to explain a relationship between the separation variables (u_0, L) and the performance variables (Π, t_0). And three-dimensional graph of N (Π, t_0) can be derived from N (u_0, L) by using the LRT. Starting from N (u_0, L), the three-dimensional graph of N (Π, t_0) is obtained, then a plain of t_0 and N can be found as a KPL cross-section in the graph N (Π, t_0).

Furthermore, PAC (Pressure-Application Coefficient) and TEC (Time-Extension Coefficient) are defined on the basis of partial differential to evaluate effectiveness of pressure or time quantitatively. Finally, the function of N (Π, t_0) can be represented as a differential equation with PAC or TEC.

In chapter 4, when using 2-μm packings with column of 2-mm internal diameter, the optimal flow rate corresponding to $u_{0,\mathrm{opt}}$ is 0.2 to 0.3 ml/min. Ginsenosides in ginseng products were analyzed with the column at the flow rate. L is applied at a maximum, because the neighborhood of $u_{0,\mathrm{opt}}$ almost gives the minimal H, H_{min}. Π and t_0 are passively determined by LRT correspondence. In the separation condition, PAC and TEC should be approximately 1.0.

In chapter 5, the linear velocity is increased to larger one than $u_{0,\mathrm{opt}}$. In case of 2-μm packings and 2-mm internal diameter, the flow rate of 6 ml/min can be applied. Determination of capsaicinoids in foods was performed under the condition of high-speed and high-resolution, because u_0 and L can be chosen comparatively freely. Although L cannot be applied efficiently due to larger H, increase of Π

permits extension of L, then t_0 can be shorten by increasing u_0. Evaluation of PAC or TEC is important to understand the effectiveness of speed and separation quantitatively.

1-4 References

1. N. Tanaka and D. V. McCalley, *Anal. Chem.*, **2016**, *88*, 279.
2. Siswoyo, L. W. Lim, and T. Takeuchi, *Anal. Sci.*, **2012**, *28*, 107.
3. K. Todoroki, T. Nakano, H. Watanabe, J. Z. Min, K. Inoue, Y. Ishikawa, and T. Toyo'oka, *Anal. Sci.*, **2014**, *30*, 865.
4. Y. Song, K. Takatsuki, T. Sekiguchi, T. Funatsu, S. Shoji, and, M. Tsunoda, Chromatography, **2016**, *37*, 111.
5. C. Okamoto, H. Yoshida, A. Nakayama, S. Kikuchi, N. Ono, H. Miyano, Y. Ino, N. Hiraoka, and T. Mizukoshi, Chromatography, **2016**, *37*, 125.
6. H. Kobayashi, M. Sukegawa, K. Fujimura, T. Kubo, and K. Otsuka, Chromatography, **2016**, *37*, 133.
7. T. Toyo'oka, *Anal. Sci.*, **2017**, *33*, 555.
8. A. Morikawa, H. Fukuoka, K. Uezono, M. Mita, S. Koyanagi, S. Ohdo, K. Zaitsu, and K. Hamase, Chromatography, **2017**, *38*, 53.
9. K. Nojima, M. Niitsu, Y. Kurosawa, T. Izawa, K. Nakayama, and Hisaaki Itoh, Chromatography, **2017**, *38*, 73.
10. Y. Nagatomo, S. Hashimoto, Y. Kishimoto, T. Hayakawa, S. Yamamoto, M. Kinoshita, and S. Suzuki, Chromatography, **2017**, *38*, 23.
11. M. Otsubo, T. Motono, S. Kitagawa, and H. Ohtani, Chromatography, **2017**, *38*, 31.
12. J. H. Knox and M. Saleem, J. Chromatogr. Sci., **1969**, *7*, 614.
13. M. Martin, C. Eon, and G. Guiochon, J. Chromatogr., **1974**, *99*, 357.
14. P. W. Carr, X. Wang, and D. R. Stoll, *Anal. Chem.*, **2009**, *81*, 5342.
15. A. J. Matula and P. W. Carr, *Anal. Chem.*, **2015**, *87*, 6578.
16. H. Kobayashi, T. Ikegami, H. Kimura, T. Hara, D. Tokuda, and N. Tanaka, *Anal. Sci.*, **2006**, *22*, 491.
17. K. Miyabe and Y. Murata, *Anal. Sci.*, **2014**, *30*, 277.
18. S. Jespers, K. Broeckhoven, and G. Desmet, *LCGC Europe*, **2017**, *30*, 284.
19. A. A. Kurganov, A. Yu. Kanat'eva, E. E. Yakubenko, T. P. Popova, and V. E. Shiryaeva, *Russ. J. Phys. Chem. A*, **2017**, *91*, 182.
20. S. R. Groskreutz and S. G. Weber, *Anal. Chem.*, **2016**, *88*, 11742.
21. N. Lambert, S. Miyazaki, M. Ohira, N. Tanaka, and A. Felinger, *J. Chromatogr. A*, **2016**, *1473*, 99.
22. O. H. Ismail, M. Catani, L. Pasti, A. Cavazzini, A. Ciogli, C. Villani, D. Kotoni, F. Gasparrini, and D. S. Bell, *J. Chromatogr. A*, **2016**, *1454*, 86.

23. A. Kurganov, A. Kanateva, and E. Yakubenko, *J. Sep. Sci.*, **2016**, *39*, 162.
24. A. Andres, K. Broeckhoven, and G. Desmet, *Anal. Chim. Acta*, **2015**, *894*, 20.
25. S. Fekete, J.L. Veuthey, and D. Guillarme, *J. Chromatogr. A*, **2015**, *1408*, 1.
26. K. Miyabe, *Anal. Sci.*, **2009**, *25*, 219.
27. K. Miyabe, *Anal. Sci.*, **2011**, *27*, 1007.
28. G. Desmet, D. Clicq, and P. Gzil, *Anal. Chem.*, **2005**, *77*, 4058.
29. P. A. Bristow and J. H. Knox, Chromatographia, **1977**, *10*, 279.
30. H. Poppe, J. Chromatogr. A, **1997**, *778*, 3.
31. J J van Deemter, F. J. Zuiderweg, and A. Klinkenberg, *Chem. Eng. Sci*.,**1956**, 5, 271.
32. G. Desmet, D. Cabooter, and K. Broeckhoven, *Anal. Chem.*, **2015**, *87*, 8593.
33. Masahito Ito, J. Miura, Mitsuo Ito, F. Umesato, K. Yasuda, Y. Takata, B. Stanislawski, J. Chromatogr., **1994**, *661*, 143.

Chapter 2. Mathematical Study on HPLC Model and Three-Dimensional Graph

2-1 Introduction

There are several studies on speed and separation in HPLC.[1-5] In this chapter, given a chosen packing support, the methods can assess the performance of the packing support as the KPL at a given pressure drop (ΔP), where the KPL shows the maximal performance that can be achieved by the packing support under the specific conditions of the linear velocity (u_0) and the column length (L). However, the KPL conditions of u_0 and L are not always adopted as conditions of practical analytical methods. In this chapter, we first investigate the three-dimensional space of the number of theoretical plates (N), t_0, and ΔP by scanning the parameter of ΔP to show the curved surface generated by KPL in the space. Then we demonstrate a method to find practical conditions of u_0 and L by investigating the three-dimensional relationship among N, t_0, and ΔP. In addition $u_{0,\mathrm{opt}}$ enables the determination of optimal performance sets of t_0 ($t_{0,\mathrm{opt}}$) and N (N_{opt}), by calculating L and ΔP automatically; and the optimal performance is shown as a straight line through the original point in the three-dimensional space.

2-2 Theoretical

Fundamental principle of KPL

The KPL is related to a number of basic equations, as shown below.[6] t_0 is proportional to L, and u_0 comes from Eq. (2-1):

$$t_0 = \frac{L}{u_0} \quad . \qquad (2\text{-}1)$$

It can also be regarded as a definition of t_0 made from u_0 and L. The column efficiency, N, is also proportional to L, and $H(u_0)$ comes from Eq. (2-2):

$$N = \frac{L}{H(u_0)} \quad . \qquad (2\text{-}2)$$

$H(u_0)$ is a specific function of u_0, the so-called van Deemter curve. Equation (2-2) shows that N can also be regarded as an expression of $H(u_0)$, which is an essential property of separative performance. $N(u_0, L)$ is also a function of u_0 and L.

$H(u_0)$ may have a minimum value. Although $H(u_0)$ is originally an arbitrary function of u_0, Eq. (2-3) is empirically adopted as a fitting function of $H(u_0)$ to discuss the results in this thesis. Equation (2-3) shows the van Deemter equation, one of the most representative expressions:[7]

$$H(u_0) = A + B\frac{1}{u_0} + Cu_0 \quad , \qquad (2\text{-}3)$$

where A, B, and C are constants depending on the packing supports.

The KPL generates a t_0-N curve at a certain ΔP by scanning the operating parameter of u_0 through Eqs. (2-1) and (2-2). It does not require Eq. (2-3), but does need Eq. (2-4). It is an advantage for the KPL that the other operating parameter, L, can be determined automatically by Eq. (2-4):[8]

$$\Delta P = \frac{\eta u_0 L}{K_V} \quad , \qquad (2\text{-}4)$$

where η is the dynamic viscosity of the mobile phase. In pressure-driven chromatography, the mathematical product of u_0 and L is bonded, because ΔP is constricted. K_V is a kind of fitting constant experimentally. In this chapter, Eq. (2-4) is the most important equation that is a fundamental principle to generate the product of u_0 and L. It can be said that the pressure-driven chromatography obeying Eq. (2-4) is the scope of this chapter. On the other hand, Eq. (2-3) is a characteristic function to give the diversity of chromatographic separation. Equations (2-1) and (2-2) are positioned as secondary functions of u_0 and L to stretch the t_0-axis and N-axis of the three-dimensional graph. Especially Eq. (2-1) can uniquely determine u_0 and L respectively by using Eq. (2-4) simultaneously.

Each of the three performance parameters, t_0, N, and ΔP, is proportional to L, as shown in Eqs. (2-1), (2-2), and (2-4), respectively. In other words, the KPL converts the van Deemter H-u_0 curve to a t_0-N curve for each L, which is automatically determined as a limit based on the specific value of ΔP. The dependency of L is an important feature of pressure-driven chromatography.

Optimal velocity

In addition, assuming Eq. (2-3) holds, $u_{0,\mathrm{opt}}$ can be estimated to obtain the minimum of $H(u_0)$ ($H_{\min}$) and the optimal N (N_{opt}), by differential calculation of Eq. (2-3), using Eq. (2-5):

$$H_{\min} = H(u_{0,opt}) \qquad (u_{0,opt} = \sqrt{\frac{B}{C}}) \quad . \qquad (2\text{-}5)$$

$u_{0,\mathrm{opt}}$ is useful and convenient for traditional determination of the optimal conditions.

From five dimensions to three dimensions

The five essential variables of t_0, N, u_0, L, and ΔP should be utilized to study separation performance in detail. However, 5-dimensional space is extremely difficult to visualize. In considering the aspects of the five variables, u_0 and L are measurement condition inputs, t_0 and N are performance outputs obtained as results, and the last variable, ΔP, is a type of undesirable ramification factor that may reach a boundary condition $\Delta P_{\max}$.

A new mathematical variable, Π, may be introduced to simplify the following discussion. Given Eq. (2-4),

$$\Pi \equiv \frac{K_V \Delta P}{\eta} \quad . \qquad (2\text{-}6)$$

Π (m^2/s) is a kind of extensive parameter to normalize ΔP with K_V and η. Π may be seen as expressing both pressure-driven strength and velocity-length product, as seen in Eq. (2-7), given Eqs. (2-1) and (2-4):

$$\Pi = u_0 L = u_0^{\,2} t_0 \quad . \qquad (2\text{-}7)$$

When Π is given, any u_0 and any L can be chosen under the condition of the constant, $\Pi = u_0 L$. In other words, when a chosen u_0 and L are used, Π will be yielded automatically, which in turn means that ΔP can be calculated by Eq. (2-6). For rapid analysis, any large u_0 can be set under the upper-limit condition, while considering Π. Then an L is automatically determined by Π. For high-resolution performance, any large L can be set, along with u_0, while considering Π as well. Π can be equally applied to u_0 or L, because u_0 and L form a pair. In addition, Ohm's law is a good analogy to explain the structure of pressure-driven chromatography, with Π corresponding to the voltage, with current u_0 and electrical resistance L in Eq. (2-7). Π is a good index for demonstrating the kinetic strength of a given analytical method, including not only column permeability in the stationary phase, but also dynamic viscosity in the mobile phase, instead of the allowable pressure drop.

The aforementioned five dimensions can be reduced to three by introducing a third axis, of Π. Π can unify u_0, L, and ΔP in one dimension, because Π is the velocity-length product $u_0 L$, and proportional to ΔP. Π is thus effective in simplifying the mathematics of chromatographic theories. L can be expressed simply as the function L (u_0, t_0) by Eq. (2-1). u_0 might be considered more important than L, because $H(u_0)$ is essentially a function not of L but of u_0 by Eq. (2-3). However, L is still useful in discussing N because of its proportional properties. L can be regarded as a kind of extensive scaling factor, because N, Π, and t_0 are all proportional to L, by Eqs. (2-2), (2-7), and (2-1), respectively. This is partly why the respective variables have good correlations with each other. In the case of $u_{0,\mathrm{opt}}$, N becomes a straight line, based on the scaling factor L, in the three-dimensional space, because of the constant H (= $H_{\min}$) with $u_{0,\mathrm{opt}}$.

Introduction of impedance time

Inverted impedance time (t_E^{-1}) is introduced to provide a simpler three-dimensional representation, by Eq. (2-8):[6]

$$t_E^{\,-1} = \frac{N^2}{t_0} \quad . \qquad (2\text{-}8)$$

t_E^{-1} is proportional to Π in Eq. (2-9) through Eqs. (2-2), (2-7), and (2-8):

$$\frac{1}{t_E(u_0)} = \frac{u_0{}^2 t_0}{\{H(u_0)\}^2} = \frac{\Pi}{\{H(u_0)\}^2} \quad . \qquad (2\text{-}9)$$

It is clear that a three-dimensional representation with t_E^{-1} is characterized by $H(u_0)$. Π is expressed in Eq. (2-10) through Eqs. (2-8) and (2-9):

$$\Pi = \{H(u_0)\}^2 \frac{N^2}{t_0} \quad . \qquad (2\text{-}10)$$

On the other hand, plate time[9] (t_P) is a function of u_0 as Eq. (2-11) through Eqs. (2-1) and (2-2):

$$t_P = \frac{t_0}{N} = \frac{H(u_0)}{u_0} \quad . \qquad (2\text{-}11)$$

t_P has a feature not to be influenced by Π directly, when compared to t_E.

2-3 Experimental

Acetonitrile of HPLC grade was purchased from Wako Pure Chemicals as a mobile phase. The UHPLC system (Hitachi High-Technologies) consisted of an L-2160U Binary pump with high pressure gradient elution, L-2200U autosampler, L-2300 column oven, L-2400U UV detector, and CDS of EZChrom Elite™ for Hitachi. The columns, also manufactured by Hitachi High-Technologies, included a LaChromUltra C18 (2 μm) column (50 mm x 2 mm), LaChrom C18 (3 μm) column (100 mm x 4.6 mm), and LaChrom C18 (5 μm) column (150 mm x 4.6 mm). The packing supports consisted of fully porous octadecylsilyl silica gel. A monolithic column of octadecylsilyl silica (75 mm x 2.3 mm), a prototype manufactured by Hitachi High-Technologies, was used for comparison.

2-4 Results and discussion

Basic performance of packing supports

$H(u_0)$ can represent a major feature of chromatography in Fig. 2-1. $H(u_0)$ or N includes the extra column dispersion without specific calculations in this experiment. u_0 is simply calculated with L divided by the hold-up time of uracil as t_0 (Eq. (2-1)). For convenience, Eq. (2-3) is used as a fitting function of $H(u_0)$. The experimental parameters A, B, and C of the different supports are shown in Table 2-1. For simplicity, η is fixed as 0.001 Pa·s in this chapter. The K_V values of different supports are also shown as hydrodynamic constants in Table 2-1. K_V is also an experimental coefficient in Eq. (2-4) to demonstrate the three-dimensional representation.

Table 2-1 Experimental values for different packing supports [a]

Packings	A / 10^{-6} m	B / 10^{-9} m^2s^{-1}	C / 10^{-3} s	K_V / 10^{-12} m^2
2-µm particle	5.1	3.3	0.27	0.007
3-µm particle	4.5	4.7	1.3	0.011
5-µm particle	6.8	3.9	2.7	0.018
Monolith	3.4	4.1	0.52	0.025

a. The parameters A, B, and C were estimated by the method of least squares through Eq. (2-3) from Fig. 1. The column permeability K_V was determined using Eq. (2-4).

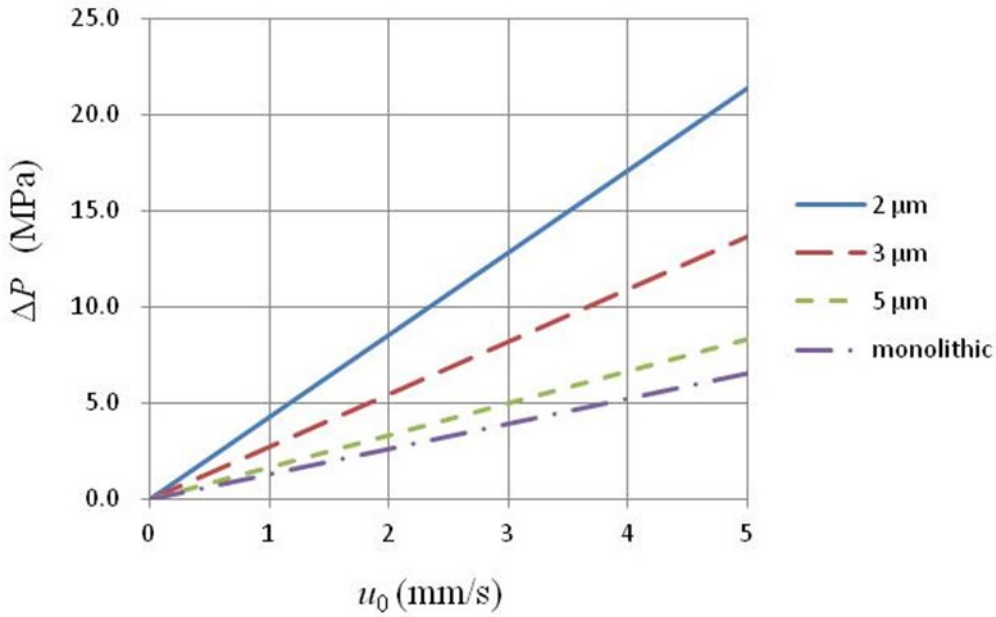

Fig. 2-1 Column permeability K_V of different packing supports.
K_V is determined from a slop of $\Delta P - u_0$ graph. Viscosity of the mobile phase: $\eta = 0.6\times10^{-3}$ Pa·s. Column length: L = 50 mm.

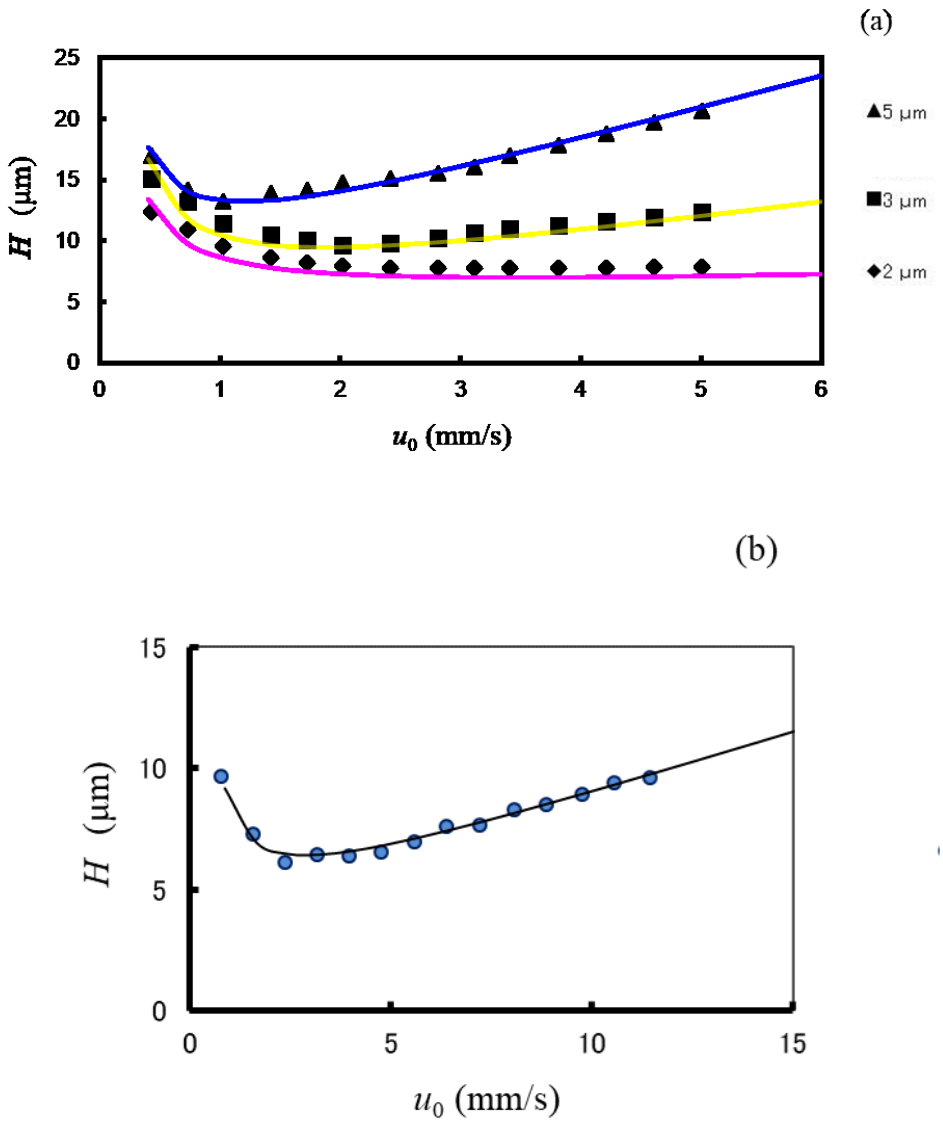

Fig. 2-2 van Deemter plots for (a) fully porous silica particles and (b) silica monolith.
The plots show typical supports (5-μm particle ▲, 3-μm particle ■, 2-μm particle ♦, and silica monolith○). The analyte was butyl benzoate for each support, and uracil was the sample measurement for the hold-up time for each support. The mobile phase consisted of 60% acetonitrile and 40% water (v/v). The column temperature was 40 °C. UV absorbance at 270 nm was used for detection. The column dimensions were 2.0 mm i. d. × 50 mm for the particle columns, and 2.3 mm o. d. × 75 mm for the monolithic column.

A precise method, based on the KPL, for determining column conditions

The KPL is expressed as a curved line on the t_0-N plain, at a specific ΔP. It indicates a performance limit of the packing support, which can be reached by the boundary condition of ΔP with specific u_0 and L. This offers a good method for assessing the packings. However, the KPL does not clearly illustrate the importance of pressure drop. And the actual conditions in the HPLC cannot be directly determined by the KPL. Three-dimensional representations of N, t_0, and ΔP or Π will be useful for finding an appropriate analytical method that includes the effect of pressure drop.[10] Figure 2-3 shows the curved surface of the KPL with 2-μm packings, in a three-dimensional representation. To generate the figure, first a basal plane was defined based on the input parameters of ΔP and t_0. Then, as a third axis, the u_0 of each point ΔP and t_0 was calculated using Eqs. (2-1) and (2-4). N was calculated using u_0 with Eqs. (2-1) and (2-2). Finally, N was built at each point of ΔP and t_0 on the basal plane, in the manner of a topographical map. Any N is available under the KPL surface, because the KPL is an upper limit on the basal plane, and u_0 and L should be adjustable for the N. Π is also shown, beside the ΔP-axis. Π is proportional to ΔP, and $\Pi = 350$ mm^2/s corresponds to $\Delta P = 50$ MPa, with a 2-μm particle and $\eta = 0.001$ Pa·s. $\Pi = 350$ mm^2/s may be achieved when $L = 50$ mm and $u_0 = 7$ mm/s, for instance.

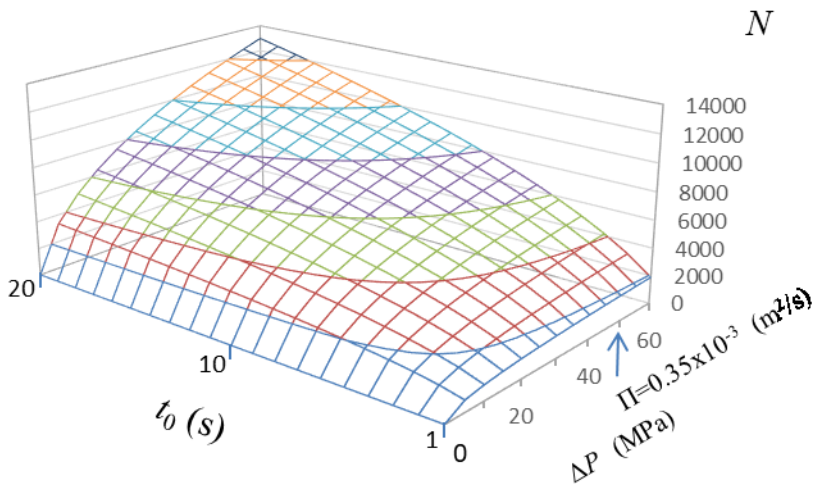

Fig. 2-3 Three-dimensional representation using plates, time, and pressure for a totally porous silica particle of 2-µm diameter.

To take an example, in the case of $t_0 = 5$ s, when ΔP increases 33% from 15 to 20 MPa, N increases 14% from 3,250 to 3,700. And when ΔP again increases 33% from 45 to 60 MPa, N increases 11% from 5,180 to 5,780. Therefore, pressure increase is not as effective for the plates at 60 MPa, as at 20 MPa. Alternatively, in the case of $N = 4{,}000$, when ΔP increases 33% from 15 to 20 MPa, t_0 decreases 23% from 7.5 s to 5.8 s. And when ΔP increases 33% from 45 to 60 MPa, t_0 decreases 14% from 3.3 s to 2.9 s. Here again, pressure increase is not as effective for speed-up at 60 MPa, as at 20 MPa.

Theoretical background

It may be seen that separation impedance[11] (E) is a good parameter to explain the performance of packings with K_V and H, by Eq. (2-12):

$$\{t_E(u_0)\}^{-1} = \frac{\Pi}{\{H(u_0)\}^2} = \frac{K_V}{\{H(u_0)\}^2}\frac{\Delta P}{\eta} = \frac{1}{E(u_0)}\frac{\Delta P}{\eta} \quad . \qquad (2\text{-}12)$$

Through Eqs. (2-8) and (2-12), we can see that N^2 is roughly proportional to both t_0 and ΔP, or Π. The slope of Fig. 2-4 can be determined to be roughly proportional to $\{E(u_0)\}^{-1}$. Therefore, the three-dimensional representation of $\{E(u_0)\}^{-1}$ on the basal plane is valuable (Fig. 2-5). A large $\{E(u_0)\}^{-1}$ is preferable, because $\{E(u_0)\}^{-1}$ is proportional to the slope in Fig. 2-4. There is a ridge line corresponding to $u_{0,\mathrm{opt}}$, which is determined uniquely on the (Π, t_0) and (ΔP, t_0) basal planes. The optimization of $u_{0,\mathrm{opt}}$ indicates only the neighbor of the ridge line in three dimensions. Although the ridge line is ideal for optimization, the large plateau of the KPL surface including the ridge line should be an acceptable domain of chromatographic conditions. It is undoubtedly necessary to avoid any dramatic cliff, such as the basal point (10 MPa, 5 s) in Fig. 2-5.

There is a straight line, $\{E(u_{0,\mathrm{opt}})\}^{-1}$, on the KPL surface of $\{E(u_0)\}^{-1}$, because $u_{0,\mathrm{opt}}$ gives a constant of $\{E(u_{0,\mathrm{opt}})\}^{-1}$ (= K_V/H_{min}^2). The maximum of E^{-1} is 1.4×10^{-4}, as the minimum of E is 7.0×10^3.

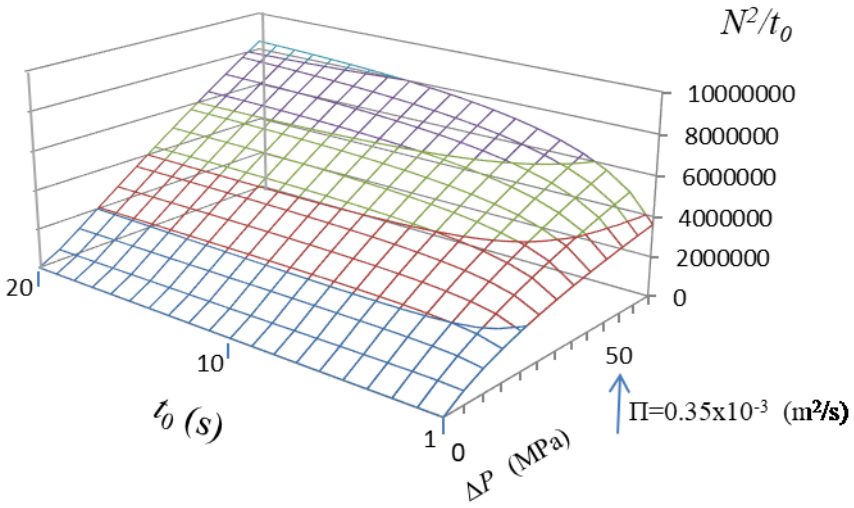

Fig. 2-4 Three-dimensional representation with inverted impedance time for a totally porous silica particle of 2-µm diameter.

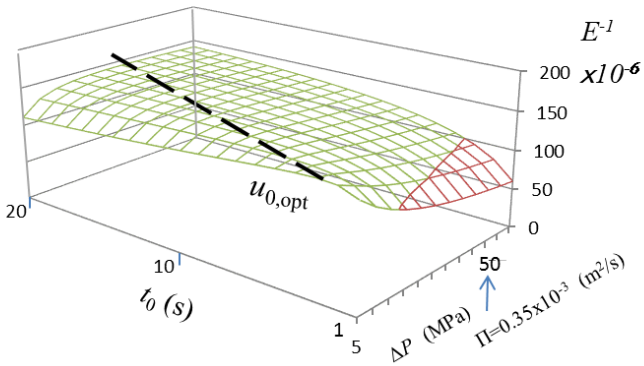

Fig. 2-5 Inverted separation impedance of 2-µm packings on the basal plane.

On different packing supports

Figure 2-6 shows three-dimensional graphs of a 3-µm particle, 5-µm particle, and monolithic column, respectively[12]. The specification of the column for maximum pressure is 20 MPa in each case. While *N* reached 13,000 plates at 60 MPa in the case of the 2-µm particle, it could reach 15,000 plates in the case of the 3-µm particle, even at 20 MPa. In the case of the 5-µm particle, a still higher *N*, of 30,000 plates or more, can be obtained, because t_0 offers another way to increase *N*, along with Π.[2]

The three-dimensional representation method is useful to show the effect of maximum pressure at a glance. For example, in the case of 2-µm particle, although *N* of 10,000 can be reached at the basal plane of 60 MPa and 13 s, *N* of 30,000 cannot be reached in Fig. 2-3. On the other hand, in the case of 5-µm particle, it is found that *N* of 30,000 can be reached at the basal plane of 20 MPa and 500 s in Fig. 2-6b. It is found that there are two contributions to reach a required number of theoretical plates. One is the maximum pressure. And the other is long retention time while considering usage of suitable packing supports.

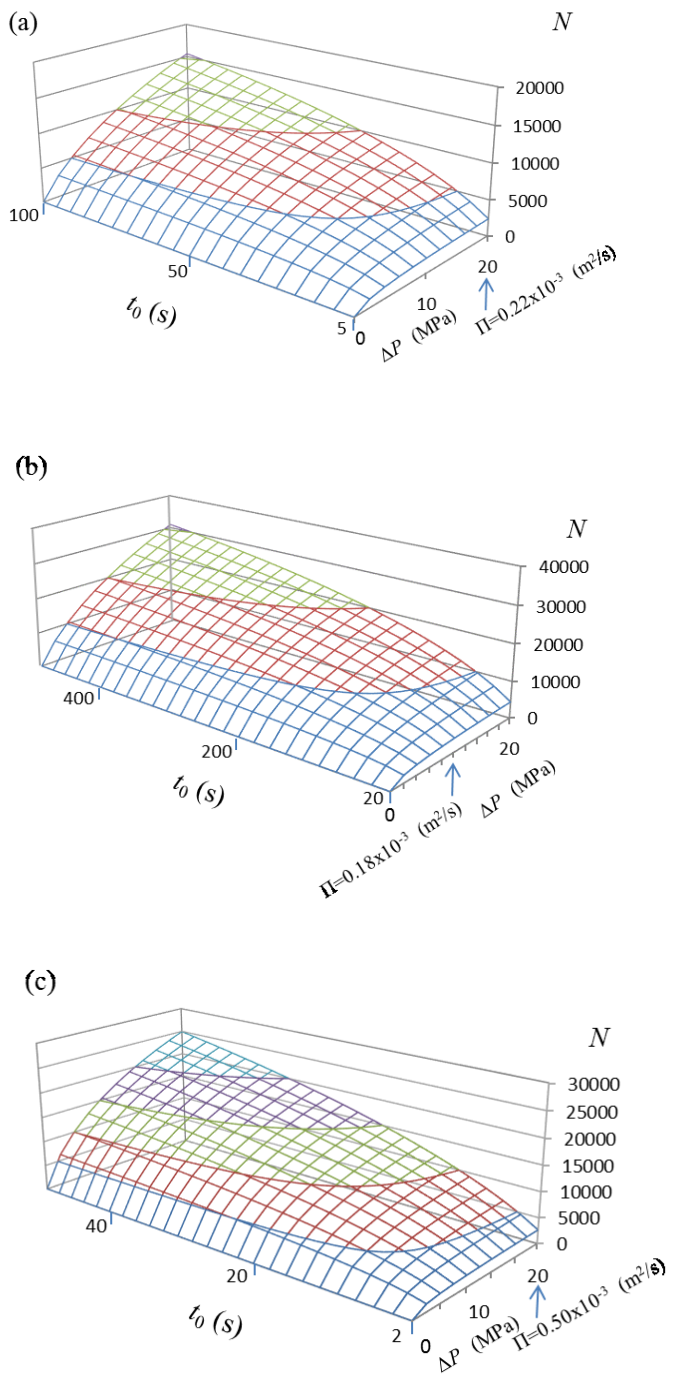

Fig. 2-6 KPL surfaces of (a) 3-μm packings, (b) 5 μm-packings, and (c) monolithic column.

Figure 2-7 shows the E^{-1} of each packing support. Each E^{-1}, including that of the monolithic column, has a large plateau near the $u_{0,opt}$ line, when compared with that of a 2-μm particle (Fig. 4); and the value of E^{-1} ($=K_V/H^2$) on each plateau is roughly the same, because the $u_{0,opt}$ line has a common H_{min} in each support. The maximums of E^{-1} for the 3-μm and 5-μm particles, and the monolith, are 1.2×10^{-4}, 1.1×10^{-4}, and 6.3×10^{-4} respectively. It is confirmed that the maximal E^{-1} for each particle diameter (d_P) is almost constant.[12] This means that K_V is inversely proportional to d_P^2, and H_{min} is proportional to d_P. It can be said that the E^{-1} of the monolithic column is significantly larger than that of the particle packing supports.

Regarding the performance of high resolution and high speed, although the optimal velocity has mainly been discussed so far, the concept of KPL was clarified recently. The KPL surface and the ridge line of optimal velocity on the surface can be shown simultaneously at one graph by expanding t_0-N plains to a three-dimensional graph with another axis of pressure or Π. In the three-dimensional representation method, to increase the number of theoretical plates, it can be determined which pressure or time to choose, because pressure and time are independent variables respectively.

A straight line emerging from $u_{0,opt}$ can be represented on the KPL surface in three dimensions, and $u_{0,opt}$ can appear as a ridge line or plateau by representing the vertical axis of E^{-1} on the basal plane. And furthermore, a three-dimensional graph of E^{-1} can be projected into that of N bi-directionally, because N corresponds one-to-one with E^{-1} on the basal plane of Π and t_0.

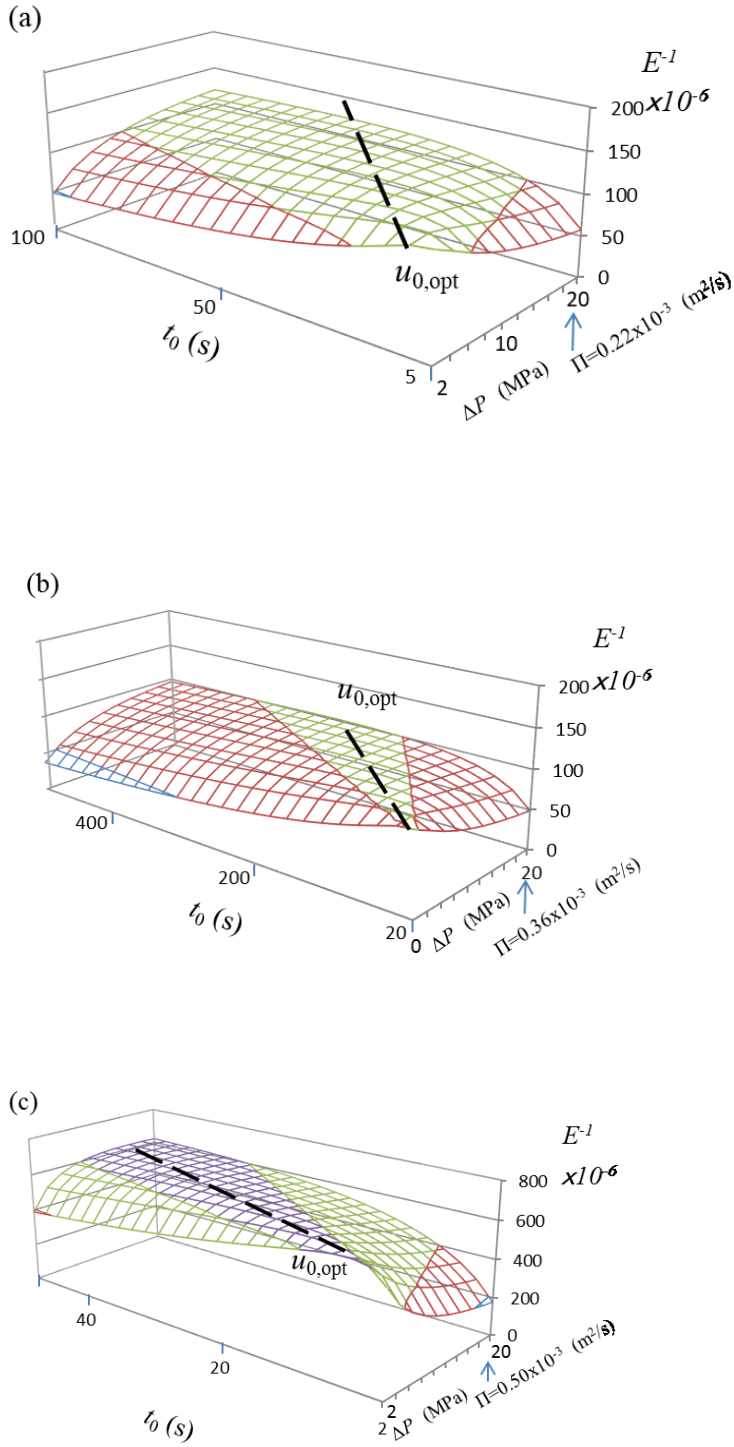

Fig. 2-7 Inverted separation impedance of (a) 3-μm packings, (b) 5-μm packings, and (c) monolithic column.

2-5 Summary

A valuable three-dimensional representation for assessing the effect of pressure in pressure-driven chromatography has been designed, using the axes of ΔP, t_0, and N, or the axes of Π, t_0, and N. In addition, a new index based on the velocity-length product Π has been defined, using K_V and η instead of ΔP; and has been shown to be useful for indicating strength in pressure-driven chromatography. A valuable method has been formulated by considering both ideal values of $u_{0,opt}$ and KPL values.

2-6 References

1. J.C. Giddings, Anal. Chem., **1965**, *37*, 60–63.
2. M. Martin, C. Eon, and G. Guiochon, J. Chromatogr., **1974**, *99*, 357.
3. U. D. Neue, J Chromatogr A, **2008**,*1184*, 107-130.
4. P. W. Carr, X. Wang, and D. R. Stoll, *Anal. Chem.*, **2009**, *81*, 5342.
5. A. J. Matula and P. W. Carr, *Anal. Chem.*, **2015**, *87*, 6578.
6. G. Desmet, D. Cabooter, and K. Broeckhoven, Anal. Chem., **2015**, *87*, 8593.
7. J J van Deemter, F. J. Zuiderweg, and A. Klinkenberg, *Chem. Eng. Sci*.,**1956**, 5, 271.
8. J. H. Knox and M. Saleem, J. Chromatogr. Sci., **1969**, *7*, 614.
9. H. Poppe, J. Chromatogr. A, **1997**, *778*, 3.
10. M. Ito and K. Shimizu, W.O. Patent Application, **2014**, 030537.
11. P. A. Bristow and J. H. Knox, Chromatographia, **1977**.
12. M. Ito, K. Shimizu, and K. Nakatani, *Anal. Sci.*, **2018**, *34*, 137-142.

Chapter 3. Mathematical Study on Three-Dimensional Graph, and New Coefficients on Two-Dimensional Curved Surface

3-1 Introduction

The relationship between speed and separation is studied again off the peripheral methodologies of KPL[1-7]. In Chapter 2. The number of theoretical plates (N) is obtained as a function of N (Π, t_0) with two independent variables of the velocity length product (Π) and the hold-up time (t_0). Π is a kind of strength variable in pressure-driven chromatography instead of the pressure drop (ΔP), and is proportional to ΔP. Π is necessary to understand the theory essentially, and is better than ΔP, because Π is not affected by either the column permeability (K_V) or the viscosity (η). The largest feature of Π is the product u_0 of and L. Weber et al. show a contour map [8] of N (u_0, L) with alternative variables of the linear velocity (u_0) and the column length (L), those correspond to separation conditions. And an axis transformation on nomogram is also referred[9].

Generally, HPLC operators search separation conditions by changing the flow rate after fixing L. u_0 is better than the flow rate to understand the theory essentially, because u_0 is not affected by either the internal diameter of the column or packing supports. Π and t_0 are obtained as the results after determining u_0 and L. The separation conditions are the cause of Π and t_0 as the performance. For example, the operators require to know the results of Π and t_0, and to see the overall relationship of N (Π, t_0). In other words, they have a concern about how large Π is related to how high speed, or how high separation. Three-dimensional graph[10, 11] of N (Π, t_0) is a good method to show the relationship. Although Π and t_0 can be directly discussed to evaluate the separation, the separation cannot quantitatively be judged only with u_0 and L. A logical process from N (u_0, L) to N (Π, t_0) is studied here.

3-2 Theoretical

3-2-1 Logarithmically rotational transformation

A new conversion method from N (u_0, L) to N (Π, t_0) has been formulated. Equations (3-1) and (3-2) can be written in logarithm from Eq. (2-1) and (2-7).

$$\log\Pi = \log u_0 L = \log u_0 + \log L \qquad (3\text{-}1)$$

$$\log t_0 = \log(\frac{L}{u_0}) = -\log u_0 + \log L \qquad (3\text{-}2)$$

Equations (3-1) and (3-2) can be represented into Eq. (3-3) in matrix notation, that is a kind of a rotation transformation.

$$\begin{pmatrix} \log\Pi \\ \log t_0 \end{pmatrix} = \begin{pmatrix} 1 & 1 \\ -1 & 1 \end{pmatrix} \begin{pmatrix} \log u_0 \\ \log L \end{pmatrix} = \sqrt{2} \begin{pmatrix} \cos 45° & \sin 45° \\ -\sin 45° & \cos 45° \end{pmatrix} \begin{pmatrix} \log u_0 \\ \log L \end{pmatrix} \qquad (3\text{-}3)$$

Equation (3-3) is called LRT (Logarithmically Rotational Transformation), and that means N (u_0, L) can be brought a coordinate conversion into N (Π, t_0). LRT correspondence is a one-to-one mapping from the basal plain (u_0, L) to the basal plain (Π, t_0). The inverse conversion is also available. Exactly describing, LRT is a bijective linear transformation of rotation with logarithmic elements, multiplying by the square root of 2.

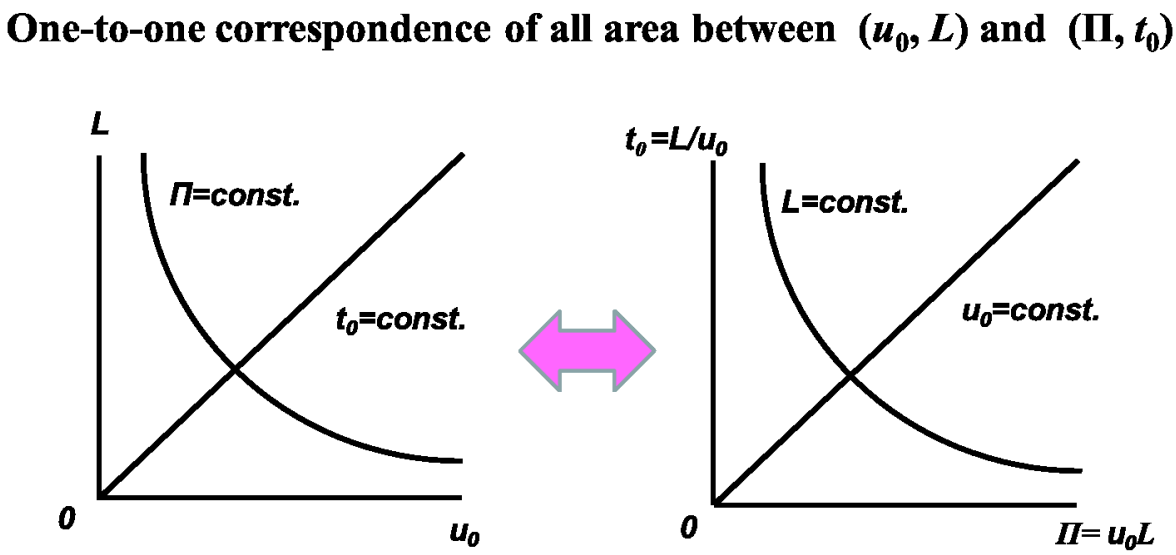

Fig. 3-1 One-to-one mapping from the basal plain (u_0, L) to (Π, t_0)

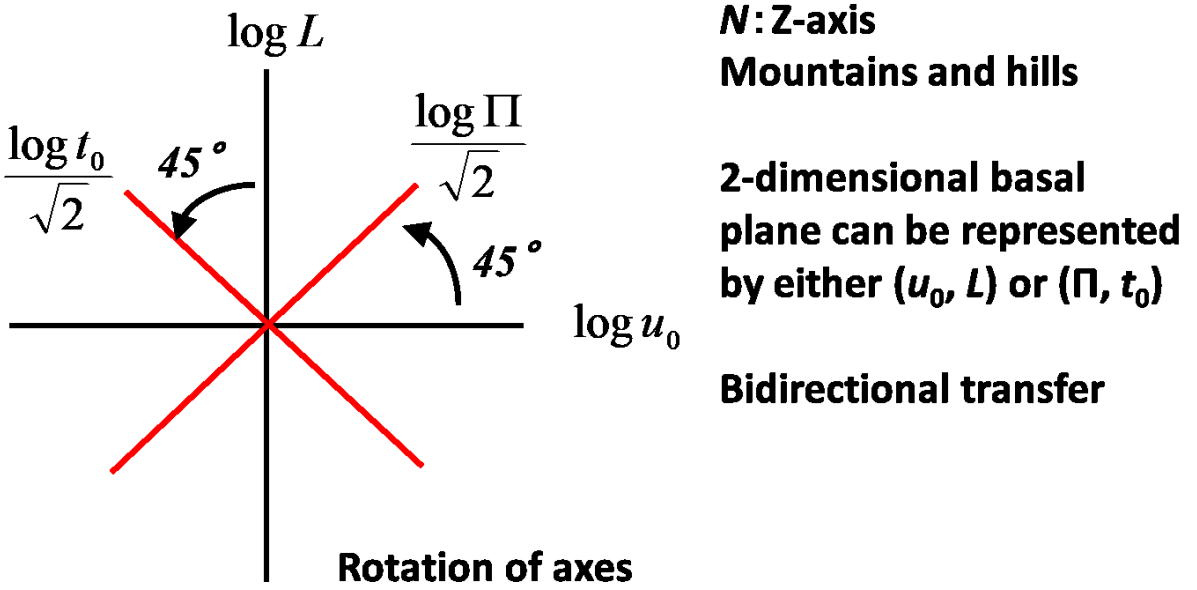

Fig. 3-2 Schematic diagram of LRT (Logarithmically Rotational Transformation)

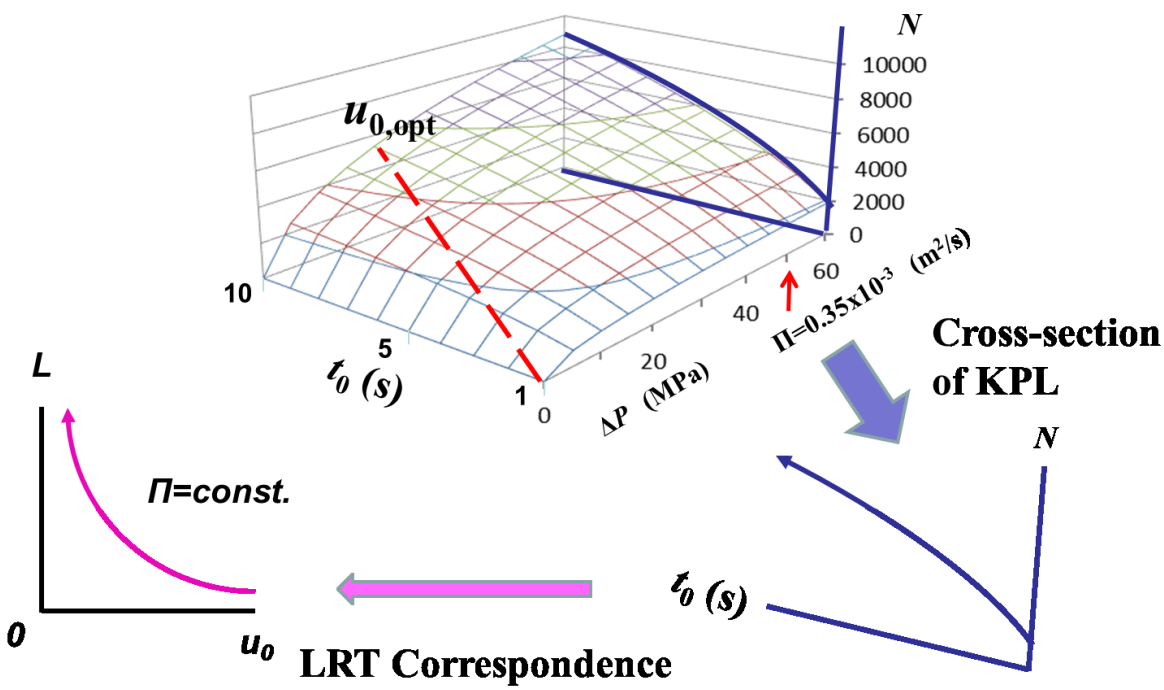

Fig. 3-3 Schematic cross-section of KPL and LRT correspondence

The representative contents of N (u_0, L) can be regarded as equivalent to those of N (Π, t_0), and there are only different axes. The representation of logarithm is a good way to understand the correspondence at a glance. The relationship of mathematical product and quotient between u_0 and L can join that of sum and difference between them through logarithm. Five-dimensional space of F (u_0, L, Π, t_0, N) to be treated in Chapter 2 can divide into three-dimensional partial space of T_1 (u_0, L, N) or T_2 (Π, t_0, N) respectively. And the partial space can easily transfer into each other through LRT correspondence.

In HPLC, T_1 (u_0, L, N) equals N (u_0, L) by changing variables u_0 and L under a condition of arbitrary packings, while fixing mobile phase, analytes, and column temperature, etc. T_2 (Π, t_0, N) is a destination to be transferred from the basal plane (u_0, L) to the coordinate (Π, t_0). In other words, two-degree-of-freedom system of u_0 and L succeeds one of Π and t_0 comprehensively. For example, if there is a column realistically, L is fixed and u_0 is variable. When operating u_0, not only t_0 but also Π changes simultaneously. Then it is found that a set of u_0 and L corresponds closely to a set of Π and t_0. And it is understandable that the correspondence is a bidirectional method to transfer from the result representation of T_2 to the casual representation of T_1, or the inverse to trace back. LRT correspondence can easily offer the basal plane of Π and t_0 as results not to be predicted only with u_0 and L by HPLC operators.

3-2-2 Pressure-application coefficients

When recognizing the function of N (Π, t_0) in the graph as two-dimensional curved surface in three-dimensional space of T_2 (Π, t_0, N), the partial differential coefficient can become an evaluating indicator. Simply, the slope of N per Π at fixed t_0 is the partial derivative of $c_{N/\Pi}$ (Eq. 3-4), that is a function with physical dimension to be specified in all basal plane of Π and t_0.

$$c_{N/\Pi}(\Pi, t_0) \equiv \left(\frac{\partial N}{\partial \Pi}\right)_{t_0} \qquad (3\text{-}4)$$

Equation (2-10) coming from impedance time is a combination of N, Π, and t_0 with $H(u_0)$. Therefore, there is a relationship of Eq. (3-5) at u_0=$u_{0,\mathrm{opt}}$, because $H_{\min}$=$H(u_{0,\mathrm{opt}})$.

$$\Pi = H_{\min}{}^2 N^2 t_0{}^{-1} \qquad (3\text{-}5)$$

Only if u_0=$u_{0,\mathrm{opt}}$, Eq. (3-6) can be derived from Eq. (3-5) with factor 2.

$$\left(\frac{\partial \Pi}{\partial N}\right)_{t_0} = 2\frac{\Pi}{N} = \frac{1}{c_{N/\Pi}} \qquad (3\text{-}6)$$

Furthermore, Eq. (3-7) comes from Eq. (3-6) only at $u_{0,\mathrm{opt}}$. However, any Π or any t_0 cannot be chosen on all the basal plane.

$$2c_{N/\Pi}(\Pi, t_0) = \frac{N(\Pi, t_0)}{\Pi} \qquad (3\text{-}7)$$

To expand the variable region of both Π and t_0 to all the basal plane, $\mu_{N/\Pi}$ is introduced as a formula similar to Eq. (3-7) (Eq. (3-8)).

$$2c_{N/\Pi}(\Pi, t_0) = \mu_{N/\Pi}(\Pi, t_0)\frac{N(\Pi, t_0)}{\Pi} \qquad (3\text{-}8)$$

$\mu_{N/\Pi}$ is defined in Eq. (3-9) with dimensionless by normalization of 1 at $u_{0,\mathrm{opt}}$, that is called PAC (Pressure-Application Coefficients) for N. $\mu_{N/\Pi}$ is a kind of adjusting factor to keep the formula of Eq. (3-7).

$$\mu_{N/\Pi} \equiv 2\frac{\Pi}{N}\left(\frac{\partial N}{\partial \Pi}\right)_{t_0} \qquad (3\text{-}9)$$

$\mu_{t/\Pi}$ is also PAC for t_0 to be defined as Eq. (3-10) as well, that is dimensionless and normalized at $u_{0,\mathrm{opt}}$.

$$\mu_{t/\Pi} \equiv -\frac{\Pi}{t_0}\left(\frac{\partial t}{\partial \Pi}\right)_{N} \qquad (3\text{-}10)$$

$\mu_{N/t}$ is also defined as TEC (Time-Extension Coefficient) as Eq. (3-11) as well.

$$\mu_{N/t} \equiv 2\frac{t_0}{N}\left(\frac{\partial N}{\partial t_0}\right)_{\Pi} \qquad (3\text{-}11)$$

The function N can be represented as a differential equation (Eq. (3-12)).

$$\begin{aligned} dN &= \left(\frac{\partial N}{\partial \Pi}\right)_{t_0} d\Pi + \left(\frac{\partial N}{\partial t_0}\right)_{\Pi} dt_0 \\ &= \frac{1}{2}\mu_{N/\Pi}\frac{N}{\Pi}d\Pi + \frac{1}{2}\mu_{N/t}\frac{N}{t_0}dt_0 \end{aligned} \qquad (3\text{-}12)$$

Equation (3-13) comes from Eq. (3-12).

$$2\frac{dN}{N} = \mu_{N/\Pi}\frac{d\Pi}{\Pi} + \mu_{N/t}\frac{dt_0}{t_0} \qquad (3\text{-}13)$$

Differential equation of $d\Pi$ is also shown as Eq. (3-14), by treating two-dimensional surface of Π (N, t_0) instead of N (Π, t_0).

$$\begin{aligned} d\Pi &= \left(\frac{\partial \Pi}{\partial N}\right)_{t_0} dN + \left(\frac{\partial \Pi}{\partial t_0}\right)_N dt_0 \\ &= \frac{2}{\mu_{N/\Pi}} \frac{\Pi}{N} dN + \frac{-1}{\mu_{t/\Pi}} \frac{\Pi}{t_0} dt_0 \end{aligned} \tag{3-14}$$

Equation (3-15) can come from Eq. (3-14) like Eq. (3-13).

$$2\frac{dN}{N} = \mu_{N/\Pi} \frac{d\Pi}{\Pi} + \frac{\mu_{N/\Pi}}{\mu_{t/\Pi}} \frac{dt_0}{t_0} \tag{3-15}$$

By comparing the coefficients of Eq. (3-13) and (3-15), Eq. (3-16) can be obtained.

$$\mu_{N/t}(\Pi, t_0) = \frac{\mu_{N/\Pi}(\Pi, t_0)}{\mu_{t/\Pi}(\Pi, t_0)} \tag{3-16}$$

Explicit expression of PAC

In the case of the van Deemter equation (Eq. (2-3)), explicit solutions of both coefficients can be obtained. First, from Eq. (3-10), $\mu_{t/\Pi}$ can be mathematically derived from Eq. (3-17):

$$\left(\frac{\partial t_0}{\partial \Pi}\right)_N = \left(\frac{\partial t_0}{\partial u_0}\right)_N \left(\frac{\partial u_0}{\partial \Pi}\right)_N \tag{3-17}$$

$$\begin{aligned} \left(\frac{\partial t_0}{\partial u_0}\right)_N &= N\left(\frac{\partial\{H(u_0)/u_0\}}{\partial u_0}\right)_N \\ &= -N\left(Au_0^{-2} + 2Bu_0^{-3}\right) \end{aligned} , \tag{3-18}$$

where, through Eqs. (2-1) and (2-2),

$$t_0 = \frac{NH(u_0)}{u_0} , \tag{3-19}$$

and through Eq. (2-3),

$$\begin{aligned} \left(\frac{\partial \Pi}{\partial u_0}\right)_N &= N\left(\frac{\partial\{u_0 H(u_0)\}}{\partial u_0}\right)_N \\ &= N\left(A + 2Cu_0\right) \end{aligned} , \tag{3-20}$$

where, through Eqs. (2-2) and (2-7),

$$\Pi = Nu_0 H(u_0) . \tag{3-21}$$

Then Eq. (3-17) can be expressed as Eq. (3-22), when Eq. (3-18) is divided by Eq. (3-20):

$$\left(\frac{\partial t_0}{\partial \Pi}\right)_N = \left(\frac{\partial t_0}{\partial u_0}\right)_N \Big/ \left(\frac{\partial \Pi}{\partial u_0}\right)_N = -\frac{Au_0 + 2B}{Au_0^3 + 2Cu_0^4} \quad , \qquad (3\text{-}22)$$

where, through Eq. (2-7),

$$u_0 = \sqrt{\frac{\Pi}{t_0}} \quad . \qquad (3\text{-}23)$$

Then $\mu_{t/\Pi}$ can be obtained on the basal plane (Π, t_0) using u_0 with Eqs. (2-13), (3-22) and (3-23):

$$\mu_{t/\Pi} = \frac{-\Pi}{t_0}\left(\frac{\partial t_0}{\partial \Pi}\right)_N = \frac{\Pi}{t_0}\left(\frac{Au_0 + 2B}{Au_0^3 + 2Cu_0^4}\right) = \frac{Au_0 + 2B}{Au_0 + 2Cu_0^2} \quad . \qquad (3\text{-}24)$$

$\mu_{t/\Pi}$ is found a function of u_0, $\mu_{t/\Pi}$ (u_0). And $\mu_{t/\Pi}$ becomes 1, given Eq. (3-24) at the optimal velocity $u_{0,\mathrm{opt}}$ with Eq. (2-5):

$$\mu_{t/\Pi} = \frac{Au_{0,opt} + 2B}{Au_{0,opt} + 2C\left(\frac{B}{C}\right)} = 1 \quad . \qquad (3\text{-}25)$$

On the other hand, to obtain an explicit solution of $\mu_{N/\Pi}$, plate time[12] $t_P = N/t_0$ can temporarily be used to generate a function with only the variable u_0 (Eq. (3-27)):

$$\left(\frac{\partial N}{\partial \Pi}\right)_{t_0} = \left(\frac{\partial N}{\partial u_0}\right)_{t_0} \Big/ \left(\frac{\partial \Pi}{\partial u_0}\right)_{t_0} \qquad (3\text{-}26)$$

$$t_P = \frac{t_0}{N} = \frac{H(u_0)}{u_0} \quad . \qquad (3\text{-}27)$$

Equation (3-27) is differentiated partially through Eqs. (2-1), (2-2), and (2-3), using u_0 (Eq. (3-28)):

$$t_0\left(\frac{\partial N^{-1}}{\partial u_0}\right)_{t_0} = \left(\frac{\partial (H(u_0)/u_0)}{\partial u_0}\right)_{t_0} = \left(-Au_0^{-2} - 2Bu_0^{-3}\right) \quad . \qquad (3\text{-}28)$$

Equation (3-29) can be given through Eq. (3-20) from Eq. (3-28):

$$t_0\left(\frac{\partial N^{-1}}{\partial \Pi}\right)_{t_0} = t_0\left(\frac{\partial N^{-1}}{\partial u_0}\right)_{t_0} / \left(\frac{\partial \Pi}{\partial u_0}\right)_{t_0} = \frac{1}{t_0}\left(-\frac{1}{2}Au_0^{-3} - Bu_0^{-4}\right) \quad , \qquad (3\text{-}29)$$

where, from Eq. (2-7),

$$\left(\frac{\partial \Pi}{\partial u_0}\right)_{t_0} = 2u_0 t_0 \quad . \qquad (3\text{-}30)$$

Equation (3-31) comes mathematically from Eq. (3-29):

$$t_0\left(\frac{\partial N}{\partial \Pi}\right)_{t_0} = -t_0 N^2\left(\frac{\partial N^{-1}}{\partial \Pi}\right)_{t_0} = \frac{N^2}{2t_0}\left(Au_0^{-3} + 2Bu_0^{-4}\right) \quad , \qquad (3\text{-}31)$$

where, through Eqs. (2-1) and (2-2),

$$N = \frac{u_0 t_0}{H(u_0)} = \frac{\Pi}{u_0 H(u_0)} \quad . \qquad (3\text{-}32)$$

In this way, $\mu_{N/\Pi}$ can also be obtained on the basal plane (Π, t_0), using u_0 with Eqs. (2-12), (3-23), and (3-31):

$$\mu_{N/\Pi} = 2\left(\frac{\partial N}{\partial \Pi}\right)_{t_0}\frac{\Pi}{N} = \frac{\Pi}{t_0}\left(\frac{Au_0 + 2B}{Au_0^3 + Bu_0^2 + Cu_0^4}\right) = \frac{Au_0 + 2B}{Au_0 + B + Cu_0^2} \quad . \qquad (3\text{-}33)$$

$\mu_{N/\Pi}$ is also a function of u_0, $\mu_{N/\Pi}$ (u_0). $\mu_{N/\Pi}$ becomes 1 as well as $\mu_{t/\Pi}$, given Eq. (3-33) at the optimal velocity $u_{0,opt}$ with Eq. (2-5):

$$\mu_{N/\Pi} = \frac{Au_{0,opt} + 2B}{Au_{0,opt} + B + C\left(\frac{B}{C}\right)} = 1 \quad . \qquad (3\text{-}34)$$

On the region of the KPL surface with $\mu_{N/\Pi}$ of 1 or more, ΔP_{max} should be adopted to obtain larger N with the same t_0, On the other hand, on that of KPL surface with μ_N of 1 or less, ΔP_{max} should be adopted carefully while considering $\mu_{N/\Pi}$ well. In some cases, exceeding pressure should be eliminated. In the case of the pressure-application coefficient of t_0, $\mu_{t/\Pi}$ should be discussed at the same height of N as well.

3-3 Results and discussion

Figure 3-4 shows the explicit values of $\mu_{N/\Pi}$ and $\mu_{t/\Pi}$ for 2-μm packings. There is a line of 1 for $\mu_{N/\Pi}$ and $\mu_{t/\Pi}$ respectively, which is obtained at $u_{0,opt}$. It is clear that there is little difference between $\mu_{N/\Pi}$ and $\mu_{t/\Pi}$. The distribution of $\mu_{t/\Pi}$ is more significant than that of $\mu_{N/\Pi}$. In the case of $\mu_{t/\Pi}$, the adjustment of u_0 may be mainly a way to make the distribution. On the other hand, in the case of $\mu_{N/\Pi}$, there may be two ways to adjust u_0 and L. That may be the reason why there is the difference of the distributions. $\mu_{t/\Pi}$ at 20 MPa and at 6 s is obtained as 0.84, and $\mu_{t/\Pi}$ at 60 MPa and at 3 s is 0.49. It is confirmed that those are almost the same as the values to be calculated by the power index formula from integration. Then N is almost 4,000 on the basal plane, because N is uniquely determined on the KPL surface. In the case of 2 μm particle, both $\mu_{N/\Pi}$ and $\mu_{t/\Pi}$ are 0.5 or less around ΔP = 50 MPa and t_0 = 2 s, because the region of the basal plane is so far from $u_{0,opt}$, and is not so effective for increasing N or decreasing t_0 even by increasing ΔP. On the other hand, on the basal plane around ΔP = 10 MPa and t_0 = 20 s, both $\mu_{N/\Pi}$ and $\mu_{t/\Pi}$ are 1.0 or more, because u_0 can get close to $u_{0,opt}$ by increasing ΔP, and H comes close to H_{min}, that is the optimal value. Furthermore, in the case of $\mu_{t/\Pi}$, it is needed to shorten L for fixing the N, because of smaller H. Then t_0 can become much smaller dually by increasing u_0 and shortening L. It is interesting that $\mu_{t/\Pi}$ is larger than $\mu_{N/\Pi}$ by the dual effect when u_0 is smaller than $u_{0,opt}$. After all, it should be recommended to let u_0 comes close to $u_{0,opt}$ on the KPL surface even at the same ΔP, when u_0 is smaller than $u_{0,opt}$. Or on the region where $\mu_{N/\Pi}$ is 1 or more, ΔP should automatically be shifted to ΔP_{max} on the KPL surface, because larger N at the same t_0 is preferable. And on the region where $\mu_{t/\Pi}$ is 1 or more, ΔP should also be shifted to ΔP_{max} on KPL surface, because smaller t_0 at the same height of N is preferable. And if the other region described below is entered before reaching ΔP_{max}, the following procedure of the other region should be obeyed. When u_0 is larger than $u_{0,opt}$, a way to increase ΔP might be a significant option to obtain the required N or t_0, while investigating coefficients of $\mu_{N/\Pi}$ or $\mu_{t/\Pi}$. Or on the region where $\mu_{N/\Pi}$ or $\mu_{t/\Pi}$ is less than 1, although ΔP_{max} of the column might be the first choice, the t_0 on the KPL surface at the ΔP_{max} should be adopted carefully while considering $\mu_{N/\Pi}$ or $\mu_{t/\Pi}$ well. It is also available to choose the straight line of $u_{0,opt}$, or to stay the neighborhood, because an exceeding pressure drop might not be so effective.

Regarding the performance of high resolution and high speed, although the optimal velocity has mainly been discussed so far, the concept of KPL was clarified recently. The KPL surface and the ridge line of optimal velocity on the surface can be shown simultaneously at one graph by expanding t_0-N plains to a three-dimensional graph with another axis of pressure or Π. In three-dimensional representation method, to increase the number of theoretical plates, it can be determined which pressure or time to choose, because pressure and time are independent variables respectively. In addition, from this method, pressure application coefficients of $\mu_{N/\Pi}$ and $\mu_{t/\Pi}$ have been proposed to understand quantitatively the difference of response by applying pressure between the neighborhood of the ridge line and the far part from the line on the KPL surface. Although it is difficult to distinguish separation conditions with bad coefficients by the original idea of KPL, the condition with exceeding pressure can be eliminated by using $\mu_{N/\Pi}$ and $\mu_{t/\Pi}$.

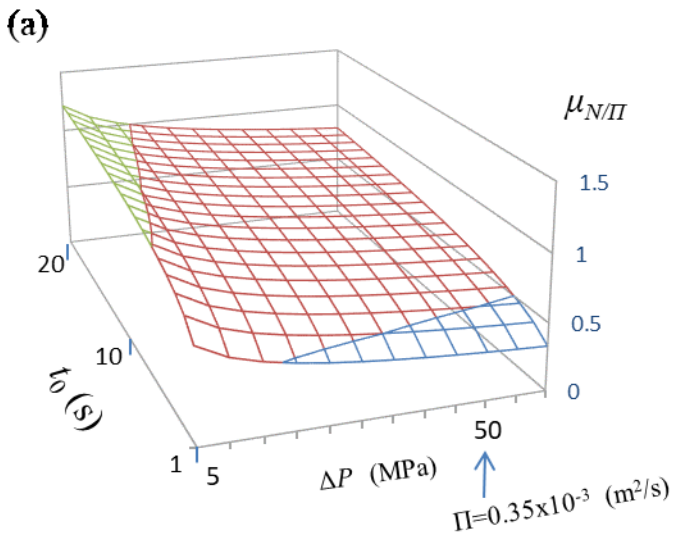

Fig.3-4a Pressure-application coefficients for *N* of 2-μm packings.

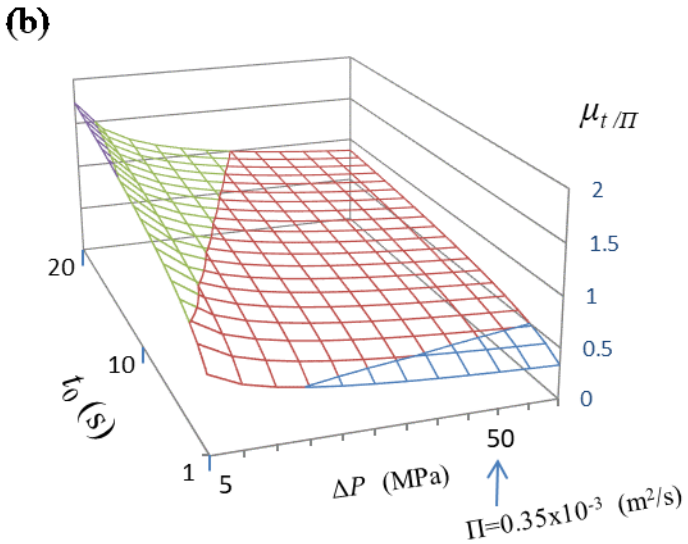

Fig.3-4b Pressure-application coefficients for t_0 of 2-μm packings.

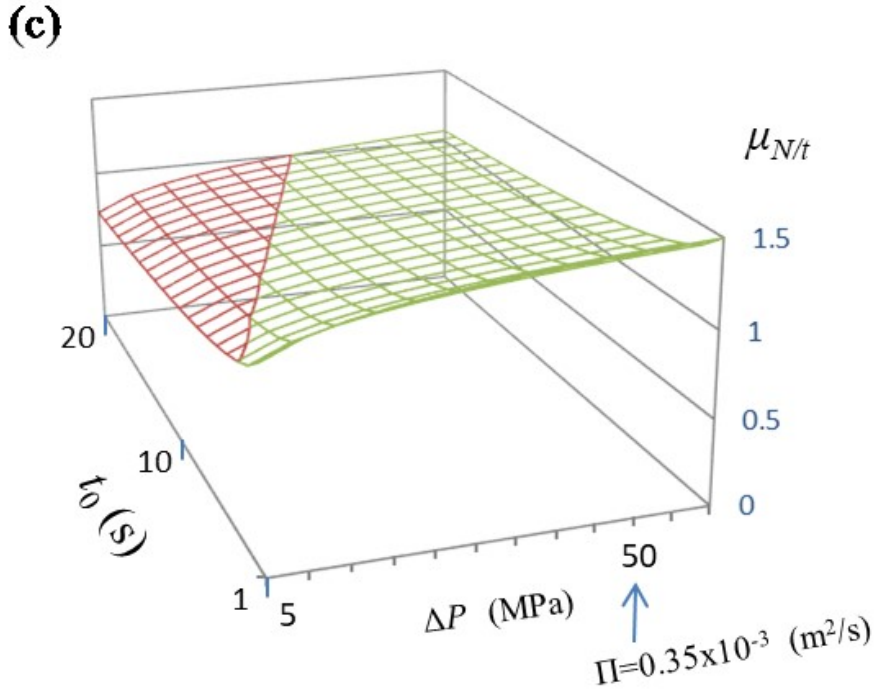

Fig.3-4c TEC of 2-μm packings

Separation conditions to be analyzed by using PAC's or TEC

Figure 3-5 shows $u_{0,opt}$ of the packing supports on the basal plane. The 5-μm particle can reach the largest Π. Although the separation performance such as H (u_0) is not shown in Fig. 3-5, the large Π is a necessary condition to reach as large N as 30,000 with the 5-μm particle. However, it needs to take as long t_0 as 500 s.

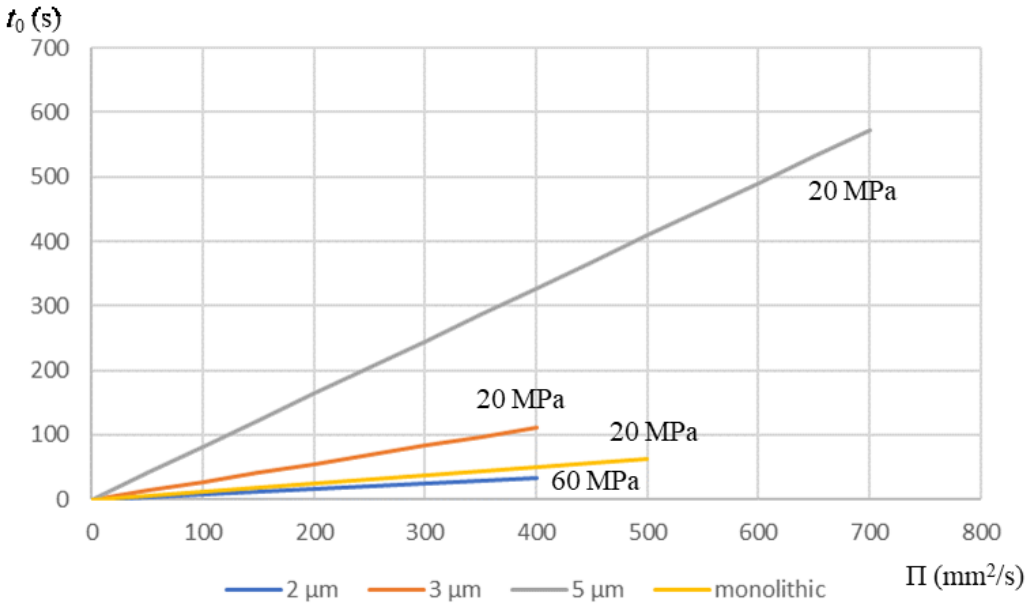

Fig. 3-5 Trajectory of optimal velocity of different packing supports.

Figure 3-6 is the contour map of N (Π, t_0) with the $u_{0,opt}$ line of the 2-μm particle. There are two regions. One is higher Π region than the $u_{0,opt}$ line. The other is lower Π region than the $u_{0,opt}$ line. Generally, the first choice is an application of the $u_{0,opt}$ line or the neighborhood. In this case, the largest N can be obtained with the given L because of H_{min}. Both t_0 and Π are uniquely calculated by using $u_{0,opt}$ and L. If N = 5,000 is requested, the horizontal curve of N = 5,000 should be watched firstly. Then the intersection point between the curve and the $u_{0,opt}$ line should be searched. The point is the solution to the request of N = 5,000, that is the basal plane (17.5 MPa, 10 s). The ΔP of 17.5 MPa equals Π of 0.12 x 10^{-3} m^2/s.

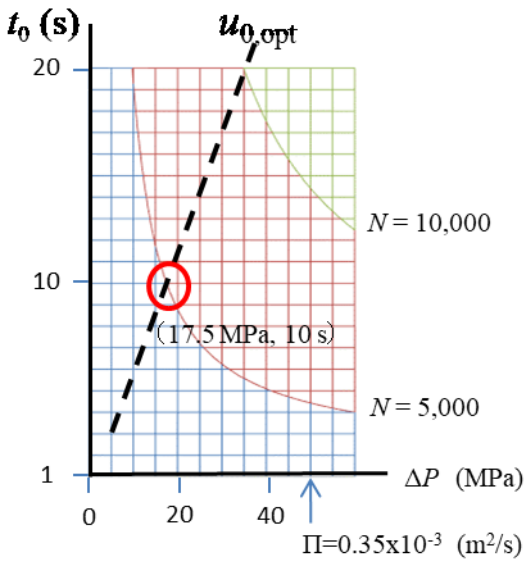

Fig. 3-6 Trajectory of optimal velocity of different packing supports

Figure 3-7 shows a countermeasure to the pressure limit of 20 MPa for example. Under 20 MPa, the horizontal curve can be chosen as the separation condition. If larger N is requested at the limit of 20 MPa, the arrow of upper direction must be chosen. To keep the limit, u_0 must be decreased along with increasing L, such as the example of glycated hemoglobin Hb A1c in Fig. 1-2.

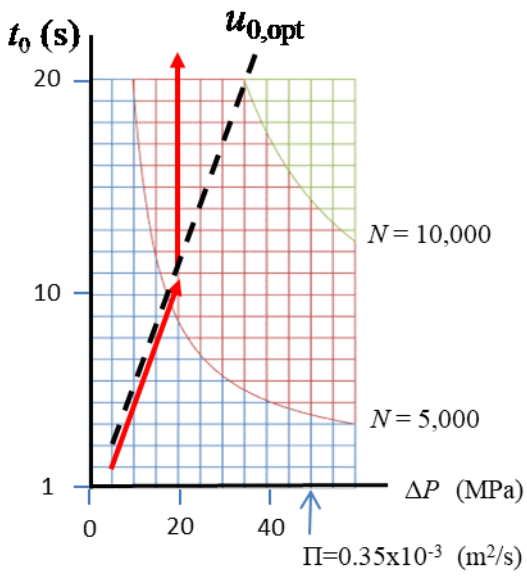

Fig. 3-7 Encounter of the pressure limit

For precise discussion, firstly the higher Π region than the $u_{0,opt}$ line is treated. Figure 3-5 shows three optimizing approaches corresponding to two PAC's and a TEC. An approach on $\mu_{N/\Pi}$ of PAC for N is a method to increase N by increasing Π at the constant t_0. By moving to the right from the $u_{0,opt}$ line in the contour map, N can be increased like climbing the hill. Then L must be increased to increase N, and u_0 must be increased to keep t_0. Simultaneously, $\mu_{N/\Pi}$ (Π, t_0) goes from 1.0 at the line to a value lower than 1.0 (Fig. 3-4a). L is applied not so efficiently ($u_0 > u_{0,opt}$), because H (u_0) gets slightly worse than H_{min}. $\mu_{N/\Pi}$ (Π, t_0) is an index to quantitatively show the slope of the hill as 1.0 to be normalized at the $u_{0,opt}$ line. For example, method developers can consider whether $\mu_{N/\Pi}$ of 0.8 is acceptable or not to increase N at a certain pressure such as 50 MPa.

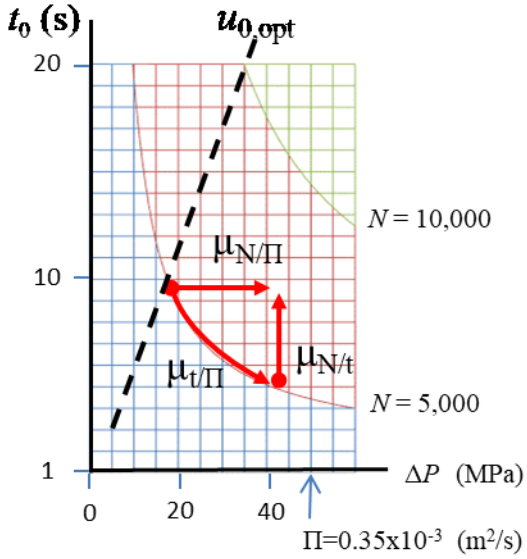

Fig. 3-8 Higher Π region than the $u_{0,opt}$ line

Next approach on $\mu_{t/\Pi}$ of PAC for t_0 is a method to decrease t_0 by increasing Π at the constant N. By moving along the horizontal curve of a certain N such as 5,000 in the contour map, t_0 can be decreased like moving laterally on the level line of a constant height. Then u_0 must be increased ($u_0 > u_{0,opt}$) to decrease t_0, and L must be increased slightly to keep N. Simultaneously, $\mu_{t/\Pi}$ (Π, t_0) goes from 1.0 at the $u_{0,opt}$ line to a value lower than 1.0 (Fig. 3-1b). L is changed not so drastically, because it is not necessary to increase N. To keep N, L is elongated a little to compensate the difference between H (u_0) and H_{min}.

The last approach on $\mu_{N/t}$ of TEC is a method to increase N by increasing t_0 at the constant Π. By moving to the upper in the contour map (Fig. 3-8), N can be increased like climbing along the straight line of a certain constant Π such as 40 MPa. Then L must be elongated to increase N, and u_0 must be decreased to keep Π. The separate condition compensates the difference between the first approach on $\mu_{N/\Pi}$ and the second approach on $\mu_{t/\Pi}$. The condition pulls L up from the goal of $\mu_{t/\Pi}$ to the goal of $\mu_{N/\Pi}$. And $\mu_{N/t}$ equals $\mu_{N/\Pi}$ divided by $\mu_{t/\Pi}$ (Eq. 3-16).

In the lower Π region than the $u_{0,opt}$ line, Figure 3-6 also shows three optimizing approaches corresponding to a TEC and two PAC's. An approach on $\mu_{N/t}$ of TEC is a method to increase N by increasing t_0 at the constant Π. By moving to the upper in the contour map (Fig. 3-9), N can be increased like climbing along the straight line of a certain constant Π such as 10 MPa. The approach is often applied, because larger N is needed under some limited pressure. Simultaneously, $\mu_{N/t}$ (Π, t_0) goes from 1.0 at the $u_{0,opt}$ line to a value lower than 1.0 (Fig. 3-4c). It means the time extension for N in the lower Π region is not so efficient as that on the $u_{0,opt}$ line.

On the other hand, $\mu_{t/\Pi}$ is larger than 1.0 in the lower Π region (Fig. 3-4a). In the region, the pressure application has a potential to increase N more than the $u_{0,opt}$ line. In the case of $\mu_{t/\Pi}$, the pressure application has also a potential to speed up more than that near the $u_{0,opt}$ line. The basal plane (Π, t_0) can easily transfer to the basal plane (u_0, L) by LRT correspondence. In other words, in the lower Π region,

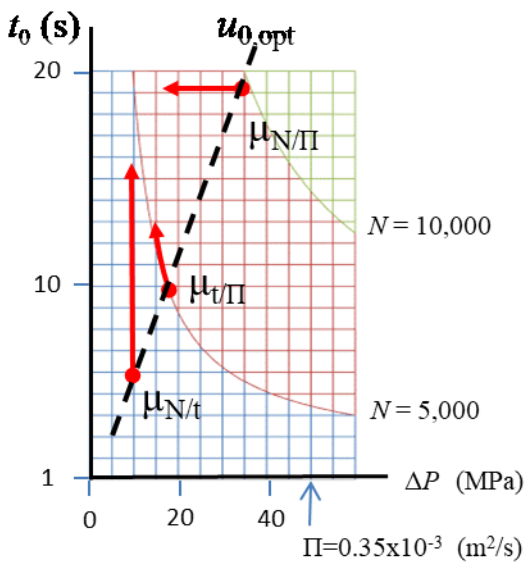

Fig. 3-9 Lower Π region than the $u_{0,opt}$ line

For example, in the case of u_0 = 6 mm/s and L = 50 mm, Π gets 0.3 x 10^{-3} m^2/s and t_0 becomes 8 s by LRT correspondence. The separation condition is plotted in the contour map, and three types of coefficients are shown (Fig. 3-10). The plot is located in the lower Π region. Therefore, N becomes larger by increasing Π than that on the $u_{0,opt}$ line, because of $\mu_{N/\Pi}$ = 0.84. t_0 gets shorter than that on the $u_{0,opt}$ line, because of $\mu_{t/\Pi}$ = 0.72. On the other hand, if time is extended, there is a potential to gain N because of $\mu_{N/t}$ = 1.16.

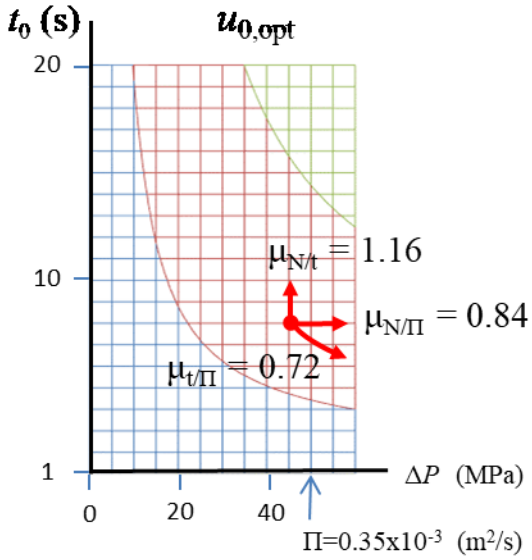

Fig. 3-10 PAC's and TEC of an example

3-4 Summary

LRT correspondence is found out to explain a relationship between the separation variables (u_0, L) and the performance variables (Π, t_0). And Three-dimensional graph of N (Π, t_0) can be derived from N (u_0, L) by using the LRT. Starting from N (u_0, L), the three-dimensional graph of N (Π, t_0) is obtain, then a plain of t_0 and N can be found as a KPL cross-section in the graph N (Π, t_0).

Furthermore, PAC (Pressure-Application Coefficient) and TEC (Time-Extension Coefficient) are defined on the basis of partial differential to evaluate effectiveness of pressure or time quantitatively. Actually, PAC has two types. One is $\mu_{N/\Pi}$ of PAC for N, and the other is $\mu_{t/\Pi}$ of PAC for t_0. The function of N (Π, t_0) can be represented as a differential equation with PAC's or $\mu_{N/t}$ of TEC. Finally, there is a relationship among $\mu_{N/\Pi}$, $\mu_{t/\Pi}$, and $\mu_{N/t}$.

3-5 References

1. G. Desmet, D. Clicq, and P. Gzil, Anal. Chem., **2005**, *77*, 4058-4070.
2. Deirdre Cabooter, Wim Decrop, Sebastiaan Eeltink, Remco Swart, Mario Ursem, François Lestremau, and Gert Desmet, Anal. Chem., **2010**, *82*, 1054–1065.
3. Sebastiaan Eeltink, Sebastiaan Dolman, Gabriel Vivo-Truyols, Peter Schoenmakers, Remco Swart, Mario Ursem, and Gert Desmet, Anal. Chem., **2010**, *82*, 7015–7020.
4. Bert Wouters, Cees Bruggink, Gert Desmet, Yury Agroskin, Christopher A. Pohl, and Sebastiaan Eeltink, Anal. Chem., **2012**, *84*, 7212–7217.
5. Eva Tyteca, Anuschka Liekens, David Clicq, Ameriga Fanigliulo, Benjamin Debrus, Serge Rudaz, Davy Guillarme, and Gert Desmet, Anal. Chem., **2012**, *84*, 7823–7830.
6. Gert Desmet and Sebastiaan Eeltink, Anal. Chem., **2013**, *85*, 543–556.
7. Leonid M. Blumberg and Gert Desmet, Anal. Chem., **2016,** *88*, 2281–2288.
8. S. R. Groskreutz and S. G. Weber, Anal. Chem., **2016**, *88*, 11742-11749.
9. I. Halász, G. Görlitz, *Angew. Chem*., **1982**, *94*, 50–62.
10. M. Ito, K. Shimizu, W.O. Patent Application, **2014**, 030537.
11. M. Ito, K. Shimizu, and K. Nakatani, *Anal. Sci.*, **2018**, *34*, 137-142.
12. H. Poppe, J. Chromatogr. A, **1997**, *778*, 3.

Chapter 4. Applicational Experiments Using Velocity near Optimal Velocity

4-1 Introduction

4-1-1 Optimal velocity

If there is a column realistically, L is fixed. Operators can only change the alternative parameter of u_0 in this thesis. For example, they have possibility to maximize N. Therefore, they can set $u_{0,opt}$ to obtain H_{min}. In one sentence, Operation using u_0 near $u_{0,opt}$ can offer the approximate maximum of N under the restrictive condition of fixed L, because H_{min} can be obtained. This chapter treats the results by u_0 near $u_{0,opt}$. However, if the maximal N under the fixed L can be ignored, the freedom of two-dimensional surface can be realized. And either t_0 or N can be obtained independently by Π, then both u_0 and L can uniquely be calculated by LRT correspondence (cf. Chapter 5).

When using 2-μm packings with column of 2-mm internal diameter, the optimal flow rate corresponding to $u_{0,opt}$ is 0.2 to 0.3 ml/min. Ginsenosides in ginseng products were analyzed with the column at the flow rate. Π and t_0 are passively determined. In the separation condition, PAC and TEC should be approximately 1.0.

4-1-2 Ginsenosides

Ginseng, a medical herb, has long been used to maintain physical vitality throughout far-Eastern countries, including Korea, China and Japan. Carl Anton Meyer, a Russian botanist, named it Panax ginseng in 1843, and the genus name Panax means "cure all" in Greek.[1] The major components of ginseng are carbohydrates such as starch, polysaccharides and cellulose (60–70%).[2–4] However, it also contains various compounds unique to ginseng, such as ginsenosides, polyacetylenes, antioxidative aromatic compounds and gomisins (gomisin-N, -A), which protect the liver[5–7], and acidic peptides that behave similar to insulin.[8–11] Ginseng saponins, which are known to be some of the major effective compounds in ginseng, are called ginsenosides. Compared to saponins found in other plants, those found in ginseng exhibit significantly different chemical structures and also induce different effects. Through modern analytical technology, chemical structures of 30 ginseng saponins have been identified in ginseng thus far. Based on their chemical structures, ginseng saponins have been classified into three groups: protopanaxadiol (PPD), protopanaxatriol (PPT) and oleanane.[1,4]

A few studies on the analysis of ginsenosides in ginseng have been reported. Soxhlet extraction, ultrasonic extraction, base hydrolysis, refluxing extraction and shaking extraction methods have been used to extract ginsenosides from ginseng with aqueous methanol/ethanol solutions as the extracting solvent[12–17]. Solid-phase extraction has been used to remove interferences. In general, high-performance liquid

chromatography (HPLC) has typically been used to separate and determine the concentrations of ginsenosides. Ultraviolet (UV), refractive index (RI) and evaporative light scattering (ELS) detection methods have been commonly used for the detection of ginsenosides.[18–25] Recently, ultra-HPLC (UHPLC) coupled with mass spectrometry (MS) has been adopted in many areas of food and biological analyses because it is rapid and provides excellent separation. UHPLC is known to be economical and environmentally friendly due to its extremely rapid analysis. Because of its fast analysis, the consumption of solvent for the mobile phase can be reduced 5- to 10-fold compared with conventional HPLC.[26–29]

This study attempted to establish a simple and effective method for the determination of the concentration of ginsenosides in ginseng and ginseng products using UHPLC coupled with a heating-block method. For the rapid analyses, sample preparation and separation were the two important aspects that were considered. To develop a rapid method of sample preparation, the ability of sample preparation methods to remove interferences was evaluated. The evaluated methods included refluxing extraction, solid-phase extraction (SPE), Soxhlet extraction and heating-block extraction. For the effective separation by chromatography, a short-length or middle-length column was used to reduce the total running time.

4-1-3 Vitamins A and E

Vitamin A is needed by the retina of the eye in the form of a specific metabolite, the light-absorbing molecule retinal, which is absolutely necessary for both scotopic and color vision. Vitamin A also functions in a very different role, as an irreversibly oxidized form of retinol known as retinoic acid, which is an important hormone-like growth factor for epithelial and other cells. Vitamin E is a generic term for tocopherols and tocotrienols. Vitamin E consists of a family of α-, β-, γ-, and δ-tocopherol and four corresponding tocotrienols. Vitamin E is a fat-soluble antioxidant that stops the production of the reactive oxygen species that are formed when fat undergoes oxidation. Of these, α-tocopherol has been studied the most as it has the highest bioavailability.[30] The difference between natural and synthetic vitamin E is their chemical structures. Natural vitamin E contains one isomer, RRR-x03B1 tocopherol, which has eight different forms: x03B1, x03B2, x03B3, and x03B4 tocopherols; and x03B1, x03B2, x03B3, and x03B4 tocotrienols. Many different tocopherol and tocotrienol derivatives have been synthesized, but these are most commonly based on racemic x03B1-tocopherol, which contains equimolar amounts of eight stereoisomers, with only one being identical to the natural RRR isomer. Synthetic vitamin E contains equimolar amounts of eight stereoisomers, of which one is identical to the natural RRR isomer.[31]

There have been many reports that vitamins A and E have a wide variety of functions that affect human health. For example, Shenai et al.[32], Pearson et al.[33], and Bental et al.[34] reported that vitamin A deficiency may contribute to the development of chronic lung disease or bronchopulmonary dysplasia (BPD) in very-low-birth-weight infants. Inconsistent results have been reported in four relatively small

randomized clinical trials in which the effect of vitamin A on the prevention of BPD was assessed. Vitamin E and γ-tocopherol, in particular, have antioxidant properties believed to be associated with the development of atherogenesis, coronary heart disease, and cancer.[35-37] As for all fat-soluble substances, the presence of lipids is essential for vitamin E absorption.[38]

Many analytical methods used to detect vitamins A and E have been studied to date. The most common method for the identification and quantification of vitamins A and E used an HPLC system combined with a UV or photodiode array detector. An LC method with a switching valve system was reported for the simultaneous determination of vitamins A, E, and D in human serum.[39] In clinical chemistry, some research has been completed to determine the vitamin E content in biological samples such as human plasma using GC combined with a flame ionization detector.[40] Other efforts used GC with a mass spectrometer to detect α- and δ-tocopherol in kiwi fruits.[41]

Recently, UHPLC coupled with a UV detector and a mass spectrometer has been adopted in many instances of food and biological analysis due to its rapid analysis and excellent separations.[42,43] Because UHPLC uses higher pressure and a shorter column than conventional HPLC (c-HPLC), peak dispersion is minimized, and the method provides improved speed, resolution, and sensitivity. Thus, it is well known that UHPLC delivers faster analysis, higher resolution, and increased sensitivity without decreasing the quality of separations. Moreover, the UHPLC method is economical and environmentally friendly due to the extremely rapid analysis. In addition to the fast analysis, the consumption of solvents for mobile phases can be reduced up to 5- to 10-fold compared with the c-HPLC method. Therefore, our study focused on the development and validation of a rapid analytical method for the determination of vitamins A and E in foods using UHPLC.[44] Furthermore, the KOH hydrolysis methods are studied with comparisons.[45-47]

4-1-4 β-Carotene

β-Carotene is an organic compound - a terpenoid, a red-orange pigment abundant in plants and fruits. Isolation of β-carotene from fruits abundant in carotenoids is commonly done using column chromatography. The separation of β-carotene from the mixture of carotenoids is based on the polarity of a compound. β-Carotene is a non-polar compound, so it is separated with a non-polar solvent such as hexane. Being highly conjugated, it is deeply colored, and as a hydrocarbon lacking functional groups, it is very lipophilic.[48]

There have been many reports that β-carotene has the wide variety of function on the human health.[49] For examples, Jialai et al.[50] and Sies et al.[51] reported that β-carotene, in addition to be an efficient quencher of singlet oxygen, can also function as a radical-trapping antioxidant. Numerous observational studies have found that major public health benefits could be achieved by increasing consumption of carotenoids-rich fruits and vegetables still appear to stand; however, the pharmacological use of

supplemental β-carotene for the prevention of cardiovascular diseases and lung cancer, particularly in smokers, can no longer be recommended.[52] Therefore, the demand of exact determination of β-carotene amount in foods is increased due to its two faces of the effect on the human health.[53,54]

A lot of the analytical methods of β-carotene have been studied to date. The most common method for identification and quantification of β-carotene has employed the HPLC system combined with an ultra violet (UV) detector. An isocratic liquid chromatographic method was reported for the simultaneous determination of vitamin C, E, and β-carotene in human plasma.[55] Especially, in the clinical chemistry, several researches have been made to determine the β-carotene in biological samples, such as human serum and tissues using liquid chromatography combined with reversed phase column and UV detection.[56,57] Others employed the normal phase HPLC in a silica gel column with n-hexane-2-propanol as the mobile phase.[58]

Dietz et al.[59] reported the reversed phase HPLC analysis of β-carotene from raw and cooked vegetable. Weissenberg et al.[60] also reported that a simple and rapid HPLC method had been devised in order to separate and quantify β-carotene present in red pepper fruits and food preparation using HPLC. A reversed-phase isocratic non-aqueous system enables the separation of β-carotene within a few minutes, with detection at 450 nm. Quantitative analysis of carotenoids and carotenoid esters in fruits by HPLC was introduced and analyzed without saponification using octadecylsilyl silica as stationary and methanol-ethyl acetate as mobile phase.[61] Recently UHPLC method coupled with mass spectrometry has been adopted in many areas of food and biological analysis due to its rapid analysis and remarkably excellent separation.[62,63] Because UHPLC has adopted the higher pressure, shorter column than conventional HPLC, minimizing peak dispersion providing improved speed, resolution, and sensitivity, it is well known that UHPLC delivers fast analysis, higher resolution, and increased sensitivity without losing separation quality. Moreover, UHPLC method has been known to be economical and environmentally friendly due to extremely rapid analysis. In concomitant with the fast analysis, the consumption of solvent for mobile phase can be reduced up to 5 to 10 fold, comparing with the conventional HPLC method. Therefore, our study was focused to evaluate the rapid analytical method for the determination of β-carotene in foods, using UHPLC.

4-2 Experimental

4-2-1 Ginsenosides

Apparatus

The UHPLC system consisted of a LaChromUltra L-2000U Series apparatus (Hitachi-High Technologies, Japan), which included the following: a mobile phase reservoir, an HPLC pump (L-2160U), an autosampler system (L-2200U) with a fixed injection volume of 5 mL, and an ultraviolet detector (L-

2400U) set to detect at 203 nm. Two different columns were used to analyze ginsenosides: a LaChromUltra C18 short-length column (2 mm i. d. x 50 mm L, 2 mm; Hitachi-High Technologies) and a LaChromUltra C18 middle-length column (2 mm i. d. x 100 mm L, 2 mm; Hitachi-High Technologies).

The gradient was prepared by mixing 20% acetonitrile (solvent A) and 80% acetonitrile (solvent B). The gradient profile for the separation of the ginsenosides by UHPLC was 100% A–0% B (0 min), which was maintained for 10 min. The gradient profile was subsequently changed linearly to 25% B in 30 min, 70% B in 10 min, 100% B in 30 min and returned to 0% B in 5 min, which was then maintained for 5 min. The flow rate in the UHPLC was 0.2 mL/min for the short-length column and 0.3 mL/min for the middle-length column. The temperature of the analytical column was maintained at 30˚C.

Reagents

The ginsenosides Rg1, Re, Rf, Rh1(S), Rg2(S), Rg2(R), Rh1(R), Rb1, Rc, F1, Rb2, Rb3, Rd, F2, Rg3(S), Rg3(R), PPT(S), PPT(R), compound K, Rh2(S), Rh2(R) and PPD (Felton Natural Products, Chengdu, P.R. China) were used. The purity of all reference standards was higher than 98%, except PPT(R), which was 90.5%. Stock standard methanolic solutions of ginsenosides at concentrations of 800–1,000 mg/L were prepared. These solutions were stored in glass bottles at 4˚C. Working ginsenoside mixtures were prepared by dilution of the stock standard solutions with methanol, depending on the sensitivity of the UV detector to each ginsenoside. Ninety-five percent ethanol (ACS reagent grade), acetonitrile (chromatographic grade) and acetic acid (ACS reagent grade) were used. All solvents were of chromatographic or HPLC grade, and other reagents were ACS reagent grade. The water was purified with a Milli-Q system (Millipore, Bedford, MA).

Test samples

Raw ginseng root, dried ginseng, ginseng tablet and red ginseng extract samples were purchased from a retail store in Seongnam City, Gyeonggi Province, Republic of Korea. On receipt, samples were stored at below 4˚C in an airtight container before analysis. The samples were mixed thoroughly to create a homogeneous mixture.

Sample preparation

Raw ginseng root samples were washed with tap water to remove impurities on the surface of the ginseng roots and then dried to remove the moisture from their surface. The roots were then chopped into small pieces. One hundred grams of the chopped roots were ground in a grinder (Super Grinder, JL-1000, Hibell, Korea) for the analysis. Dried ginseng samples and ginseng tablets were ground in a grinder (Super Grinder, JL-1000) to pass a 40-mesh screen. A portion of the red ginseng extract sample was taken without any pretreatment.

Extraction of ginsenosides from the samples

Refluxing extraction

One gram of ground ginseng powder was placed into a 250 mL Erlenmeyer flask and 70 mL of 50% aqueous methanol was added. The mixture was refluxed for 1 h at 80˚C. The extraction was repeated two additional times, and the combined extracts were concentrated in vacuo at a temperature less than 60˚C. The residue was dissolved in 25 mL of 20% aqueous acetonitrile solution, filtered through a 0.20 mm PTFE membrane (SRP 15, Sartorius, Japan), and analyzed.

Solid phase extraction

One gram of ginseng powder was placed into a 250 mL Erlenmeyer flask and 70 mL of 50% aqueous methanol was added. The mixture was refluxed for 1 h at 80˚C. The extraction was repeated two additional times, and the combined extracts were concentrated in vacuo at a temperature less than 60˚C. The residue was dissolved in 25 mL of 20% aqueous acetonitrile solution and filtered through a 0.20-mm PTFE membrane (SRP 15, Sartorius). The solution (0.5 mL) was loaded onto a preconditioned SPE Sep-Pak Vac C18 cartridge (12 cc, 2 g; Waters, Iceland). The cartridge was placed in a 10 mL syringe, cleaned with 5 mL of methanol and then preconditioned with 20 mL of water. The sample solution was applied to the SPE cartridge, which was subsequently washed with 20 mL of water and then washed with 15 mL of 30% methanol. The ginsenosides were then slowly eluted using 5 mL of methanol. The eluted solution was filtered through a 0.20 mm PTFE membrane (SRP 15, Sartorius), and subjected to UHPLC analysis.

Soxhlet extraction

A total of 1.0 g of ginseng powder was placed in a thimble for Soxhlet extraction and extracted at 90˚C for 16 h with 100 mL of 100% methanol. When the extraction was completed, the mixture was allowed to stand and cool to room temperature. The extract was concentrated in vacuo at 60˚C, then dissolved in 20 mL of 50% aqueous acetonitrile, filtered through a 0.20 mm PTFE membrane (SRP 15, Sartorius), and subjected to UHPLC analysis.

Heating-block extraction

A portion of ginseng powder and ginseng products (100–500 mg) were dissolved with 10 mL of 50% aqueous methanol in a 20 mL vial. The ginsenosides were then extracted at 80˚C for a given period of time (10, 20 or 30 min) on a heating block. The extract was gently decanted into a 25 mL volumetric flask. The extraction process was performed a second time. All of the extracts were combined in the 25 mL volumetric flask, and 50% aqueous methanol was added to bring the flask to its final volume. The extracts were filtered through a 0.20 mm syringe filter into a sample vial for UHPLC injection.

Calibration graphs

Calibration graphs for UHPLC were based on the peak areas obtained after injection of 5 mL of ginsenoside solutions at four concentration levels, depending on the UV sensitivity in the range of 2.6–40.4 mg/kg. The solutions were prepared through the dilution of ginsenoside stock solutions with 100% methanol, depending on the concentration of the standardized ginsenoside stock solutions.

Statistical analysis

The recovery experiments were performed at intra-day (n = 12) and inter-day (n = 3) intervals, and the results were expressed as the mean ± standard deviation (SD). Comparisons of extraction efficiency of ginsenosides in ginseng powder were analyzed as a one-way analysis of variance (ANOVA). The program used for statistical calculations was SPSS 13.0 for Windows (Lead Tools, Lead Technologies, Charlotte, NC).

4-2-2 Vitamins A and E

Apparatus

(a) *UHPLC system.*—LaChromUltra L-2000U Series apparatus (Hitachi-High Technologies Corp., Tokyo, Japan), including the following: an eluent reservoir; Model L-2200U UHPLC pump; Model L-2200U autosampler; and EZChrom Elite software for Hitachi (Version 3.1.8b).

(b) *UHPLC analytical column.*—LaChromUltra C18 (particle size 2 μm, 2 mm id, 50 mm length; Hitachi-High Technologies Corp.).

(c) *UHPLC analytical detector*.—L-2485U fluorescence detector (Hitachi-High Technologies Corp.), excitation wavelength 340 nm and emission wavelength 460 nm for vitamin A, and excitation wavelength 298 nm and emission wavelength 325 nm for vitamin E. Flow cell capacity is 3 μL.

(d) *UHPLC mobile phase.*—Distilled water–methanol solution (5 + 95, v/v) as solvent A and pure methanol as solvent B.

(e) *Flow rate.*—0.3 mL/min.

(f) *Heating block.*—TECHE DB-3D, Barloworld Scientific Ltd, Staffordshire, UK.

Reagents

(a) *Retinol (>95%, C20H30O, MW 286.45, CAS No. 68- 26-8); retinol acetate (99.3%, C22H32O2, MW 328.5, CAS No. 127-47-9); retinol palmitate (94.7%, C36H60O2, MW 524.9, CAS No. 79-81-2); DL-α-tocopherol (99.5%, C29H50O2, MW 430.0, CAS No. 10191-41-0); γ-tocopherol (99.1%, C28H48O2, MW 416.7, CAS No. 54-28-4); and δ-tocopherol (93.1%, C27H46O2, MW 402.7, CAS No.*

119-13-1) stock solutions.—Weigh accurately 0.0891 g retinol, 0.100 g retinol acetate, 0.100 g retinol palmitate, 0.100 g α-tocopherol, 0.100 g δ-tocopherol, and 0.025 g γ-tocopherol into a 50 mL volumetric flask containing 0.02 g butylated hydroxy toluene (BHT). Add tetrahydorofuran to the volumetric flask to dissolve the solids and produce solutions of approximately 1692.9, 1956.0, 1894.0, 1990.0, 1862.0, and 495.5 mg/kg, respectively (Supelco, Bellefonte, PA).

(b) *Other reagents.*—Tetrahydrofuran, petroleum ether, and acetonitrile (J.T. Baker, Phillipsburg, NJ), and dimethyl sulfoxide (DMSO) and acetic acid (Sigma-Aldrich, St. Louis, MO) were used. All solvents were of chromatographic or HPLC grade, and other reagents were ACS reagent grade.

Test Samples

A powdered skim milk sample was purchased in a local market in Seongnam City, Korea. The powdered skim milk sample was stored at room temperature in an airtight container prior to analysis. All other samples for analysis were also purchased in the local market in Seongnam City, Korea.

Sample Preparation

Sample preparation for the rapid method was based on the KOH hydrolysis method in the AOAC *Official Method*SM (16) and the Korean food code (17). Samples of approximately 0.5 g were transferred into 22 mL vials (solid caps with 30 mm PTFE liner; Supelco). A 5 mL amount of anhydrous ethanolic 1 M KOH with 0.02 M BHT was added. The vial was then tightly capped and placed in a heating block at 100°C for 30 min to carry out saponification. After saponification, the vial was placed in the dark and allowed to cool to room temperature for about 15 min. Then, 5.00 mL saturated sodium chloride solution and 10.00 mL petroleum ether were added. The vial was shaken vigorously for 5 min and placed in the dark for 10 min; 3.00 mL of the supernatant was then transferred into a 20 mL test tube. After removing the petroleum ether at 40°C using a Turbo-vap evaporator (Caliper Life Science, Hopkinton, MA), the concentrate was reconstituted to 3.00 mL by adding a reconstitution solvent comprising methanol–isopropanol (1 + 1, v/v) with 0.02 M BHT adjusted to pH 5.85 with acetic acid. Finally, the sample solution was filtered through a 0.2 μm syringe filter into a small glass vial for *UHPLC* analysis. The KOH hydrolysis method following the AOAC *Official Method* (16), the Korean food code (17), and the DMSO hydrolysis method of Kwak et al. (18) were used as comparisons with the rapid method.

Statistical Analysis

The obtained results were subjected to statistical analysis using the program SPSS 13.0 for Windows (LEAD Technologies, Inc., Chicago, IL). Vitamins A and E were analyzed using a one-way analysis of variance (ANOVA) and a paired sample *t*-test technique.

4-2-3 β-Carotene

Materials

Red pepper powder samples were purchased in the local market in Seongnam, Korea, and samples were stored at room temperature in an airtight container prior to analysis. All other samples for the applicability were also purchased in the local market in Seongnam, Korea. Standard β-carotene (>95%, C40H56, Fw 536.87, CAS 404-86-4) was purchased from Sigma-Aldrich (St. Louis, MO, USA). To make a stock solution for quantitation, weight accurately 0.2630 g β-carotene and 0.02 g butylated hydroxyl toluene (BHT), and dissolve in ethyl acetate: acetonitrile: acetic acid (30:68:2, v/v/v) with 0.22 mM BHT in a volumetric flask to produce a solution of approximately 2,500 μg/g. Other reagents such as ethylacetate and petroleum ether (ACS reagent grade), acetonitrile (chromatographic grade), and acetic acid (ACS reagent grade) were used.

Sample preparation

The sample preparation was based on the conventional method except saponification procedure. Approximate 0.5 g of samples was taken into 22-mL vial (solid caps with PTFE liner 20-mm, Supelco, Bellefonte, PA, USA) and then 10 mL anhydrous ethanolic 1 N KOH and 0.02 g BHT were added, followed by tightly capping the tube. The vial was placed in a heating block (TECHNE DB-3D; Barloworld Scientific Ltd., Stone, UK) at 100°C for 30 min to saponify. After saponification, the vial was placed in a dark place and was allowed about 30 min in a room temperature to cool down. The supernatant was transferred from the vial into a 250-mL brown separating funnel through a filter paper (Whatman No. 2). Twenty mL of saturated NaCl solution and 40 mL of petroleum ether containing 0.22 mM BHT were added into the separating funnel. The separating funnel was vigorously shaken for 5 min, followed by collecting the supernatant into the 250-mL of round-bottom flask. The procedure above was repeated again, and all the extracts were combined. After removing the petroleum ether under 40°C using a rotary evaporator, the concentrate was reconstituted up to 200 mL with a mobile phase into a volumetric flask. Finally, the sample solution was filtered through a 0.2-μm syringe type filter into a small glass vial for UHPLC analysis.

Effect of BHT on the stability of β-carotene

β-Carotene has been known to be light sensitive compound and deterioration can be easily occurred during storage and pretreatment of the sample. To avoid the change of total amount in samples during storage and pretreatment, it is recommended that BHT be added in the standard stock solution as well as sample solution for β-carotene analysis. For the rapid analysis of β-carotene, we adopted the heating block method instead of a refluxing method as a new way of reducing saponification time, accordingly, it was expected that the concentration of β-carotene could be affected by the procedure of

sample preparation. At this point of view, we have evaluated the effect of BHT on the stability of β-carotene during method validation.

Analysis of β-carotene

The concentration of β-carotene was determined using UHPLC. The UHPLC system (LaChromUltra L-2000U Series; Hitachi-High Technologies Corp., Hitachinaka, Japan) was equipped with a mobile phase reservoir, UHPLC pump (Model L-2200U), an autosampler of 5 μL injection at a fixed volume. LaChromUltra C18 (2 μm, 2 mm i.d.×50 mm L, Hitachi-High Technologies Corp.) was used as an analytical column. Mobile phase was ethylacetate: acetonitrile: acetic acid (30:68:2, v/v/v) with 0.22 mM BHT and flow rate was 0.2 mL/min. Detector was UV detector (Model L-2400U; Hitachi-High Technologies Corp.) set at the wavelength of 450 nm. For comparison purpose, c-HPLC analysis was performed according to Korea Food Code.

Calibration graph

Calibration graph for UHPLC was based on peak area and prepared by injecting 5 μL of 0.5, 1.0, 5.0, and 25.0 μg/mL solutions prepared by the dilution of β-carotene stock solutions with a mobile phase.

4-3 Results and discussion

4-3-1 Ginsenosides

Separation of ginsenosides in ginseng using UHPLC

Figure 4-1 shows typical chromatograms for the analysis of 22 of ginsenoside standards and red ginseng extract using the 100 mm C18 column under optimized instrument conditions. The optimization of the mobile phase led to a satisfactory resolution. Although the use of the 100-mm column resulted in better separation using UHPLC, the retention times of the ginsenosides were similar to those obtained with the 50-mm column, and the 50-mm column can be used in routine analyses. The resolution of ginsenosides by UHPLC with a 100-mm column appeared to be sufficient to separate 22 ginsenosides for the quantification.

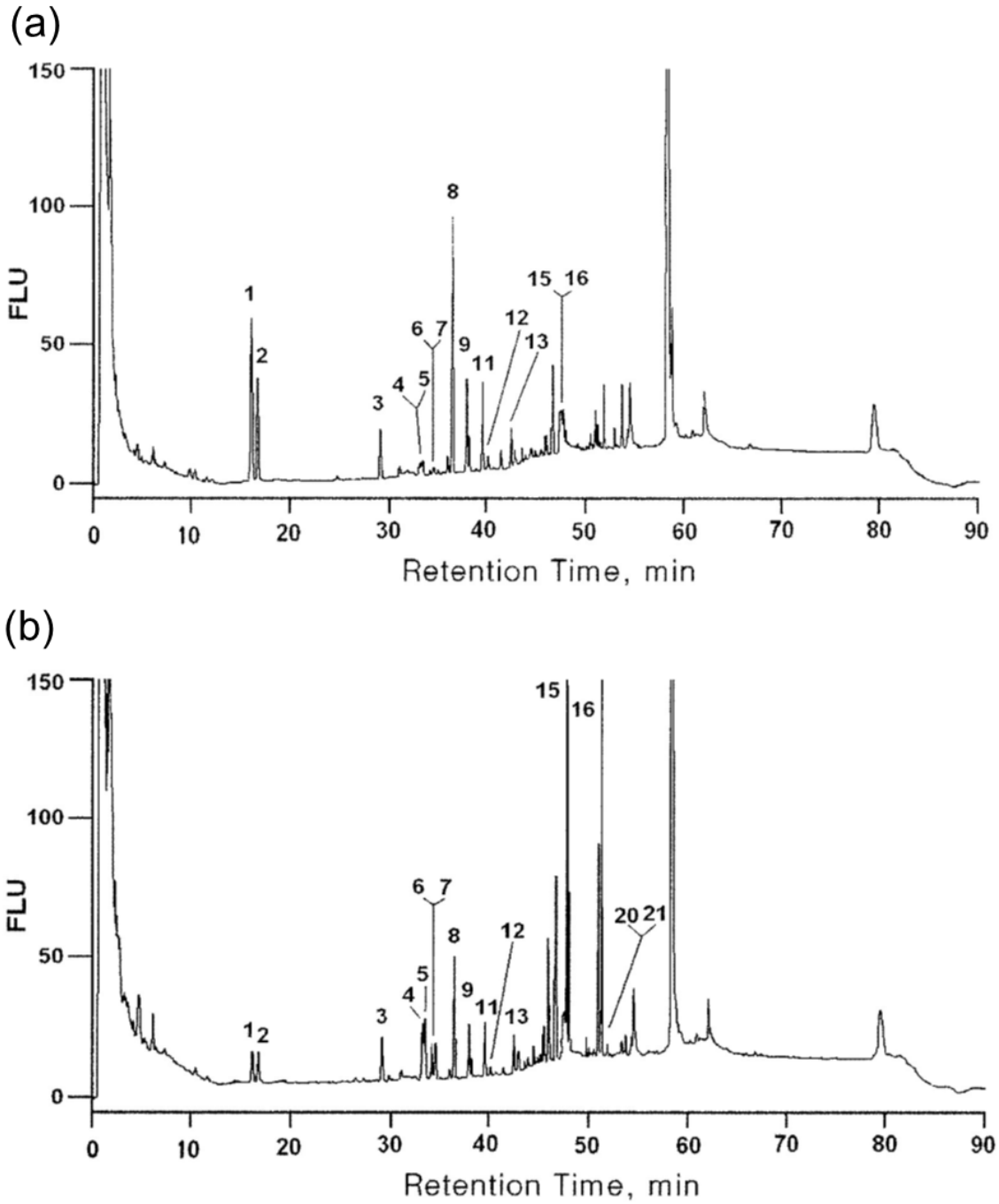

Fig. 4-1 UHPLC chromatograms of: ginsenoside standards (a); red ginseng extract (b). The chromatographic separation was performed on a middle-length C18 column (2 mm i. d. × 100 mm L, particle size 2 mm; Hitachi-High Technologies, Japan). Peaks: 1, Rg1; 2, Re; 3, Rf; 4, Rh1(S); 5, Rg2(S); 6, Rg2(R); 7, Rh1(R); 8, Rb1; 9, Rc; 10, F1; 11, Rb2; 12, Rb3; 13, Rd; 14, F2; 15, Rg3(S); 16, Rg3(R); 17, PPT(S); 18, PPT(R); 19, compound K; 20, Rh2(S); 21, Rh2(R); 22, PPD.

Evaluation of the sample preparation method

The effect of the sample preparation method on the extraction efficiency of ginsenosides from ginseng powder using the 50-mm column was evaluated and found to be suitable for routine analyses. Because of the different concentrations of ginsenosides in ginseng, Rg1, Re, Rf, Rh1(S), Rg2(S), Rg2(R)+Rh1(R) (mixture as two analytes), Rb1, Rc, Rb2, Rb3 and Rd were selected as target compounds to compare the extraction efficiencies of the various sample preparation techniques. First, ginsenosides were extracted twice with 70 mL of 50% methanol at 80˚C and then injected the sample solution into the UHPLC without any purification procedures to confirm the impurities in ginseng. Many impurities in ginseng were eluted at the beginning of the injection. However, when ginsenosides in ginseng were eluted, few impurities were co-eluted with the target ginsenosides. To remove the impurities, we employed the SPE clean-up procedures. The sample clean-up step did not appear to significantly remove the impurities from the ginsenosides. The Soxhlet method was applied to effectively extract ginsenosides; however, the extraction efficiency of the Soxhlet method was not as effective as the refluxing method in the extraction of Rg1, Re, Rf, Rb1, Rc, Rb2, Rb3 and Rd.

Table 4-1 presents a comparison of the results of the extraction efficiencies of the various sample preparation methods. Three kinds of sample preparation methods were evaluated: refluxing, SPE and Soxhlet extracts. Among the three kinds of preparations, refluxing extraction was the most efficient in the extraction of all ginsenosides, followed by the SPE and Soxhlet methods, in decreasing order of effectiveness (Table 4-1).

Table 4-1

Comparison of the Extraction Efficiencies of the Various Sample Preparation Methods* (mg/kg)

Analytes	Refluxing (n = 5)	SPE (n =7)	Soxhlet (n = 3)
Rg1	1,913+223	1,333+337	818+72
R	1,361+167	1,002+220	332+29
Rf	641+77	420+128	635+6
Rh1(S)	6+3	14+6	0
Rg2(S)	66+54	18+28	0
Rg2(R) + Rh1(R)	26+32	35+32	0
Rb1	1,534+108	1,168+373	3,374+358
Rc	702+80	524+319	1,206+106
Rb2	422+51	267+84	798+66
Rb3	50+7	32+8	119+10
Rd	70+37	43+28	222+24

*Note: Values represent the mean of analyses ± SD. As described in the text, the chromatographic separation was performed on a short-length C18 column (2 mm i. d. × 50 mm L, particle size 2 μm; Hitachi-High Technologies).

Evaluation of the heating-block method

Extraction time

A comparison of the extraction efficiencies as a function of the extraction time was evaluated. Based on the results obtained using the refluxing method as a control, the heating-block method exhibits no significant difference. The extraction times were set to 10, 20 or 30 min. Based on ANOVA results, the F-ratio and F-critical value of the extraction method were 0.007 and 2.839, which indicates that no significant difference in the extraction efficiency was observed among the extraction conditions at a significant level of 0.05. Therefore, there was no significant difference between the extraction times of 10, 20 or 30 min, and the extractions were mostly completed within 20 min.

Comparison of extraction efficiencies by sample amounts

The sample amount is sometimes an important parameter with respect to the extraction efficiency, because the extraction efficiency can be affected by the ratio between the sample amount and the amount of extracting solvent. Four different sample amounts were used to compare the extraction efficiency using the heating-block method: 0.1, 0.2, 0.25 and 0.5 g. Based on the ANOVA results, the F-ratio of the sample amount was 0.007, and its F-critical value was 2.839, which indicates that no significant difference among the sample amounts was observed at a significance level of 0.05. Therefore, the optimum sample amount was 0.2 g based on the consideration of homogeneity and the ease of sample handling.

Method validation

Linearity, limit of detection and limit of quantification

To determine the linearity, four different concentrations of ginsenosides were selected in a working range from 2.6 to 40.4 mg/mL for the 22 ginsenosides and analyzed using a UHPLC method. Each solution was injected three times, and the average values of triplicate analyses are presented in Table 4-2. Regression analysis revealed a good correlation coefficient ($r^2 > 0.99$), as shown in the table. For the determination of the linearity of individual ginsenosides, the sensitivity was calculated using the four concentrations of the standard described previously, depending on the UV sensitivity, and the results are presented in Table 4-2. The limit of detection (LOD) and limit of quantification (LOQ) values for the method were estimated at SD/b ratios of 3 and 10, where SD and b represent the standard deviation of the intercept and the slope of the regression line, respectively. The LODs ranged from 0.6 mg/kg for Rb2 and Rg3(S) to 1.2 mg/kg for PPT(S) and PPD. The LOQs ranged from 1.8 mg/kg for Rg3(S) to 3.7 mg/kg for PPT(S) (Table 4-2).

Table 4-2 Calibration and Sensitivity Data of the Ginsenosides*

Analytes	Linear range mg/kg	r^2	LOD, mg/kg	LOQ, mg/kg
Rg1	2.9-36.8	0.9995	0.7	2.1
Re	3.2-39.6	0.9996	1.0	2.9
Rf	2.9-36.0	0.9996	0.7	2.2
Rh1(*S*)	2.9-36.0	0.9996	0.7	2.2
Rg2(*S*)	2.6-32.8	0.9994	0.8	2.3
Rg2(*R*)	2.9-36.8	0.9995	0.9	2.7
Rh1(*R*)	3.0-37.2	0.9995	0.8	2.5
Rb1	3.5-36.0	0.9995	1.1	3.3
Rc	2.9-36.4	0.9996	0.8	2.3
F1	2.9-36.8	0.9995	0.7	2.2
Rb2	2.9-36.8	0.9996	0.6	1.9
Rb3	2.9-36.8	0.9996	0.7	2.3
Rd	2.9-36.8	0.9995	0.8	2.6
F2	2.9-36.0	0.9996	0.7	2.1
Rg3(*S*)	3.1-38.8	0.9995	0.6	1.8
Rg3(*R*)	3.0-37.6	0.9995	0.7	2.1
PPT(*S*)	2.9-36.4	0.9996	1.2	3.7
PPT(*R*)	3.0-36.0	0.9995	1.0	2.9
K	2.9-36.8	0.9996	0.8	2.3
Rh2(*S*)	3.5-40.4	0.9996	1.1	3.3
Rh2(*R*)	2.6-32.8	0.9994	0.7	2.2
PPD	4.0-38.4	0.9987	1.2	3.6

*Note: The chromatographic separation was performed on a middle-length C18 column (2 mm i. d. × 100 mm L, particle size 2 μm; Hitachi-High Technologies).

Precision and accuracy

The precision and accuracy data were compared for the ginsenosides in ginseng powder for UHPLC analysis, as illustrated in Table 4-3. Intra-day (n = 12) and inter-day (n = 3) repeatability tests for precision were performed on the 12 ginsenosides in ginseng powder. The relative standard deviations (RSDs) for intra-day and inter-day repeatability are presented in Table 4-3. The RSDs for the intra-day and inter-day repeatability were less than 14.6 and 14.7%, except for the mixture of Rg2(R) and Rh1(R), which showed RSDs of 18.0 and 24.2%, respectively.

Table 4-3 Precision Data of the Ginsenosides in Ginseng Powder*

Analytes	Intra-day, % (n=12)	Inter-day, % (n=3)
Rg1	6.1	3.7
Re	3.8	4.6
Rf	5.2	8.7
Rh1(*S*)	13.3	13
Rg2(*S*)	14.6	14.7
Rg2(*R*)+ Rh1(*R*)	18.0	24.2
Rb1	6.1	8.9
Rc	5.9	8.7
Rb2	6.6	9.3
Rb3	6.6	10.3
Rd	12.9	11.2

*Note: Data were expressed as the RSDs. The chromatographic separation was performed on a short-length C18 column (2 mm i. d. × 50 mm L, particle size 2 μm; Hitachi-High Technologies). †The initial ginsenoside concentrations were estimated to be: Rg1, 1,978 mg/kg; Re, 1,849 mg/ kg; Rf, 645 mg/kg; Rh1(S), 36 mg/kg; Rg2(S), 60 mg/kg; Rg2(R) t Rh1(R), 18 mg/kg; Rb1, 2,150 mg/kg; Rc, 653 mg/kg; Rb2, 483 mg/kg; Rb3, 77 mg/kg; Rd 111 mg/kg.

To study the accuracy of the heating-block method, recovery experiments were performed using a standard addition method. The recovery of the standard that was added to the assay samples was calculated using the following equation:

$$\text{Recovery (\%)} = [(C_t - C_u)/C_a] \times 100$$

where C_t is the total concentration of the analyte found, C_u is the concentration of the analyte present in the original ginseng powder and C_a is the concentration of the pure analyte added to the ginseng powder. To obtain the accuracy data, six ginsenosides were selected: Rg1, Re, Rf, Rb1, Rc and Rb2, because the concentrations of ginsenosides in ginseng powder exhibited an excessively broad range between ginsenosides. Therefore, three different concentrations were added to the ginsenosides based on the initial concentration of ginsenosides in ginseng powder. Most of the recovery ratios were greater than 98.1% for Re, as shown in Table 4-4.

Table 4-4 Recovery test of Ginsenosides in Ginseng Powder*

Analytes	Initial conc. of ginseng, mg/kg	Amount Added, mg/kg	Recovery, %
Rg1	2045	731	100.0
		1462	100.9
		2924	101.3
Re	1278	906	98.1
		1811	99.5
		3622	99.3
Rf	571	318	99.4
		637	101.0
		1274	100.2
Rb1	1979	894	100.3
		1788	102.0
		3575	102.2
Rc	596	339	100.1
		678	102.4
		1356	102.2
Rb2	450	269	98.5
		537	101.2
		1074	100.8

*Note: The chromatographic separation was performed on a short-length C18 column (2 mm i. d. × 50 mm L, particle size 2 μm; Hitachi-High Technologies).

Analyses of real samples

The proposed method based on UHPLC was used to determine 22 ginsenosides in ginseng powder. The retention times were used to identify the 22 ginsenosides, and an external calibration procedure was applied for quantification. Table 4-5 shows the results obtained from four samples. Ginsenosides were found in all of the samples, and the contents of ginsenosides ranged from 44 mg/kg for Rc to 667 mg/kg for Rg1 in ginseng root (Table 4-5).

Table 4-5 Concentration of Ginsenosides in Various Ginseng Products* (mg/kg)

Analytes	Raw ginseng root [a] (n=3)	Dried ginseng root [b] (n=3)	Ginseng tablet [c] (n=3)	Red Ginseng extract [d] (n=3)
Rg1	705.8±32.0	2183.6±14.5	4059.0±41.5	23.8±0.6
Re	184.6±9.5	1329.8±15.1	2351.5±25.7	20.8±0.1
Rf	57.0±8.7	508.3±0.5	947.7±16.8	27.2±0.2
Rh1(S)	0.0	27.8±6.8	204.7±8.1	27.5±0.0
Rg2(S)	0.0	40.8±2.8	233.0±18.1	33.2±0.2
Rg2(R)	0.0	13.7±2.5	71.8±0.9	19.1±0.1
Rh1(R)	0.0	0.0	76.8±3.2	16.9±0.3
Rb1	113.3±16.2	2088.7±35.7	7034.7±46.2	97.1±0.0
Rc	60.4±11.1	558.7±17.2	2472.7±22.4	38.7±0.0
Rb2	44.8±12.6	475.0±32.1	1965.0±33.3	34.5±0.2
Rb3	0.0	74.6±2.9	265.3±4.6	5.3±0.2
Rd	0.0	102.2±4.9	607.1±3.0	17.7±0.1
Rg3(S)	0.0	0.0	113.6±5.9	111.2±2.5
Rg3(R)	0.0	0.0	51.2±1.5	48.5±0.8
K	0.0	0.0	0.0	0.0
Rh2(S)	0.0	0.0	0.0	0.0
Rh2(R)	0.0	0.0	0.0	0.0

*Note: Sample preparations are described in 4-2-1 experimental. The chromatographic separation was performed on a middle-length C18 column (2 mm i. d. × 100 mm L, particle size 2 μm; Hitachi-High Technologies).

4-3-2 Vitamins A and E

Comparison of Elution Time by UHPLC with c-HPLC

The chromatograms of the retinol and tocopherol standards that were separated by c-HPLC and UHPLC are illustrated in Figure 4-2. The typical c-HPLC method requires a considerable amount of analysis time (around 45 min) and a considerable amount of solvent consumption for successful chromatographic

analysis, due to the long period of time for which the method runs. However, UHPLC requires a considerably shorter analysis time (around 16 min) to achieve the same chromatographic separation as c-HPLC, as is shown in Figure 4-2. In addition, the UHPLC method is economically and environmentally friendly as a result of the rapid analysis. Because of the fast analysis, the consumption of solvents used as the mobile phase can be reduced at least 2.5-fold (Figure 4-2).

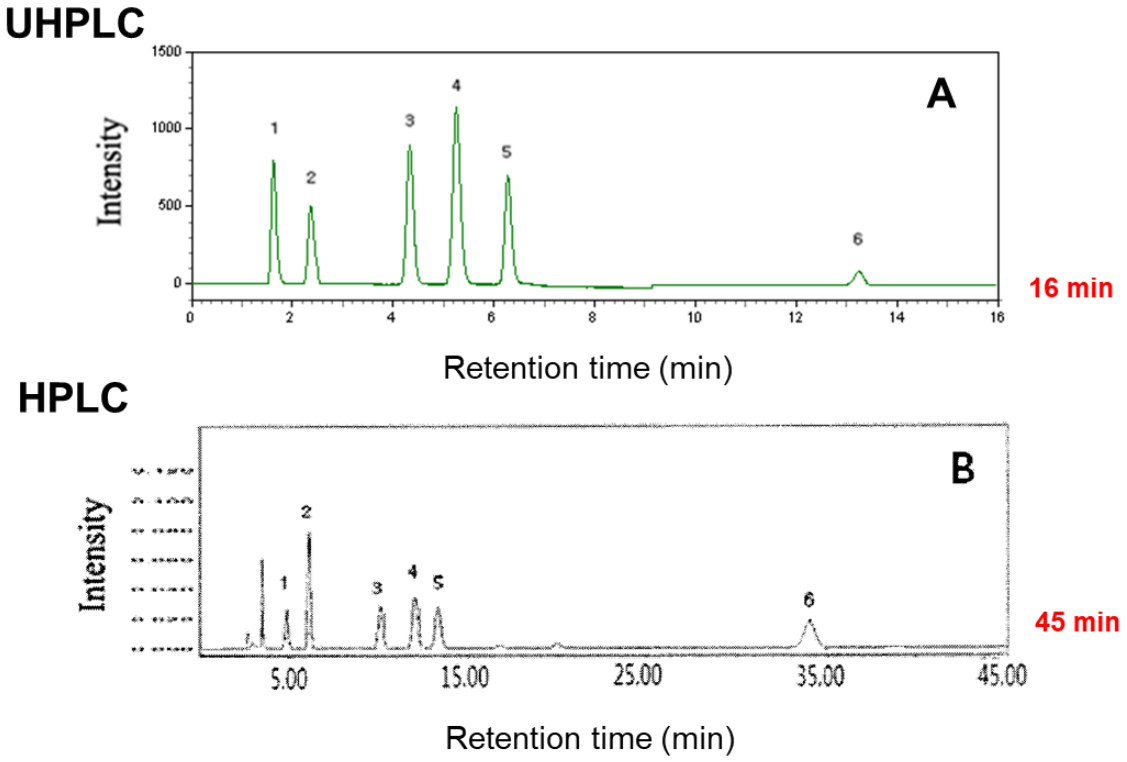

Fig. 4-2 Typical chromatograms of vitamins A and E. (A) Standard analyzed by UHPLC, column: LaChromUltra C18, particle size 2 μm, 2 mm id, length 75 mm (Hitachi-High Technologies Corp.). Flow rate 0.3 mL/min, injection volume 3 μL. (B) Standard analyzed by c-HPLC; column: CapCell pak C18 UG120, particle size 5 μm, 4.6 mm id, length 250 mm (Shisheido, Tokyo, Japan). Flow rate 1.0 mL/min, injection volume 10 μL. 1, retinol; 2, retinol acetate; 3, δ-tocopherol; 4, γ-tocopherol; 5, α-tocopherol; 6, retinol palmitate.

Linearity

To determine the linearity, five different concentrations of retinol standards (only four for retinol palmitate) were used between the following working ranges of 0.0090 and 9.9900 mg/kg for the UHPLC analysis: 0.015 to 15.09 mg/kg for retinol acetate, 0.0015 to 0.7448 mg/kg for δ-tocopherol, 0.0012 to 0.5946 mg/kg for γ-tocopherol, 0.0046 to 2.3084 mg/kg for α-tocopherol, and 0.1000 to 25.0000 mg/kg for retinol palmitate. Each solution was injected 12 times, and the values represent the average of the analyses. The regression analysis revealed good correlation coefficients (r^2) from 0.9984 to 1.0000. The results are reported in Table 4-6.

Table 4-6 Calibration and sensitivity data of vitamins A and E

Components	Linear range (mg kg^{-1})	r^2	LOD^a (mg kg^{-1})	LOQ^a (mg kg^{-1})
Retinol	0.0090 -9.9900	1.0000	0.0148	0.0450
Retinol-acetate	0.0150-15.0900	0.9999	0.0517	0.1566
delta-tocopherol	0.0015-0.7448	0.9992	0.0014	0.0042
gamma-tocopherol	0.0012-0.5946	0.9992	0.0017	0.0053
alpha-tocopherol	0.0046-2.3084	0.9984	0.0138	0.0418
Retinol-palmitate	0.1000-25.0000	1.0000	0.0900	0.2726

a. Values represent the mean of intra-day (n = 15) analysis

LOD and LOQ

We calculated the sensitivity using the five concentrations of standard described above for the determination of linearity. The results are reported in Table 4-6. The LOD and the LOQ values for the method were estimated at an SD/b ratio of 3 and 10, where SD and b stand for the SD of the intercept and slope of for retinol, 0.0517 mg/kg for retinol acetate, 0.0014 mg/kg for δ-tocopherol, 0.0017 mg/kg for γ-tocopherol, 0.0138 mg/kg for α-tocopherol, and 0.0900 mg/kg for retinol acetate. The LOQ was 0.0450 mg/kg for retinol, 0.1566 mg/kg for retinol acetate, 0.0042 mg/kg for δ-tocopherol, 0.0053 mg/kg for γ-tocopherol, 0.0418 mg/kg for α-tocopherol, and 0.2726 mg/kg for retinol acetate (Table 4-6).

Accuracy and Precision

We compared the precision and accuracy data of vitamins A and E for the rapid method in this research with two conventional analytical methods (a KOH hydrolysis method and a DMSO hydrolysis method). Intraday (n = 3) and interday (n = 5)
repeatability tests for precision were performed for vitamins A and E in powdered skim milk. The RSDs for intraday and interday repeatability are given in Tables 4-7 to 4-9. In order to study the accuracy of the methods, recovery experiments were carried out using the standard addition method. The recovery of the standard that was added to the assay samples was calculated using the following equation:

$$\text{Recovery (\%)} = [(C_t - C_u)/C_a] \times 100$$

where C_t is the total concentration of the analyte found, C_u is the concentration of the analyte presents in the original powdered skim milk, and C_a is the concentration of the pure analyte added to the powdered skim milk.

The recoveries were within the range of 81.37–92.99% for the rapid method, 72.18–101.01% for the KOH hydrolysis method, and 81.70–94.59% for the DMSO hydrolysis method. The RSD for the interday repeatability was also estimated. The RSD was less than 9.12% for the rapid method, less than 10.25% for the KOH hydrolysis method, and less than 6.49% for the DMSO hydrolysis method (Tables 4-7 to 4-9).

Table 4-7 Precision and accuracy data of vitamins A and E by the DMSO hydrolysis method with powdered skim milk[a]

Components	Spiked amount (mg kg^{-1})	Intra-day (RSD, %)	Inter-day (RSD, %)	Recovery[b], %
Retinol	0.68	2.75	5.34	90.24±4.83
	4.23	0.88	4.63	83.38±3.87
	8.46	0.81	2.48	82.57±2.04
Retinol acetate	0.74	2.36	5.16	83.21±4.28
	4.89	1.08	4.39	81.70±3.94
	9.78	0.76	1.67	81.82±1.37
delta-tocopherol	0.11	2.12	3.59	86.08±3.09
	0.70	0.94	3.59	83.95±3.17
	1.40	0.59	1.24	83.31±1.05
gamma-tocopherol	0.16	1.56	4.80	83.13±4.05
	0.99	0.79	4.20	84.88±3.57
	1.98	0.59	2.01	84.04±1.71
alpha-tocopherol	0.32	1.44	5.76	94.59±5.41
	1.99	0.80	6.49	90.46±5.87
	3.98	0.73	3.67	89.17±3.40

a. Amount of powdered skim milk taken = 0.5 g; values represent the mean of intra-day (n = 3) and inter-day (n = 5); the amount of vitamins in powdered skim milk in the initial sample was estimated to be 0.0 mg kg^{-1}.

b. Values represent the mean of inter-day (n = 5) analyses ± standard deviation

Table 4-8 Precision and accuracy data of vitamins A and E by the KOH hydrolysis method with powdered skim milk[a]

Components	Spiked amount (mg kg^{-1})	Intra-day (RSD, %)	Inter-day (RSD, %)	Recovery[b], %
Retinol	0.68	3.15	10.25	101.01±10.35
	4.23	2.28	7.58	82.72±6.27
	8.46	1.71	7.29	82.04±5.98
delta-tocopherol	0.11	4.26	6.18	85.86±5.32
	0.70	1.66	4.06	84.61±3.44
	1.40	1.23	5.49	85.52±4.68
gamma-tocopherol	0.16	3.39	7.34	82.26±5.96
	0.99	1.71	5.52	74.82±4.13
	1.98	0.81	4.05	77.62±3.14
alpha-tocopherol	0.32	3.02	8.15	79.65±6.48
	1.99	1.95	8.63	72.18±6.24
	3.98	1.09	6.72	74.18±4.98

a. Amount of powdered skim milk taken = 1.0 g; values represent the mean of intra-day (n = 3) and inter-day (n = 5); the amount of vitamins in powdered skim milk in the initial sample was estimated to be 0.0 mg kg^{-1}.

b. Values represent the mean of inter-day (n = 5) analyses ± standard deviation

Table 4-9 Precision and accuracy data of vitamins A and E by the rapid method with powdered skim milk[a]

Components	Spiked amount (mg kg^{-1})	Intra-day (RSD, %)	Inter-day (RSD, %)	Recovery[b], %
Retinol	0.68	0.92	8.42	91.11±7.66
	4.23	2.52	5.09	86.13±4.38
	8.46	1.93	5.51	84.58±4.33
delta-Tocopherol	0.11	2.85	6.32	81.37±5.19
	0.70	4.68	9.12	82.30±7.75
	1.40	1.03	6.68	81.84±6.39
gamma-Tocopherol	0.16	1.15	3.27	88.62±2.77
	0.99	1.87	2.93	88.43±2.58
	1.98	1.20	3.41	88.22±3.01
alpha-Tocopherol	0.32	1.20	5.38	91.24±4.91
	1.99	1.61	3.31	92.62±3.03
	3.98	1.50	3.78	92.99±3.52

a. Amount of powdered skim milk taken = 0.5 g; values represent the mean of intra-day (n = 3) and inter-day (n = 4); the amount of vitamins in powdered skim milk in the initial sample was estimated to be 0.0 mg kg^{-1}.

b. Values represent the mean of inter-day (n = 5) analyses ± standard deviation

To compare recovery and precision results for each preparation method, we used one-way ANOVA (*F*-test) and paired sample *t*-test techniques. The *F*-test was executed to identify significant differences among the three methods. The *t*-test was executed to identify significant differences of the individual method in precision and accuracy. Recovery and interday (RSD) results in Tables 4-7 to 4-9 were used as raw data. The results of the *F*-test indicated significant differences among the three methods in precision and accuracy. The result of the *t*-test by the SPSS program indicated no significant difference between the rapid method and the DMSO hydrolysis method in precision and accuracy. However, it showed a significant difference in the precision and accuracy obtained when the rapid method and KOH hydrolysis method were used. The rapid method had recovery and precision similar to that of the DMSO hydrolysis method, but was better than the KOH hydrolysis method in precision and accuracy, as shown in Tables 4-10 and 4-11, respectively. The benefits of using the rapid method for the detection vitamins A and E in foods are reducing the pretreatment time to approximately 1/3 that of the KOH hydrolysis method, and reducing the volume of solvent to approximately 1/20 of that used with the KOH hydrolysis method (Tables 4-10 and 4-11).

Table 4-10 Comparison of recovery results (interday, n = 5) of the analysis of vitamins A and E by the DMSO hydrolysis method, the KOH hydrolysis method, and the rapid method

	DMSO	KOH	Rapid
Mean[a]	86.32	81.84	91.11
SD[b]	3.70	7.24	4.21
RSD[c]	4.28	8.85	4.82
F-test[d]		3.54 (3.28)	
t-test[d] (DMSO-Rapid)		-1.22 (1.80)	
t-test[d] (KOH-Rapid)		-2.02 (1.80)	
t-test[d] (DMSO-KOH)		-1.81 (1.80)	

a. n = 15 for all the methods

b. SD = standard deviation

c. RSD = relative standard deviation

d. Tabulated values of t and F at p = 0.05 are shown in parentheses

Table 4-11 Comparison of precision results (interday, n = 5) in RSD of the analysis of vitamins A and E by the DMSO hydrolysis method, the KOH hydrolysis method, and the rapid method

	DMSO	KOH	Rapid
Mean[a]	3.98	6.77	5.27
SD[b]	1.49	1.76	1.98
RSD[c]	37.31	25.94	37.54
F-test[d]		6.98 (3.28)	
t-test[d] (DMSO-Rapid)		-1.62 (1.80)	
t-test[d] (KOH-Rapid)		1.92 (1.80)	
t-test[d] (DMSO-KOH)		7.24 (1.80)	

a. n = 15 for all the methods

b. SD = standard deviation

c. RSD = relative standard deviation

d. Tabulated values of t and F at p = 0.05 are shown in parentheses

Applicability

The application of a UHPLC method using a heating block for the saponification of the sample was examined with various foods. The results are represented in Table 7. Because the UHPLC method uses a higher pressure and a shorter column than the c-HPLC method, peak dispersion is minimized, analysis speed is improved, and high resolution and good sensitivity are obtained. Even though c-HPLC can use a column as short as 7.5 cm in length, sometimes the resolution is not good enough to separate vitamins A and E in foods due to their complex matrixes. We found that good separation could be achieved, without losing resolution quality, by using the UHPLC method with a heating block to saponify the food samples, as shown in Table 4-12.

Table 4-12 Applicability results of vitamin A (retinol) and vitamin E (sum of α-, γ-, and δ-tocopherol) in various foods

Foods	Vitamin A[a], mg kg^{-1}	Vitamin E[a], mg kg^{-1}
Egg-1	3.43±0.08	11.48±0.27
Egg-2	2.98±0.11	23.44±0.70
Egg-3	3.67±0.08	34.63±1.22
Egg-4	3.68±0.14	11.27±0.05
Egg-5	3.44±0.15	58.11±0.68
Egg-6	3.58±0.18	59.68±3.82
Powdered formula-1	9.68±0.23	162.45±2.49
Powdered formula-2	9.47±0.23	93.60±6.60
Powdered formula-3	12.35±0.83	133.41±10.84
Dietary supplement-1	271.72±23.79	5374.98±252.80
Dietary supplement-2	198.91±6.96	3691.83±83.04
Dietary supplement-3	17.391±0.85	260.20±17.569

a. Values represent the mean of intra-day (n = 3) analyses ± standard deviation

4-3-3 β-Carotene

Comparison of elution time by UHPLC with c-HPLC

The chromatograms of β-carotene standard separated by c-HPLC and UHPLC were illustrated in Fig. 4-3. The typical c-HPLC requires a considerable amount of analysis time (around 20 min) and considerable amount of solvent consumption for successful chromatographic analysis due to time of long-running. However, UHPLC requires a short analysis time (around 5 min) for the achievement of the same chromatographic separation as c-HPLC, as shown in Fig. 1. It can be considered that UHPLC method has been economically and environmentally friendly due to rapid analysis. Because of the fast analysis, the consumption of solvent for mobile phase can be reduced at least 4 fold.

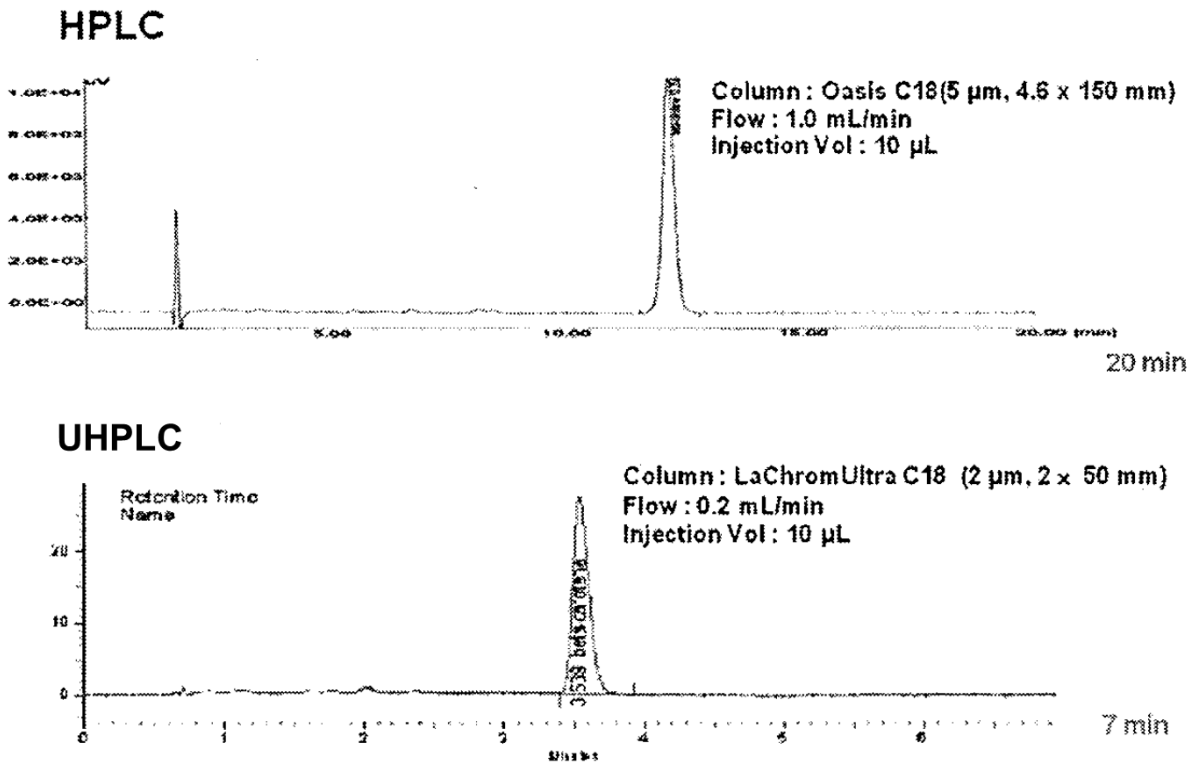

Fig. 4-3 Typical chromatograms of β-carotene. (A) Standard analyzed by c-HPLC, column: Atlantis column dC_{18} (particle size 5 µm, 4.6 mm i. d., length 150 mm; Waters, Ireland). Flow rate 1.0 mL/min, injection volume 20 µL; (B) standard analyzed by UHPLC; column: LaChromUltra C18 (particle size 2 µm, 2 mm i. d. length 50 mm, Hitachi-High Technologies Corp.). Flow rate 0.2 mL/min, injection volume 5 µL.

Linearity

To determine the linearity, 4 different concentrations of β-carotene standards were used in a working range from 0.5 to 25.0 µg/mL for UHPLC method by regression lines. Each solution was injected 3 times and the values represented the average of triplicate analysis. Regression analysis revealed a good relation (correlation coefficient R^2=0.9999 for β-carotene both without and with BHT). The graph showed a negligible intercept, which was calculated by the least-square method's regression equation.

Limit of detection (LOD) and limit of quantitation (LOQ)

The calibration and sensitivity data of both β-carotene with BHT and without BHT were compared. The results are represented in Table 4-13. The LOD and the LOQ values of the method were

estimated at an SD/b ratio of 3 and 10, where SD and b stand for the standard deviation of the intercept and slope of the regression line, respectively. LOD was 0.28 μg/mL for β-carotene with BHT and 0.62 μg/mL without BHT. LOQ was 0.84 μg/mL for β-carotene with BHT and 1.89 μg/mL without BHT. β-Carotene with BHT indicates more stable and less changeable than β-carotene without BHT at the same storage conditions. It has been revealed that the method with BHT had approximately 2 times more sensitivity than that without BHT. It can be elucidated that the differences of LOD and LOQ with and without BHT is caused by instability of standard solution of β-carotene in absence of BHT during analysis as well as sample preparation. Therefore, it is recommended that BHT should be added during preparation of standard solution as well as at the first stage of sample preparation.

Table 4-13 Calibration and sensitivity data of β-carotene

Component	Linear range (μg/mL)	r^2	LOD (μg/mL)	LOQ (μg/mL)
Beta-carotene (with BHT)	0.10 – 25.0	0.9999	0.28	0.84
Beta-carotene (w/o BHT)	0.10 – 25.0	0.9999	0.62	1.89

All values represent the mean of intra-day (n=3) and inter-day (n=15)

Precision and accuracy

Intra-day repeatability (n=3) and inter-day (n=12) test was performed on β-carotene in red pepper powder for UHPLC methods. The relative standard deviations for intra-day repeatability at the spiked amounts at 1.4, 4.3, and 12.8 μg/g revealed 2.4, 2.4, and 7.5% and inter-day repeatability revealed 4.3, 3.9, and 7.6 %, respectively, as shown in Table 2. In order to study the accuracy of the methods, recovery experiments were carried out with the standard addition method. The recovery of the added standard to the assay samples was calculated from:

$$\text{Recovery (\%)} = [(C_t - C_u)/C_a] \times 100$$

where C_t is the total concentration of the analyte found, C_u is the concentration of the present analyte in the original red pepper powder, and C_a is the concentration of the pure analyte added to the original red

pepper powder. The results are given in Table 2. The average recoveries obtained were quantitative 84.4-87.7%, indicating good accuracy of the UHPLC method.

Table 4-14 Precision and accuracy data of β-carotene in red pepper powder[a]

Components	Spiked amount (μg/g)	Intra-day (RSD%)	Inter-day (RSD%)	Recovery (%)
β-carotene	1.38	2.38	4.29	84.36±2.55
	4.25	2.36	3.87	87.68±3.74
	12.75	7.5	7.75	85.78±5.32

[a]Amount of rd pepper powder taken = 0.5 g; values represent the mean of intra-day (n=3) and inter-day (n=12); the amount of beta-carotene of r*ed pepper powder* in the initial sample was estimated to be 0.35±0.03 in test vials.

Applicability

Application of UHPLC method coupled with a heating block for the saponification of sample has been examined with the various foods. Because UHPLC method has adopted the higher pressure and shorter column than conventional HPLC, peak dispersion is minimized, analysis speed is improved, and resolution and sensitivity is provided. In the meantime, the conventional HPLC can adopted as a short column as 5 cm in length, but, the resolution is sometimes not good enough to separate β-carotene in foods due to complex matrix of the food samples. We have found that the good separation can be achieved without losing resolution quality, using UHPLC method coupled with a heating block for the saponification of food samples. Moreover, UHPLC method has been known to be economical and environmentally friendly due to extremely rapid analysis because of the shorter column. In concomitant with the rapid analysis, the consumption of solvent for mobile phase can be reduced up to 5 to 10 fold, comparing with the conventional HPLC method.

Comparison results of the analysis β-carotene in red pepper powders are illustrated in Table 3. It is postulated that two methods have no significant difference in the results. To apply the analysis method to various foods, 6 samples, containing a different amount of β-carotene, were analyzed by the UHPLC methods. The results showed that the UHPLC method could be applicable to the wide variety of foods including strawberry, tomato, pomegranate, and red pimento and achieved the good separation without hindrance of interferences in foods as shown in Table 4-15.

Table 4-15 Applicability of the UHPLC methods to various foods

Foods	β-carotene (mg/kg)
Red pepper powder	137.48±31.16
Strawberry	0.56±0.01
Tomato	0.82±0.02
Pomegranate	0.52±0.05
Red pimento - 1	2.47±0.07
Red pimento - 2	1.56+0.04

4-4 Summary

Ginsenosides

A sensitive, precise and effective heating-block method was developed for the reliable analysis of 22 ginsenosides in ginseng products. The benefits of UHPLC analysis coupled with the heating-block method include reducing the volume of extraction solvent to approximately 1/5, while maintaining high resolution, effective separation and easy handling. Apparently, UHPLC can offer significant improvements in speed, sensitivity and resolution compared with conventional HPLC, and this bodes well for future applications.

Vitamins A and E

A rapid and novel UHPLC method for the determination of vitamins A (retinol) and E (α-, γ-, and δ-tocopherol) was validated in terms of its precision, accuracy, and linearity. Intraday (n = 3) and interday (n = 5) repeatability tests for precision were performed for vitamins A and E in powdered skim milk. The precision and accuracy data of vitamins A and E for the rapid method were compared with two conventional analytical methods, KOH hydrolysis, and DMSO hydrolysis. It was found that the rapid method had similar recovery and precision compared to the DMSO hydrolysis method, but was better than the KOH hydrolysis method in terms of precision and accuracy. The UHPLC method is economical and environmentally friendly as a result of the extremely rapid analysis time and use of the shorter column. In addition, the rapid analysis, the consumption of mobile phase solvents can be reduced up to 4-fold compared to the KOH hydrolysis method.

β-Carotene and analyses by using optimal velocity

UHPLC methods by using optimal velocity ($u_{0,opt}$) were validated in terms of precision, accuracy, and linearity according FDA and ICH guidelines, and good results obtained within acceptable criteria. Advantage of UHPLC analysis in foods of β-carotene by using $u_{0,opt}$ are reducing the retention time (t_R) to approximately 1/4 t_R, reducing the volume of mobile phase to approximately 1/15, remaining a good separation and easy handling. It seems that UHPLC systems can offer significant improvements in speed, sensitivity, and resolution compered with conventional HPLC. First of all, UHPLC by using $u_{0,opt}$ can be expected well for future applications with good similarity to HPLC. In the next chapter, applications using larger velocity than $u_{0,opt}$ are studied about the advantages of the speed and the separation in food analyses.

Velocity near $u_{0,opt}$

The velocity is near $u_{0,opt}$ in the separation condition of Ginsenosides.[64] That means L are applied almost the most efficiently for N. Therefore, PAC's and TEC are approximately 1.0. Then again t_0 is not free, and should be fixed by $u_{0,opt}$ and L. The analysis of vitamins A and E in foods[27] is categorized in the conditions. And the analysis of β-carotene in foods[44] is also categorized in the conditions as well.

4-5 References

1. Cho, J., Han, Y., Oh, H., Park, H., Seong, H., and Park, J., Understanding of Korean Ginseng. The Society for Korean Ginseng. Hanlim Press, Seoul, Korea, **1995**, 35–54.
2. Lee, C.H., Nam, K.Y., Choi, K.J., *Korean Journal of Food Science and Technology*, **1978**, *10*, 263.
3. Gil, B., *Korean Journal of Food Science and Technology*, **2003**, *35*, 1003.
4. Lee, C.R., Whang, W.K., Shin, C.G., Lee, H.S., Han, S.T., Im, B.O., et al., *Korean Journal of Food Science and Technology*, **2004**, 36, 847.
5. Kim,H.J., Chun, Y.J., Park, J.D., Kim, S.I., Roh, J.K., and Jeong, T.C., *Planta Medica*, **1997**, 63, 415.
6. Prasain, J.K., Kadota, S., Basnet, P., Hase, K., and Namba, T, *Phytomedicine*, **1996**, *2*, 297.
7. Korivi, M., Hou, C.W., Huang, C.Y., Lee, S.D., Hsu, M.F., Yu, S.H., et al., Evidence-Based Complementary and Alternative Medicine, **2012**, *932165*, 1.
8. Ng, T.B., Li, W.W., and Yeung, H.W., *Journal of Enthnopharmacology*, **1987**, *21*, 21.
9. Lee, W.K., Kao, S.T., Liu, I.M., and Cheng, J.T., *Clinical and Experimental Pharmacology and Physiology*, **2006**, *33*, 27.
10. Shang, W., Yang, Y., Zhou, L., Jiang, B., Jin, H., and Chen, M., *Journal of Endocrinology*, **2008**, *198*, 561.
11. Zhang, Z., Li, X., Lv, W., Yang, Y., Gao, H., Yang, J., et al., Molecular Endocrinology, **2008**, *22*, 186.
12. Shin, J.Y., Choi, E.H., and Wee, J.J., *Korean Journal of Food Science and Technology*, **2001**, *33*, 166.

13. Shin, J.Y., Choi, E.H., and Wee, J.J., *Korean Journal of Food Science and Technology*, **2001**, *33*, 282.
14. Sun, B.S., Gu, L.J., Fang, Z.M., Wang, C.Y., Wang, Z., and Sung, C.K., Food Science and Biotechnology, **2009**, *18*, 561.
15. Hong, H.D., Sim, E.M., Kim, K., Rho, J., Rhee, Y.K., Cho, C.W., Food Science and Biotechnology, **2009**, *18*, 565.
16. Kanazawa, H., Nagata, Y., Matsushima, Y., Tomoda, M., and Takai, N., *J. Chromatogr.*, **1990**, *507*, 327.
17. Fuzzati, N., Gabetta, B., Jayaker, K., Pace, R., and Peterlongo, F., *J. Chromatogr. A*, **1999**, *854*, 69.
18. Court, W.A., Hendel, J.G., and Elmi, J., *J. Chromatogr. A*, **1996**, *755*, 11.
19. Zhu, S., Zou, K., Cai, S., Meselhy, M., and Komatsu, K., *Chemical & Pharmaceutical Bulletin (Tokyo)*, **2004**, *52*, 995.
20. Li, L., Zhang, J.L., Sheng, Y.X., Guo, D.A., Wang, Q., and Guo, H.Z., *Journal of Pharmaceutical and Biomedical Analysis*, **2005**, *38*, 45.
21. Wan, J.B., Li, S.P., Chen, J.M., and Wang, Y.T., *Journal of Separation Science*, **2007**, *30*, 825.
22. Du, X.W., Wills, R.B.H., and Stuart, D.L., *Food Chemistry*, **2004**, *86*, 155.
23. Petersen, T.G.and Palmqvist, B., *J. Chromatogr. A*, **1990**, *504*, 139.
24. Kanazawa, H., Nagata, Y., Matsushima, Y., and Tomoda, M., *J. Chromatogr. A*, **1993**, *630*, 408.
25. Chan, T.W.D., But, P.P.H., Cheng, S.W., Kwok, I.M.Y., Lau, F.W., Xu, H.X., *Anal. Chem.*, **2000**, *72*, 1281.
26. Ha, J., Seo, H.Y., Shim, Y.S., Nam, H.J., Seog, H., Ito M., and Nakagawa H., *J. AOAC International*, **2010**, *93*, 1905.
27. Shim, Y.S., Kim, K.J., Seo, D., Ito, M., Nakagawa, H., and Ha, J., *J. AOAC International*, **2012**, *95*, 517.
28. Leandro, C.C., Hancock, P., Fussell, R.J., and Keely, B.J., *J. Chromatogr. A*, **2006**, *1103*, 94.
29. Leandro, C.C., Hancock, P., Fussell, R.J., and Keely, B.J., *J. Chromatogr. A*, **2007**, *1144*, 161.
30. Wikipedia, The Free Encyclopedia, Vitamins A and Vitamin E, http://en.wikipedia.org/wiki/vitamin_ A; and http://en.wikipedia. org/wiki/vitamin_ E (accessed December 28, 2010)
31. Pusterla, N., Puschner, B., Steidl, S., Collier, J., Kane, E., and Stuart, R.L., *Vet. Rec.*, **2010**, *166*, 366.
32. Shenai, J., Kenney, K., Chytil, F., and Stahlman, M., *J. Pediatr.*, **1987**, *111*, 269.
33. Pearson, E., Bose, C., and Snidow, T., *J. Pediatr.*, **1992**, *121*, 420.
34. Bental, R.Y., Cooper, P. A., Cummins, R.R., Sandler, D.L., Wainer, S., and Rotschild, A., *S. Afr. J. Food Sci. Nutr.*, **1994**, *6*, 141.
35. Öhrvall, M., Sundlöf, G., and Vessby, B., *J. Intern. Med.*, **1996**, *239*, 111.
36. Stone, W.L., Papas, A.M., LeClair, I.O., Qui, M., and Ponder, T., *Cancer Detect. Prev.*, **2002**, *26*, 78.
37. Gackowski, D., Kowalewski, J., Siomek, A., and Olinski, R., *Int. J. Cancer*, **2005**, *114*, 153.
38. Bruno, R.S., Leonard, S.W., Park, S.I., Zaho, Y., and Traber, M.G., *Am. J. Clin. Nutr.*, **2006**, *83*, 299.

39. Mata-Granados, J.M., Quesada Gómez, J.M., and Luque de Castro, M.D., *Anal. Chim. Acta*, **2009**, *403*, 126.
40. Demirkaya, F. and Kadioglu, Y., *J. Biochem. Biophys. Meth.*, **2009**, *70*, 363.
41. Fiorentino, A., Mastellone, C., D'Abrosca, B., Pacifico, S., Scognamiglio, M., Cefarelli, G., Caputo, R., and Monaco, P., *Food Chem.*, **2009**, *115*, 187.
42. Paliakov, E.M., Crow, B.S., Bishop, M.J., Norton, D., George, J., and Bralley, J.A., *J. Chromatogr. B*, **2009**, *877*, 89.
43. De Brouwer, V., Storozhenko, S., Stove, C.P., Van Daele, J., Van Der Straeten, D., and Lambert, W.E., *J. Chromatogr. B*, **2010**, *878*, 509.
44. Ha, J.H., Shim, Y.S., Seo, H.Y., Nam, H.J., Ito, M., and Nakagawa, H., *Food Sci. Biotechnol.*, **2010**, *19*, 1199.
45. Official Methods of Analysis, *18th Ed., AOAC INTERNATIONAL*, **2005**, Gaithersburg, MD, Method 992.06.
46. Korea Food and Drug Administration, **2009**, Korea Food Code, Korea Food Industry Association, Seoul, Korea.
47. Kwak, B.M., Lee, K.W., Ahn, J.H., and Kong, U.Y., *Korean J. Food Sci. Technol.*, **2004**, *36*, 189.
48. Wikipedia, The Free Encyclopedia. Beta-carotene. Available from http://en.wikipedia.org/wiki/beta-Carotene. (accessed December 10, 2009)
49. Bertram JS. Carotenoids as cancer preventive agents. In: Retinoids and Carotenoids in Dermatology. Vahlquist A, Duvic M (eds). Informa Healthcare USA, Inc., New York, NY, USA, **2007**, 307-310.
50. Jialai I, Norkus EP, Cristol L, and Grundy SM., *Biochim. Biophys. Acta*, **1991**, *1086*, 134.
51. Sies H, Stahl W, and Sundquist AR., *Ann. NY Acad. Sci.*, **1992**, *669*, 7.
52. Mayne ST., *FASEB J.*, **1996**, *10*, 690.
53. Burton GW. and Ingold KU., *An unusual type of lipid oxidant. Science*, **1984**, *224*, 569.
54. Peto R, Doll R, Buckley JD, and Sporn MB., *Nature*, **1981**, *290*, 201.
55. Zhao B, Tham SY, Lai MH, Lee LKH, and Moochhala SM., *J. Pharm. Pharm. Sci.*, **2004**, *7*, 200.
56. Driskell WJ, Bashor MM, and Neese JW., *Clin. Chem.*, **1983**, *29*, 1042.
57. Stahl W, Sundquist AR, Hanusch M, Schwarz W, and Sies H., *Clin. Chem*., **1993**, *39*, 810.
58. Aaran RK and Nikkari TJ., *J. Pharmaceut. Biomed.*, **1988**, *6*, 853.
59. Dietz JM, Kantha SS, and Erdman Jr JW., *Plant Food Hum. Nutr.*, **1988**, *38*, 333.
60. Weissenberg M, Levy A, Schaeffler I, Menagem E, and Barzilai M., *Chromatographia*, **1997**, *46*, 399.
61. Gregory KG, Chen TS, and Philip T., *J. Food Sci.*, **2006**, *52*, 1071.
62. Estella-Hermoso de Mendoza A, Campanero MA, Mollinedo F, and Blanco-Prieto MJ., J. Chromatogr. B, **2009**, *877*, 4035.
63. Mallett DN and Ramirez-Molina C., *J. Pharmaceut. Biomed.*, **2009**, *49*, 100.
64. J. Ha, Y.-S. Shim, D. Seo, K. Kim, M. Ito, and H. Nakagawa, *J. Chromatogr. Sci.*, **2013**, *51*, 355.

Chapter 5. Applicational Experiments Using Larger Velocity than Optimal Velocity

5-1 Introduction

5-1-1 Capsaicinoids

Analysis of capsaicinoids in such foods as chili, paprika, and chili oil is considered to be relatively simple due to simple method of sample preparation, including solvent extraction, filtration by syringe-type membrane filter, and analysis by chromatographic techniques.[1-6] Some of the foods such as gochujang (one of the traditional foods in Korea), kimchi, and chili sauce have to follow the multiple step, including extraction, purification, filtration, and analysis.

Manufacturing gochujang requires many pretreatment processes to remove such impurities as interfere with analysis before the content of capsaicin is determined, since the raw materials of gochujang include soybean, wheat flour, glucose, and sugar.[7,8] It has been reported that the concentration of capsaicinoids in gochujang varieties ranges from 10 to 100 mg/kg; varieties of mild taste contain from 10 to 30 mg/kg and strong taste are characterized by a content higher than 70 mg/kg, reaching to approximate 100 mg/kg.[9,10]

It has been reported that the concentration of capsaicinoids in fresh peppers is variable. Variability is dependent upon the relative pungency of the pepper type and geographical origin of the pepper.[11] The concentration of capsaicinoids in foods is also variable depending on the variety of the pepper and the characteristics of capsicum oleoresin used in manufacturing process. Moreover, the amount of ingredients used in manufacturing process of foods can affect the extraction efficiency of capsaicinoids. To analyze the capsaicinoids in foods, optimization of analytical methods including extraction, purification, and instrumental parameters is required.

Ha et al.[12,13] have performed the gas chromatographic analysis of capsaicin in gochujang and foods. In their studies, it has been reported that for the gas chromatographic analysis of capsaicinoids in foods, the sample preparation not only follow the multiple-step to remove the interferences in foods but also requires a large consumption of solvent during sample preparation, resulting in environmentally unfriendly, time consuming, and high cost.

Recently, UHPLC method coupled with mass spectrometry has been adopted in many areas of food and biological analysis due to its rapid analysis and remarkably excellent separation.[14,15] UHPLC method also has been known to be economical and environmentally friendly due to extremely rapid analysis. In concomitant with the fast analysis, the consumption of solvent for mobile phase can be reduced up to 5 to 10 fold, comparing with the conventional HPLC method.[16,17] Therefore, our study is focused to develop the rapid analytical method for the determination of capsaicin and dihydrocapsaicin content in foods, using UHPLC. Capsaicinoids in foods which were blended to a homogeneous consistency, were

extracted with 95% ethanol in a 250-mL round-bottom flask jointed on a refluxing condenser for a given period of time. Then, a portion of the filtrated sample extract is directly analyzed by UHPLC.

5-1-2 Capsaicin in gochujang

Determination of capsaicinoids in such foods as chilli, paprika, and chilli oil has been carried out using relatively simple methods of sample preparation, including solvent extraction and filtration by a syringe-type membrane filter, and analysis by chromatographic techniques.[18–21] Analysis of some of the foods, such as *Gochujang* (a traditional food in Korea), *Kimchi*, and chilli sauce, require multiple steps, including extraction, purification, filtration, and determination. Recently, the analytical method for capsaicinoids in *Gochujang* by HPLC was endorsed as type II and by GC as type IV in the 30th section of the CODEX Alimentarius Committee Methods of Analysis and Sampling, Balatonalmadi, Hungary, March 9–13, 2009. Since then, the need for capsaicinoid analysis has rapidly increased in Korea as well as in many other Asian countries. Moreover, the Korean government is trying to establish the criteria of hot taste labeling based on concentration of capsaicinoids in foods, instead of scoville heat units. This kind of implementation has required the analysis of capsaicinoids in foods to be more effective and rapid than is possible using the conventional method.

Meanwhile, the manufacture of *Gochujang* requires many pretreatment processes to remove impurities that interfere with the analysis before the content of capsaicin is determined, since the raw materials of *Gochujang* include soybean, wheat flour, glucose, and sugar.[22,23] It has been reported that the concentration of capsaicinoids in *Gochujang* varieties ranges from 10 to 100 mg/kg; varieties of mild taste contain from 10 to 30 mg/kg, and those of strong taste are characterized by a content from 70 to about 100 mg/kg.[24,25] Ha et al.[26,27] have performed the GC analysis of capsaicin in *Gochujang* and foods. For the GC analysis of capsaicinoids in foods, the sample preparation requires multiple steps to remove the interferences in foods and a large consumption of solvent, resulting in an environmentally unfriendly, time-consuming, and high cost procedure.

Recently, UHPLC coupled with MS has been adopted in many areas of food and biological analysis due to its rapidity and excellent separation.[28,29] UHPLC has been known to be economical and environmentally friendly due to extremely rapid analysis. Because of the fast analysis, the consumption of solvent for the mobile phase can be reduced up to 5- to 10-fold compared with conventional HPLC (c-HPLC).[30,31]

Therefore, our study focused on the development of a rapid analytical method for the determination of capsaicin (CAP) and dihydrocapsaicin (DHC) content in *Gochujang* using a heating block coupled with UHPLC. Capsaicinoids in *Gochujang*, which is blended to a homogeneous consistency, are extracted with pure methanol in 22 mL vials on the heating block to reduce the time of extraction.

Then, a portion of the filtered sample extract is directly analyzed by UHPLC.

5-2 Experimental

5-2-1 Capsaicinoids

Materials

Gochujang, chilli oil, kimchi, and snack were purchased from the supermarket in Seongnam, Gyeonggi, Korea. On receipt, samples are given a unique sample number and were stored at below 4˚C in an airtight container. All other samples should be mixed thoroughly so as to be a homogeneous mixture prior to analysis.

Sample preparation

Weigh approximate 5 g of samples into 250-mL boiling flask. Add 50 mL 95% ethanol and several glass beads, and attach flask to a reflux condenser. Gently reflux it for a given hour at 90˚C and let it cool. Transfer the extract into a 50-mL volumetric flask and wash the residue with additional 95% ethanol to fill up 50 mL. Filter 1-4 mL solution through a 0.20-µm syringe filter into small glass vial. Use it for UHPLC analysis.

Reagents

Stock solution of capsaicinoids was prepared as follow; weigh accurately 10 mg of capsaicin (>97%, C18H27NO3, Fw 305.42, CAS 404-86-4; Sigma-Aldrich, St. Louis, MO, USA) and dihydrocapsaicin (>90%, C18H29NO3, Fw 307.42, CAS 19408-84-5; Sigma-Aldrich) and dissolve in 10 mL 95% ethanol in a volumetric flask to produce a solution of approximately 1 mg/mL. Ethanol (95%, ACS reagent grade), acetonitrile (chromatographic grade), and acetic acid (ACS reagent grade) were used. All solvents were of chromatographic or HPLC grade, and other reagents were ACS reagent grade.

Analysis of capsaicinoids

The concentration of capsaicinoids was determined using UHPLC. The UHPLC system (LaChromUltra L-2000U Series; Hitachi-High Technologies Corp., Hitachinaka, Japan) was equipped with a mobile phase reservoir, UHPLC pump (Model L-2200U), an autosampler system of 10 µL injection at a fixed volume. LaChromUltra C18 (2 µm, 2 mm i.d.×50 mm L, Hitachi-High Technologies Corp.) was used as an analytical column. Mobile phase was acetonitrile: 1% acetic acid in water (6:4, v/v) and flow rate was 0.6 mL/min. Detector was L-2485U fluorescence detector (Hitachi-High Technologies Corp.), set at excitation wavelength 280 nm, emission wavelength 325 nm.

Calibration graph

Calibration graph for UHPLC were based on peak area and were prepared by injecting 2 μL of the 0.2, 0.5, 1.0, 2.5, and 10.0 μg/mL solutions prepared by dilution of capsaicin and dihydrocapsaicin stock solutions with 95% ethanol.

5-2-2 Capsaicin in gochujang

Apparatus

(a) *UHPLC system*.—LaChromUltra L-2000U Series apparatus (Hitachi High-Technologies Corp., Tokyo, Japan), including the following: an eluent reservoir; Model L-2160U UHPLC pump, Model L-2200U autosampler, and EZChrom Elite software for Hitachi (Version 3.1.8b).

(b) *UHPLC analytical column*.—LaChromUltra C18 (50 x 2 mm id, 2 μm particle size; Hitachi High-Technologies Corp.).

(c) *UHPLC detector*.—L-2485U fluorescence detector (Hitachi High-Technologies Corp.), excitation wavelength 280 nm, emission wavelength 325 nm, and flow cell capacity 3 mL.

(d) *UHPLC mobile phase*.—Acetonitrile–1% acetic acid in water (6 + 4, v/v).

(e) *Flow rate*.—0.6 mL/min.

(f) *Heating block*.—TECHNE DB-3D (Barloworld Scientific Ltd, Staffordshire, UK).

Reagents

(a) *CAP [>97%, C18H27NO3, formula weight (FW) 305.42, CAS No. 404-86-4] and DHC (>90%, C18H29NO3, FW 307.42, CAS No. 19408-84-5) stock solutions*.—Weigh accurately 10 mg each of CAP and DHC and dissolve in 10 mL 95% ethanol in separate volumetric flasks to produce solutions of approximately 1 mg/mL (Sigma, St. Louis, MO).

(b) *Other reagents*.—95% ethanol (ACS reagent grade),
acetonitrile (chromatographic grade), and acetic acid (ACS reagent grade) were used. All other solvents were chromatographic or HPLC grade, and other reagents were ACS reagent grade.

Test Samples

Gochujang samples were purchased from the supermarket in Seongnam City, Gyeonggi Province, Republic of Korea. On receipt, samples were given a unique sample number and stored at below 4°C in an airtight container prior to analysis. All samples were mixed thoroughly so as to be a homogeneous mixture prior to analysis.

Sample Preparation

For the high-efficiency extraction of capsaicinoids in *Gochujang*, spread several glass beads (No. 3, Glastechnique Mfg, Lauda-Königshofen, Germany) on the bottom of a 22-mL vial with a solid cap having a 20 mm PTFE liner (Supelco, Bellefonte, PA), and place a piece of ADVANTEC No. 2 filter paper (cut to 1 × 1 cm) on the glass beads. Weigh approximately 0.2 g *Gochujang* on the filter paper to avoid direct contact of *Gochujang* with the wall of the vial. Add 15 mL methanol, and place the vial on a heating block held at 90°C. Extract capsaicinoids for 1 h and allow to cool. Transfer the extract into a 25-mL volumetric flask and wash the residue with additional methanol to fill up to 25 mL. Filter 1 mL solution through a 0.20 mm syringe filter into a small glass vial, and use it for UHPLC analysis (9).

Calibration Graphs

Calibration graphs for UHPLC were based on peak area and were prepared by injecting 2 mL 0.2, 0.5, 1.0, 2.5, and 10.0 mg/mL solutions prepared by dilution of CAP and DHC stock solutions with 95% ethanol.

5-3 Results and discussion

5-3-1 Capsaicinoids

Effect of extraction time

Extraction time plays an important role for efficient extraction depending on the concentration of capsaicinoids and sample matrix. It is necessary to optimize the time of extraction to achieve high extraction efficiency. In general, the extraction ratio of capsaicinoids in foods was increased in concomitant with increase of extraction time, the experiments were performed with gochujang (one of the traditional fermented foods) as a test sample by different extraction time (1, 3, 5, 6, and 7 hrs.) to evaluate the optimum extraction time. The results indicated that 95% extraction ratio of capsaicinoids could be achieved within 6 hrs. extraction. In the gochujang, the concentration of capsaicin is higher than that of dihydrocapsaicin, showing that extraction time of capsaicin required longer than that of dihydrocapsaicin.

It seemed that the penetration of extraction solvent into gochujang was affected by the concentration of capsaicinoids due to its high amount of sugars (approximate 20%) and the viscous property of gochujang. In consequence, we purchased the 3 kinds of gochujang products (high-capsaicinoid gochujang, middle-capsaicinoid gochujang and low-capsaicinoid gochujang) and the effect of capsaicinoids concentration in gochujang on extraction ratio has been evaluated. In the case of the low concentration of capsaicinoids in gochujang (Low), shorter time required for extraction of capsaicinoids as 3 hrs., however, in the case of the high concentration (High), the longer time required up to 6 hrs. or

more, indicating that the higher concentration of capsaicinoids requires the longer extraction time.

Linearity

To determine the linearity, 5 different concentrations of capsaicin standards were used in a working range from 0.2 to 10.0 μg/mL for the UHPLC method (Fig. 5-1). Each solution was injected 3 times and the average values of triplicate analysis were represented in Table 5-1. The calibration graph for capsaicin and dihydrocapsaicin was linear from 0.2 to 10.0 μg/mL for the UHPLC method. Regression analysis revealed a good relation (correlation coefficient r^2=0.9995 for capsaicin and 0.9999 for dihydrocapsaicin). The graph showed a negligible intercept, which was calculated by the least square method's regression equation.

Table 5-1 Calibration and sensitivity data of the UHPLC method for the determination of capsaicinoids (μg/kg)

Component	Linear range (μg/mL)	R^2	LOD, μg/mL	LOQ, μg/mL
Capsaicin	0.10 – 10.0	0.9995	0.054	0.163
Dihydrocapsaicin	0.10 – 10.0	0.9999	0.053	0.160

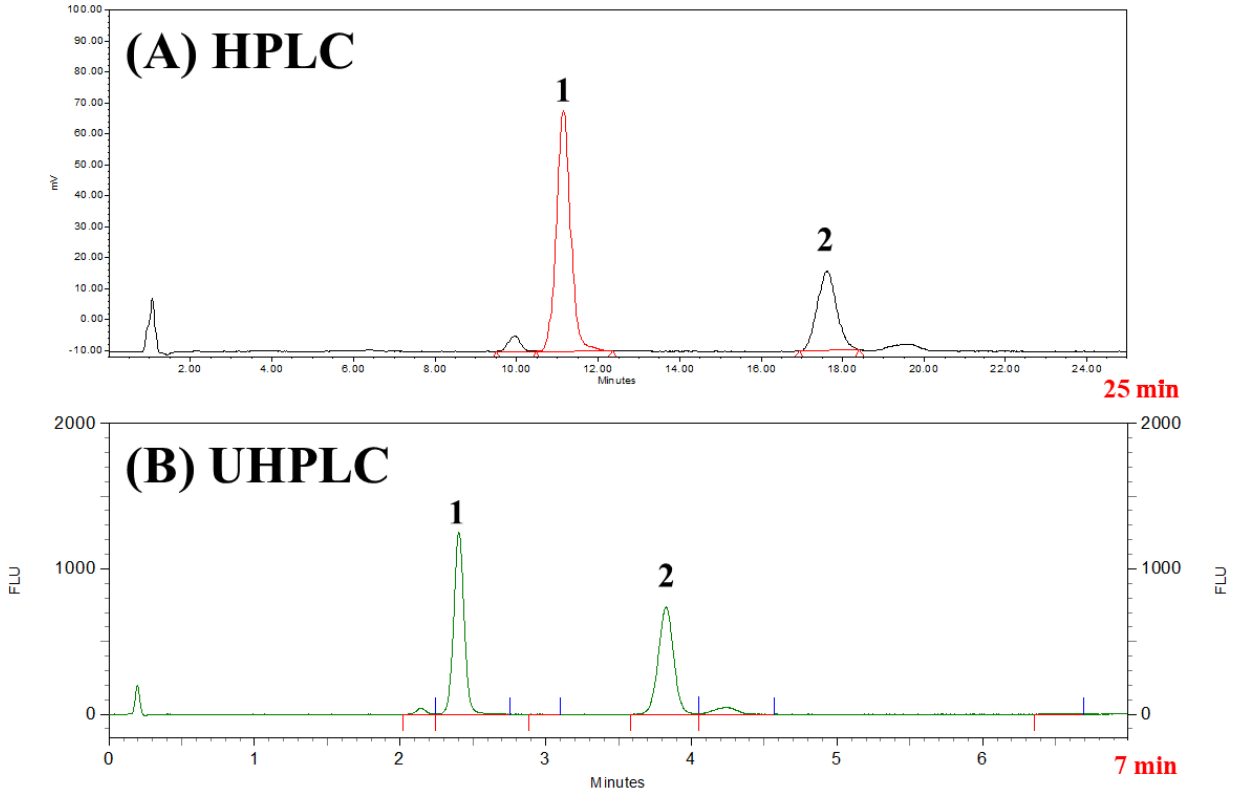

Fig. 5-1 Typical chromatograms for capsaicinoids in standards.

(A) standards by c-HPLC; column Mightysil RP18GP (particle size 5 µm, 150 × 4.6 mm id; Kanto Chemical Co., Chuoku, Japan), flow rate 1.5 mL/min, injection volume 20 µL

(B) standards by UHPLC; column: LaChromUltra C18 (particle size 2 µm, 50 × 2 mm id; Hitachi High-Technologies Corp.), flow rate 0.6 mL/min, injection volume 2 µL; FLU = fluorescence.

Limit of detection (LOD) and limit of quantitation (LOQ)

The LOD and LOQ values were estimated at an SD/b ratio of 3 and 10, where SD and b stand for the standard deviation of the intercept and slope of the regression line, respectively. LOD was 0.054 μg/mL for capsaicin and 0.053 μg/mL for dihydrocapsaicin. LOQ was 0.163 μg/mL for capsaicin and 0.160 μg/mL for dihydrocapsaicin.

Repeatability

Intra-day repeatability (n=14) test was performed on capsaicin and dihydrocapsaicin for the UHPLC methods. The relative standard deviations for intraday repeatability were revealed 4.71% for capsaicin and 5.83% for dihydrocapsaicin as shown in Table 5-2.

Table 5-2

Intra-day repeatability data of the UHPLC method for the determination of capsaicinoids in gochujang

(mg/kg)

Number of samples	Amount of samples (g)	CAP	DHC
1	5.0088	28.13	14.24
2	5.0030	27.12	13.70
3	5.0084	27.84	14.36
4	5.0019	30.44	15.59
5	5.0016	28.41	14.68
6	5.0037	28.68	14.63
7	5.0078	29.27	15.29
8	5.0046	28.38	14.51
9	5.0043	28.55	14.66
10	5.0831	30.88	16.19
11	5.0656	29.56	15.43
12	5.0379	31.80	16.73
13	5.0192	31.17	16.38
14	5.0325	29.87	15.34
Mean		29.29	15.12
SD[a]		1.38	0.88
RSD[b], %		4.71	5.83

[a]SD = Standard deviation.

[b]RSD = Relative standard deviation.

Precision and accuracy

Intra- and inter-day precision data of the UHPLC method were given in Table 5-3, indicating that the relative standard deviation of intra- and inter-day are better than 5.21% for capsaicin and 9.79% for dihydrocapsaicin. In order to study the accuracy of the UHPLC methods, recovery experiments were carried out with the standard addition method. The recovery of the added standard to the assay samples was calculated from:

$$\text{Recovery (\%)} = [(C_t - C_u)/C_a] \times 100$$

where C_t is the total concentration of the analyte found, C_u is the concentration of the present analyte in the original gochujang, and C_a is the concentration of the pure analyte added to the original gochujang. The results were given in Table 5-3. The average recoveries obtained were quantitative (91.1-94.8% for capsaicin, 91.4-97.0% for dihydrocapsaicin), indicating good accuracy of the UHPLC methods.

Table 5-3 Intra- and inter-day precision and accuracy data of the UHPLC method for the determination of capsaicinoids in gochujang

Components	Spiked amount (μg/g)	Intra-day (CV%)	Inter-day (CV%)	Recovery (%)
Cap	19.7	3.07	13.12	94.0
	39.4	4.51	4.53	94.8
	98.4	2.42	3.27	91.1
DHC	8.8	6.51	9.79	97.0
	17.5	5.81	5.18	93.4
	43.8	5.00	6.63	91.4

[a] : sample weight 5.0g, concentration of capsaicin and dihydrocapsaicin was 29.3 and 15.1 mg/kg, respectively.

Applicability

UHPLC method has been known to be economical and environmentally friendly due to extremely rapid analysis. In concomitant with the fast analysis, the consumption of solvent for mobile phase can be reduced up to 5 to 10 fold, comparing with the conventional HPLC method. To apply UHPLC method to various food products, 7 samples, containing a different amount of capsaicin, were analyzed by the UHPLC methods (Table 5-4). The results showed that the UHPLC method can be applicable to the wide variety of foods containing chilli powder, demonstrating the good separation without hindrance of interferences in foods as shown in Fig. 5-1.

Table 5-4

Applicability data of the UHPLC method for the determination of capsaicinoids in various foods

(mg/kg)

Foods	Capsaicin	Dihydrocapsaicin
Gochujang 1	16.3±0.06	15.7±0.03
Gochujang 2	35.8±0.05	22.6±0.02
Gochujang 3	95.0±0.06	44.4±0.07
Gochujang 4	28.5±0.9	14.6±0.6
Red pepper seed oil	290±0.5	146±0.5
Kimchi	2.29±0.15	1.30±0.06
Snack	4.50±0.02	3.64±0.06

5-3-2 Capsaicin in gochujang

Comparison of Elution Time by UHPLC with c-HPLC

Chromatograms of capsaicinoid standards by c-HPLC and UHPLC are shown in Figure 5-1. In HPLC, generally the elution times can be reduced by using a smaller particle size of the stationary phase and a short column length, as shown in Figure 5-1. The typical c-HPLC analysis required a considerable amount of time (around 25 min) and solvent consumption for successful chromatographic analysis of capsaicinoids. However, UHPLC required a short analysis time (around 6 min) for the achievement of the same chromatographic separation as c-HPLC. Therefore, it can be considered that UHPLC analysis is economical and environmentally friendly due to extremely rapid analysis. Because of the fast analysis, the consumption of solvent for the mobile phase can be reduced at least 4-fold.

Effect of Extraction Solvent

The solvents commonly used to extract capsaicinoids have been reported to be methanol, ethanol, and acetone. Due to the relatively high amount of moisture (>50%) and sugar (>20%) in *Gochujang*, the efficiency of the solvent to extract capsaicinoids from *Gochujang* was examined. Extraction of capsaicinoids from *Gochujang* (approximately 0.2 g) was performed twice with 10 mL solvent for 30 min on the heating block at 90°C, and the extracts were combined to yield a volume of 25 mL for the analysis. We found that methanol was the most effective solvent to extract the capsaicinoids from *Gochujang* (Table 5-5).

Table 5-5 Relative extraction efficiency of CAP and DHC in *Gochujang* by different solvents

Solvents	CAP		DHC	
	Gochujang M[b]	*Gochujang* S[c]	*Gochujang* M	*Gochujang* S
Methanol	92.9[d]	100.0	86.2	100.9
Ethanol, 95%	45.6	84.5	43.0	90.1
Ethanol, 100%	31.0	83.5	29.4	86.1
Acetone	20.1	14.4	20.5	15.5

[a] the amount of capsaicinoids in the initial sample was estimated to be 28.2 (M), 57.1 (S) μg/g for capsaicin; 24.2(M) and 35.5(S) μg/g for dihydrocapsaicin, respectively.

[b] *Gochujang* M has a mild taste.

[c] *Gochujang* S has a strong taste.

[d] values represent the mean of triplicate analyses.

Optimum Amount of Sample Taken

Because *Gochujang* has a wide range of capsaicinoid concentration depending on the variety of chili powder used as a raw material and, thus, the extraction efficiency depends on the sample amount, the optimum amount of *Gochujang* to be taken for analysis was determined. Extraction of capsaicinoids was carried out twice with 10 mL methanol for 30 min on the heating block at 90°C. The extracts were transferred into a 25 mL volumetric flask, and the residue was washed with additional methanol to fill up to 25 mL. The results of the *F*-test showed that the amount of sample taken significantly affected the extraction efficiency, as shown in Table 2. It was found that 0.1 or 0.2 g sample gave better results. When 0.5 or 1.0 g of *Gochujang* was taken, it seemed that penetration of methanol into *Gochujang* was not as effective as expected due to the high amount of sugar (20%) and the viscosity of *Gochujang*. Therefore, although the total amount of CAP and DHC in 0.5 g *Gochujang* S (strong taste) and 1.0 g *Gochujang* M (mild taste) was almost the same, 1 h extraction time was not enough, and longer extraction time was

needed for the *Gochujang* when a high amount of sample was taken. For the rapid analysis of CAP and DHC in *Gochujang*, it was found that the optimum amount of *Gochujang* taken for the determination of CAP and DHC was approximately 0.1–0.2 g. However, due to the viscous properties of *Gochujang*, it was a little difficult to take a small amount of sample into a 22 mL vial. Therefore, it was found that the optimum amount of *Gochujang* taken for the determination of CAP and DHC was approximately 0.2 g.

Table 5-6 Effect of sample amount taken on the determination of capsaicinoids

Capsaicinoids	Products	0.1 g	RSD[b],%	0.2 g	RSD, %	0.5 g	RSD, %	1.0 g	RSD, %
CAP, μg/g	Gochujang M[c]	27.6[a] ±1.35	4.89	26.9±1.23	4.57	25±1.19	4.76	21.4±1.08	5.05
	Gochujang S[c]	56.8±4.26	7.5	56.4±1.92	3.4	45.3±1.51	3.33	39.6±1.68	4.24
F-test of sample amount[d]				86.79 (2.82)					
DHC, μg/g	Gochujang M	19.7±1.45	7.36	19.1±0.79	4.14	19.1±0.89	4.66	16.3±0.81	4.97
	Gochujang S	34.8±3.16	9.08	34.7±1.23	3.54	27.8±1.05	3.78	24.3±1.04	4.28
F-test of sample amount[d]				60.48(2.82)					

[a] mean for all samples (n = 12).
[b] RSD = Relative standard deviation.
[c] the amount of capsaicinoids in the initial sample was estimated to be 28.2 (M), 57.1 (S) μg/g for capsaicin; 24.2(M) and 35.5(S) μg/g for dihydrocapsaicin, respectively.
[d] Tabulated values of the *F*-test at P = 0.05 are shown in parentheses.

Optimal Conditions for Extraction of Capsaicinoids

Optimal conditions for extraction of CAP and DHC were determined. Two solvent amounts and four extraction times were tested. The overall extraction efficiency was determined by comparing the total extractable CAP and DHC concentrations. Of the tested variables, the extraction time most significantly affected extraction efficiency. Considering the two variables, optimum amounts of extraction solvent and extraction time were approximately 15 mL and 60 min, respectively, as shown in Table 5-7. The extraction result of *Gochujang* M with 10 mL methanol was less effective than expected, even though the total amount of capsaicinoids in *Gochujang* M was almost half that of the CAP and DHC of *Gochujang* S. The reason for this discrepancy was not clear, but the viscous property of *Gochujang* caused by high sugar and moisture contents might be one of the reasons.

Table 5-7 Optimization of extraction conditions of CAP and DHC

Components	Products[a]	Amount of solvent used, mL	Time, min	Mean[b] ± SD	RSD, %
CAP, μg/g	M	10	20	17.8 ± 0.5	2.81
			40	22.4 ± 0.8	3.57
			60	25.0 ± 1.5	6.00
			80	26.9 ± 1.0	3.72
		15	20	27.5 ± 1.2	4.36
			40	28.1 ± 0.4	1.42
			60	29.8 ± 0.6	2.01
			80	30.6 ± 1.1	3.59
	S	10	20	43.1 ± 1.6	3.71
			40	48.2 ± 0.5	1.04
			60	53.0 ± 2.0	3.77
			80	52.5 ± 1.7	3.24
		15	20	54.1 ± 2.7	4.99
			40	58.6 ± 1.6	2.73
			60	60.8 ± 0.8	1.32
			80	60.0 ± 1.3	2.17
DHC, μg/g	M	10	20	13.5 ± 0.1	0.74
			40	17.0 ± 0.8	4.71
			60	19.5 ± 0.9	4.62
			80	20.1 ± 0.7	3.48
		15	20	21.2 ± 0.8	3.77
			40	22.2 ± 0.7	3.15
			60	23.0 ± 0.4	1.74
			80	23.2 ± 0.7	3.02
	S	10	20	26.8 ± 1.1	4.10
			40	30.4 ± 0.5	1.64
			60	35.3 ± 1.0	2.83
			80	36.9 ± 1.7	4.61
		15	20	34.6 ± 2.4	6.94
			40	36.8 ± 1.2	3.26
			60	41.9 ± 1.2	2.86
			80	42.5 ± 1.3	3.06

[a] Amount of *Gochujang* taken = 0.2 g.

[b] Values represent the mean of triplicate analyses.

Linearity

To determine the linearity, five different concentrations of CAP and DHC standards were used in a working range from 0.2 to 10.0 mg/mL for the UHPLC method. Each solution was injected three times. Regression analysis revealed a good relationship (R^2 = 0.9995 for CAP and 0.9999 for DHC). The graphs showed a negligible intercept, which was calculated by the least-squares method's regression equation. Calibration data are shown in Table 5-8.

Table 5-8 Calibration and sensitivity data of capsaicinoids

Component	Linear range, μg/mL	R^2	LOD, μg/mL	LOQ, μg/mL
CAP	0.10 – 10.0	0.9995	0.054	0.163
DHC	0.10 – 10.0	0.9999	0.053	0.160

LOD and LOQ

The LOD and LOQ values were estimated at an SD/b ratio of 3 and 10, respectively, where SD stands for the SD of the intercept and b for the slope of the regression line. LOD was 0.05 mg/mL for CAP and 0.05 mg/mL for DHC. LOQ was 0.16 mg /mL for CAP and 0.16 mg /mL for DHC. Sensitivity data are given in Table 5-8.

Accuracy and Precision

In order to study the accuracy of the methods, recovery experiments were carried out with the standard addition method. The recovery of the standard added to the assay samples was calculated from:

$$\text{Recovery (\%)} = [(C_t - C_u)/C_a] \times 100$$

where C_t is the total concentration of the analyte found, C_u is the concentration of the analyte present in the original *Gochujang* sample, and C*a* is the concentration of the pure analyte added to the original *Gochujang* sample. The intraday and interday precision of the method was determined using *Gochujangs* M and S spiked at the 10, 25, and 50 mg/g CAP and DHC. Data for intraday accuracy were based on the analysis of triplicate samples fortified at the three levels. Interday accuracy data were based on the analysis of each sample extracted at the three levels described above. The results obtained are given in Table 5-9. The average recoveries obtained were quantitative (93.6–103.8%), and the method's

repeatability and reproducibility were satisfactory (RSD <6.27%) for the capsaicinoids at the three levels of fortification.

Table 5-9 Accuracy and precision data for the determination of CAP and DHC in *Gochujang* using heating block method coupled with UHPLC

Parameter	Components	Products	Amount added, μg/g	Recovery[a] ± SD, %	RSD, %
Intraday (n = 3)	CAP	M[b]	10	94.5±1.45	1.53
			25	98.8±3.13	3.17
			50	97.4±2.26	2.32
		S[c]	10	94.1±3.58	6.27
			25	103.8±3.09	2.98
			50	97.5±3.49	3.58
	DHC	M	10	95.4±4.56	4.78
			25	99.6±4.76	4.78
			50	98.6±4.95	5.02
		S	10	94.2±3.23	3.42
			25	103.8±4.31	4.15
			50	100.7±3.80	3.77
Interday (n = 9)	CAP	M	10	93.6±4.14	4.42
			25	98.0±0.81	0.83
			50	95.5±3.00	3.14
		S	10	97.6±3.92	4.02
			25	102.2±2.95	2.89
			50	97.1±4.54	4.68
	DHC	M	10	96.1±3.92	4.08
			25	97.1±1.81	1.86
			50	95.7±1.19	1.24
		S	10	98.2±0.55	0.56
			25	100.6±4.33	4.30
			50	96.5±3.52	3.65

[a] Amount of solvent : 15 mL, extraction time 1 h.
[b] M : a mild taste Gochujang
[c] S : a strong taste Gochujang

Applicability

To evaluate application of the heating block method coupled with UHPLC to various *Gochujang* products, 12 samples containing a different amount of CAP and DHC were analyzed with this method and AOAC Method **995.03**, which is applicable for the determination of capsaicinoids in ground red pepper and oleoresins. The results showed that the heating block method coupled with UHPLC was almost 10% more effective than AOAC Method **995.03** for the extraction of capsaicinoids in *Gochujang*. The Pearson correlation (0.9991 for CAP and 0.9971 for DHC) reflected a significantly positive relationship between the two methods as given in Table 5-10. It was found that by replacing a refluxing method based on AOAC Method **995.03** with the proposed heating block method, the extraction time could be significantly reduced from 5 to 1 h without loss of extraction efficiency.

Table 5-10

Applicability of the heating block method coupled with UHPLC to various *Gochujang* products[a]

Products	CAP					DHC				
	u-HPLC	RSD,%	AOAC 995.03	RSD.%	D.[b], %	u-HPC	RSD,%	AOAC 995.03	RSD,%	D., %
Gochujang 01	20.5	3.71	18.8	4.3	8.3	15.3	4.93	14.1	7.53	7.8
Gochujang 02	24.8	4.43	22.6	3.5	8.9	16.5	3.56	15	2.73	9.1
Gochujang 03	20.3	1.91	18.6	3.3	8.4	15.5	1.72	13.9	2.71	10.3
Gochujang 04	12.1	4.71	10.8	3.47	10.7	10.4	3.84	9.4	4.37	9.6
Gochujang 05	28.5	3.24	26.6	4.33	6.7	18.1	2.75	17	3.54	6.1
Gochujang 06	8	2.89	7.5	9.11	6.3	5.6	6.87	5.4	9.06	3.6
Gochujang 07	22.6	1.69	20.5	5	9.3	17.1	1.72	15.3	3.74	10.5
Gochujang 08	9.5	3.78	8.2	1.64	13.7	7.8	2.78	6.5	4.22	16.7
Gochujang 09	11.7	2.19	10	6.24	14.5	8.6	4.84	7.2	3.37	16.3
Gochujang 10	8.1	5.36	7.5	6.7	7.4	9.9	6.8	9.6	6.8	3
Gochujang 11	11.1	3.77	9.6	1.73	13.5	7.4	4	6.2	2.99	16.2
Gochujang 12	23.2	2.78	21.3	2.17	8.2	26	3.29	23.4	2.73	10
Mean	16.7		15.2		9.7	13.2		11.9		9.9

[a] Results are in units of μg/g; *t*-test of CAP = 0.53 (1.72) at P = 0.05 and *t*-test of DHC = 0.55 (1.72) at P = 0.05, respectively; Pearson correlation = 0.9991 for CAP and 0.9971 for DHC, respectively.

[b] Difference : Calculated from (value $_{u\text{-}HPLC}$ – value $_{AOAC}$)/value $_{u\text{-}HPLC}$ x 100.

Larger velocity than $u_{0,opt}$

In the analytical method of capsaicinoids[32,33], on the basal plane of t_0 = 8 s and Π = 315 mm^2/s, $\mu_{N/\Pi}$ of PAC for N is 0.84. Then, $\mu_{t/\Pi}$ of PAC for t_0 is 0.72. $\mu_{N/t}$ of TEC is 1.16, that is 0.84 divided by 0.72 (Fig. 5.2). If the time is extended at the same Π, more N can be obtained efficiently. 1.16 means a potential capability of time. This condition gives TEC the potential, and Π gains N, that is $\mu_{N/\Pi}$. That comes from $\mu_{N/\Pi} > \mu_{t/\Pi}$. When increasing Π from the line of $u_{0,opt}$, $\mu_{N/\Pi} > \mu_{t/\Pi}$. Although $\mu_{N/\Pi}$ lifts N at the same t_0, $\mu_{t/\Pi}$ shortens t_0 at the same N. At the result, $\mu_{t/\Pi}$ gains the potential of TEC $\mu_{N/t}$ rather than $\mu_{N/\Pi}$ in the graph of N (Π, t_0). Therefore, $\mu_{N/\Pi} > \mu_{t/\Pi}$. The analysis of capsaicin and dihydrocapsaicin in gochujang is categorized in this condition.

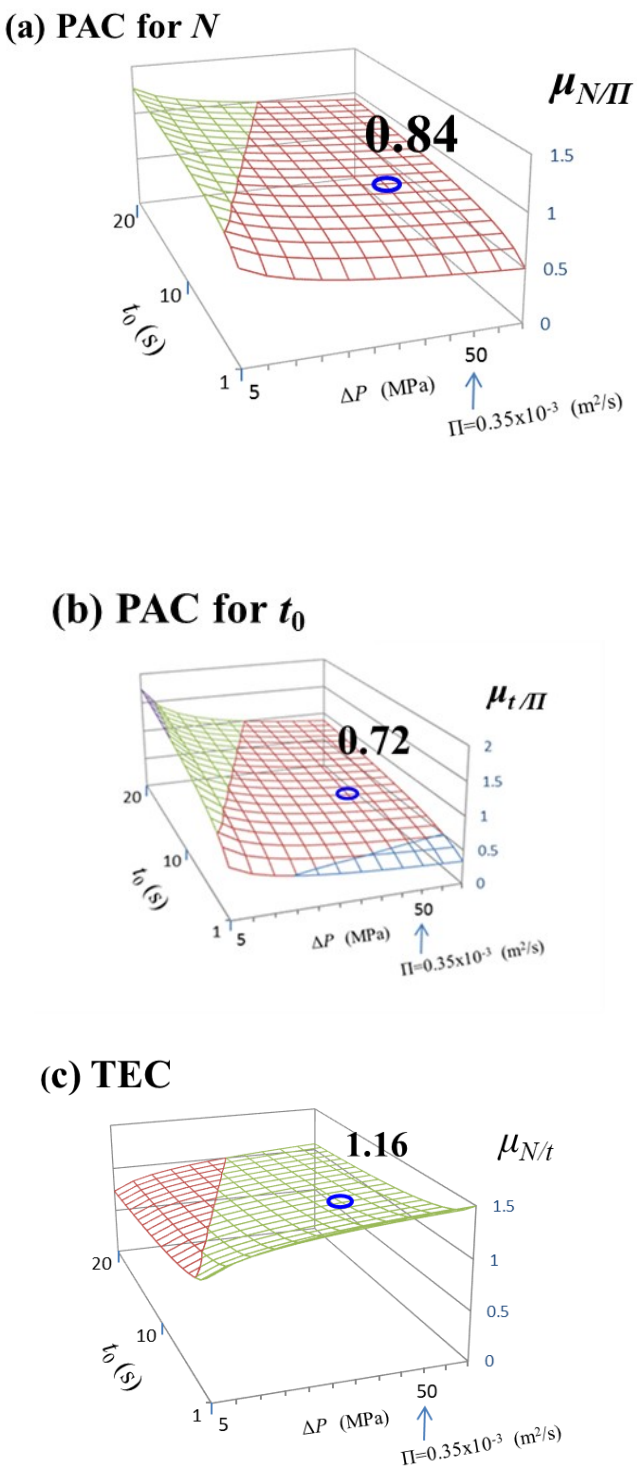

Fig. 5-2 Three-dimensional Position of regarding analysis of capsaicinoids with 2-μm packings. (a) PAC for N; (b) PAC for t_0; (c) TEC

5-4 Summary

A sensitive, precise, and specific heating block method was developed for the reliable analysis of CAP and DHC in *Gochujang*. Benefits of the heating block method coupled with UHPLC analysis are reducing the reliable analysis time at least 4-fold, high resolution, and easy handling compared with the c-HPLC method based on AOAC Method **995.03**.

TEC $\mu_{N/t}$ of 1.16 means a potential capability of time. On the other hand, $\mu_{N/\Pi}$ = 0.84 and $\mu_{t/\Pi}$ = 0.72. The condition gives TEC the potential, and Π can gain *N*, that is $\mu_{N/\Pi}$. When increasing Π, we have got a freedom on both speed and separation. Although $\mu_{N/\Pi}$ lifts *N* at the same t_0, $\mu_{t/\Pi}$ shortens t_0 at the same *N*. At the result, $\mu_{t/\Pi}$ gains the potential of TEC $\mu_{N/t}$ rather than $\mu_{N/\Pi}$ in the graph of *N* (Π, t_0).

When studying separation conditions, it is necessary to balance t_0 and *N*, under allowance of the pressure, while watching the graph of *N* (Π, t_0). Otherwise, we have only a way to obtain higher *N* by elongating *L* at the same pressure, the lower side of Π from the line of $u_{0,opt}$ in the graph of *N* (Π, t_0). At that time, although $\mu_{N/\Pi}$ of PAC for *N* becomes larger than 1.0, TEC $\mu_{N/t}$ becomes lower than 1.0.

5-5 References

1. Todd PH, Bensinger MG, and Riftu T., *J. Food Sci.*, **1977**, *42*, 660.
2. Iwai K, Suzuki T, and Fujiwake H., *J. Chromatogr.*, **1979**, *172*, 303.
3. Reilly CA, Crouch DJ, and Yost GS., *J. Forensic Sci.*, **2001**, *46*, 502.
4. Chiang GH., *J. Food Sci.*, **1986**, *51*, 499.
5. Perucka I and Oleszek W., *Food Chem.*, **2000**, *71*, 287.
6. AOAC. Official Method of Analysis of AOAC Intl. 18th ed. Method 995.03. Association of Official Analytical Chemists, Gaithersburg, MD, USA, **2005**.
7. Kim KS, Park JB, and Kim SA., *J. Korean Soc. Food Sci. Nutr.*, **2007**, *36*, 759.
8. Chae IS, Kim HS, Ko YS, Kang MH, Hong SP, and Shin D., *Korean J. Food Sci. Technol.*, **2008**, *40*, 626.
9. Kwon DJ., *Korean J. Food Sci. Technol.*, **2004**, *36*, 81.
10. Oh HI and Park JM., *Korean J. Food Sci. Technol.*, **1997**, *29*, 1166.
11. Reilly CA, Crouch DJ, and Yost GS., *J. Forensic Sci.*, **2001**, *46*, 502.
12. Ha J, Han KJ, Kim KJ, and Jeong SW., *J. AOAC Int.*, **2008**, *91*, 387.
13. Hawer W, Ha J, Hwang J, and Nam Y., *Food Chem.*, **1994**, *49*, 99.
14. Estella-Hermoso MA, Campanero MA, Mollinedo F, and Blanco-Prieto MJ., *J. Chromatogr. B*, **2009**, *877*, 4035.
15. Marin JM, Gracia-Lor E, Sancho JV, Lopez FJ, and Hernandez, F., *J. Chromatogr. A*, **2009**, *1216*,

1410.
16. Hoffman PG, Lego MC, and Galetto WG., *J. Agr. Food Chem.*, **1983**, *31*, 1326.
17. Saria A, Lembeck F, and Skofitsch G., *J. Chromatogr.*, **1981**, *208*, 41.
18. Kawada, T., Watanabe, T., Katsura, K., Takami, H., and Iwai, K., *J. Chromatogr.*, **1985**, *329*, 99.
19. Lee, K.R., Suzuki, T., Kobashi, M., Hasegawa, K., and Iwai, K., *J. Chromatogr.*, **1976**, *123*, 119.
20. Official Methods of Analysis, **2005**, 18th Ed., AOAC INTERNATIONAL, Gaithersburg, MD, Method 995.03.
21. Reillly, C.A., Crouch, D.J., and Yost, G.S., *J. Forensic Sci.*, **2001**, *46*, 502.
22. Jung, J. and Kang, S., *Korean J. Food Sci. Technol.*, **2000**, *32*, 42.
23. Kwon, D., *Korean J. Food Sci. Technol.*, **2004**, *36*, 81.
24. Kim, D., *Korean J. Food Sci. Technol.*, **2005**, *37*, 449.
25. Lee, S., Lim, I., and Yoo, B., *Korean J. Food Sci. Technol.*, **2003**, *35*, 44.
26. Hawer, W., Ha, J., Hwang, J., and Nam, Y., *Food Chem.*, **1994**, *49*, 99.
27. Ha, J., Han, K., Kim, K., and Jeong, S., *J. AOAC Int.*, **2008**, *91*, 387.
28. Estella-Hermoso de Mendoza, A., Campanero, M.A., Mollinedo, F., and Blanco-Prieto, M.J., *J. Chromatogr. B*, **2009**, *877*, 4035.
29. Mallett, D.N. and Ramirez-Molina, C., *J. Pharm. Biomed. Anal.*, **2009**, *49*, 100.
30. Hoffman, P.G., Lego, M.C., and Galetto, W.G., *J. Agric. Food Chem.*, **1983**, *31*, 1326.
31. Saria, A., Lembeck, F., and Skofitsch, G., *J. Chromatogr.*, **1981**, *208*, 41.
32. J. Ha, H.-Y. Seo, Y.-S. Shim, H.-J. Nam, H. Seog, M. Ito, and H. Nakagawa, *J. AOAC International*, **2010**, *93*, 1905.
33. J. Ha, H.-Y. Seo, Y.-S. Shim, D.-W. Seo, H. Seog, M. Ito, and H. Nakagawa, *Food Sci. Biotechnol.*, **2010**, *19*, 1005.

Chapter 6. Conclusions

First of all, velocity length product of Π has been defined as a strength of pressure-driven chromatography, that is $\Pi = u_0L$. Π has a feature not to be influenced from K_V or η. And three-dimensional graph of N (Π, t_0) has been represented. Operators can easily obtain information on the speed of t_0 and the separation of N as HPLC performance from the graph. Simultaneously, the separation conditions u_0 of L and can be calculated uniquely. The three-dimensional graph is regarded as accumulated two-dimensional graphs of t_0-N in KPL methods.

Next, an alternative three-dimensional graph of N (u_0, L) is simple to show separation conditions. LRT idea can convert N (u_0, L) into N (Π, t_0) in both directions. And N (Π, t_0) represents the same two-dimensional surface as N (u_0, L). The basal plane is only different from each other. In addition, the relationship among u_0, L, Π, t_0, and N has become well-known by LRT.

Based on the slopes of the two-dimensional surface, PAC for N has been defined to analyze the efficiency on additional N by increasing the pressure. PAC for t_0 has been defined as well. In case of velocity far from $u_{0,opt}$, the performance of t_0 and N can be understood well by PAC.

Finally, ginsenosides and capsaicinoids have been analyzed as applicational experiments. That analysis corresponds to optimal velocity with H_{min}, that is a priority of N. And this analysis is related with velocity far from $u_{0,opt}$, that is balanced with t_0 and N.

Acknowledgements

I would like to express my sincere thanks to Professor Kiyoharu Nakatani for his regard to my works.

I am very grateful to Dr. Jaeho Ha (Chairman of World Institute of Kimchi, Korea) and his colleagues for their helpful cooperation.

I thank Dr. Hiroyoshi Minakuchi, President of Kyoto Monotech Co., Ltd., for his assistance regarding the study's monolithic column.

I am grateful to Professor Gert Desmet (VUB, Belgium) for his advice.

I would like to express my gratitude to Professor Emeritus Hiroshi Nakamura (Tokyo University of Science) for his teaching.

I am also grateful to our colleagues of Hitachi High-Tech Science Corporation and the related companies for their helps.

I wish to thank all the members of Nakatani Laboratory of University of Tsukuba for their friendship.

And I thank my family for their understanding.

List of Publications

[1] M. Ito, K. Shimizu, and K. Nakatani, *Anal. Sci.*, **2018**, *34*, 137-142.

[2] J. Ha, Y.-S. Shim, D. Seo, K. Kim, M. Ito, and H. Nakagawa, *J. Chromatogr. Sci.*, **2013**, *51*, 355–360.

[3] Y.-S. Shim, K.-J. Kim, D. Seo, M. Ito, H. Nakagawa, and J. Ha, *J. AOAC International*, **2012**, *95*, 517-522.

[4] J. Ha, Y.-S. Shim, H.-Y. Seo, H.-J. Nam, M. Ito, and H. Nakagawa, *Food Sci. Biotechnol.*, **2010**, *19*, 1199-1204.

[5] J. Ha, H.-Y. Seo, Y.-S. Shim, D.-W. Seo, H. Seog, M. Ito, and H. Nakagawa, *Food Sci. Biotechnol.*, **2010**, *19*, 1005-1009.

[6] J. Ha, H.-Y. Seo, Y.-S. Shim, H.-J. Nam, H. Seog, M. Ito, and H. Nakagawa, *J. AOAC International*, **2010**, *93*, 1905-1911.